Université de Montréal

Co-encapsulation of enzymes and antibodies for chemical deactivation of pathogens on paper

par

Arash Atashi

Département de chimie
Faculté des arts et des sciences

Mémoire présenté à la Faculté des études supérieures et postdoctorales
en vue de l'obtention du grade de Maître ès sciences (M.Sc.)
en chimie

Décembre, 2015

Université de Montréal

Faculté des études supérieures et postdoctorales

Ce mémoire intitulé :

Co-encapsulation of enzymes and antibodies for chemical deactivation of pathogens on paper

Présenté par :

Arash Atashi

a été évalué par un jury composé des personnes suivantes :

Prof. Jean-François Masson, président-rapporteur

Prof. Dominic Rochefort, directeur de recherche

Prof. Karen C. Waldron, membre du jury

Résumé

Le papier bioactif est obtenu par la modification de substrat du papier avec des biomolécules et des réactifs. Ce type de papier est utilisé dans le développement de nouveaux biocapteurs qui sont portables, jetables et économiques visant à capturer, détecter et dans certains cas, désactiver les agents pathogènes. Généralement les papiers bioactifs sont fabriqués par l'incorporation de biomolécules telles que les enzymes et les anticorps sur la surface du papier. L'immobilisation de ces biomolécules sur les surfaces solides est largement utilisée pour différentes applications de diagnostic comme dans immunocapteurs et immunoessais mais en raison de la nature sensible des enzymes, leur intégration au papier à grande échelle a rencontré plusieurs difficultés surtout dans les conditions industrielles. Pendant ce temps, les microcapsules sont une plate-forme intéressante pour l'immobilisation des enzymes et aussi assez efficace pour permettre à la fonctionnalisation du papier à grande échelle car le papier peut être facilement recouvert avec une couche de telles microcapsules.

Dans cette étude, nous avons développé une plate-forme générique utilisant des microcapsules à base d'alginate qui peuvent être appliquées aux procédés usuels de production de papier bioactif et antibactérien avec la capacité de capturer des pathogènes à sa surface et de les désactiver grâce à la production d'un réactif anti-pathogène. La conception de cette plate-forme antibactérienne est basée sur la production constante de peroxyde d'hydrogène en tant qu'agent antibactérien à l'intérieur des microcapsules d'alginate. Cette production de peroxyde d'hydrogène est obtenue par oxydation du glucose catalysée par la glucose oxydase encapsulée à l'intérieur des billes d'alginate. Les différentes étapes de cette étude comprennent le piégeage de la glucose oxydase à l'intérieur des microcapsules d'alginate, l'activation et le renforcement de la surface des microcapsules par ajout d'une couche supplémentaire de chitosan, la vérification de la possibilité d'immobilisation des anticorps (immunoglobulines G humaine comme une modèle d'anticorps) sur la surface des microcapsules et enfin, l'évaluation des propriétés antibactériennes de cette plate-forme vis-à-vis l'*Escherichia coli* K-12 (*E. coli* K-12) en tant qu'un représentant des agents pathogènes. Après avoir effectué chaque étape, certaines mesures et observations ont été faites en utilisant diverses méthodes et techniques analytiques telles que la méthode de Bradford pour dosage des protéines, l'électroanalyse d'oxygène, la

microscopie optique et confocale à balayage laser (CLSM), la spectrométrie de masse avec désorption laser assistée par matrice- temps de vol (MALDI-TOF-MS), etc. Les essais appropriés ont été effectués pour valider la réussite de modification des microcapsules et pour confirmer à ce fait que la glucose oxydase est toujours active après chaque étape de modification. L'activité enzymatique spécifique de la glucose oxydase après l'encapsulation a été évaluée à 120±30 U/g. Aussi, des efforts ont été faits pour immobiliser la glucose oxydase sur des nanoparticules d'or avec deux tailles différentes de diamètre (10,9 nm et 50 nm) afin d'améliorer l'activité enzymatique et augmenter l'efficacité d'encapsulation.

Les résultats obtenus lors de cette étude démontrent les modifications réussies sur les microcapsules d'alginate et aussi une réponse favorable de cette plate-forme antibactérienne concernant la désactivation de *E. coli* K-12. La concentration efficace de l'activité enzymatique afin de désactivation de cet agent pathogénique modèle a été déterminée à 1.3×10^{-2} U/ml pour une concentration de 6.7×10^{8} cellules/ml de bactéries. D'autres études sont nécessaires pour évaluer l'efficacité de l'anticorps immobilisé dans la désactivation des agents pathogènes et également intégrer la plate-forme sur le papier et valider l'efficacité du système une fois qu'il est déposé sur papier.

Mots-clés: Papier antibactérien / Encapsulation de la glucose oxydase / Microcapsules d'alginate / Inhibition de croissance de E. coli

Abstract

Bioactive paper is obtained through the modification of paper substrate with biomolecules and reagents. It is used in the development of novel biosensors that are portable, disposable and inexpensive, aimed at capturing, detecting and in some cases deactivating pathogens. Generally bioactive papers are made by incorporating biomolecules such as enzymes and/or antibodies on to paper. The immobilization of such biomolecules on solid surfaces is widely used for different diagnostic applications such as in immunosensors and immunoassays but due to the sensitive nature of enzymes, their large scale incorporation into paper has faced several difficulties especially under industrial papermaking conditions. The functionalization of paper at large scale is possible because paper can be easily coated with a layer of microcapsules, which have proven to be an efficient immobilization platform for enzymes and to allow.

In this study, we developed a generic alginate-based platform incorporating microcapsules that can be applied to current paper production processes to prepare antibacterial bioactive paper with the ability to capture pathogens on its surface and to deactivate them by producing an anti-pathogenic agent. The design of the antibacterial platform is based on constant production of hydrogen peroxide as the antibacterial agent inside the alginate microcapsules. Hydrogen peroxide production is achieved through oxidation of glucose, catalyzed by the enzyme glucose oxidase encapsulated inside the alginate beads. The different steps of development included the entrapment of glucose oxidase inside alginate microcapsules, the reinforcement and surface activation of microcapsules by adding an additional layer of chitosan, investigating the possibility of immobilization of antibodies (human immunoglobulin G as a model antibody) on the surface of microcapsules and, finally, verifying the antibacterial properties of the system against *Escherichia coli* K-12 (*E. coli* K-12) as a representative pathogen. During development, certain measurements and observations were made using various analytical methods and techniques such as Bradford protein assay, oxygen electroanalysis, optical and confocal laser canning microscopy (CLSM), matrix assisted laser desorption/ionization- time of flight mass spectrometry (MALDI-TOF-MS), etc. Appropriate tests were performed to validate the successful modification of microcapsules and to ensure that glucose oxidase is still active after each modification. It was found that the encapsulated glucose oxidase maintained the specific enzymatic activity of 120±30 U/g. Subsequent efforts were made to immobilize glucose oxidase

on gold NPs of two different diameters (10.9 nm and 50 nm) to enhance the enzymatic activity and increase the encapsulation efficiency.

The results obtained during this study demonstrate successful modifications on alginate microcapsules and also a successful response of such antibacterial platform regarding deactivation of the pathogen representative, *E. coli* K-12. The threshold for the enzymatic activity was found to be 1.3×10^{-2} U/ml for *E. coli* K-12 growth inhibition of 6.7×10^{8} cells/ml. Further studies are needed to assess the efficiency of immobilized antibody in the capture of pathogens and also to incorporate the platform onto paper and to validate the efficiency of the system once it is coated on paper.

Keywords: Antibacterial paper/ Glucose oxidase encapsulation/ Alginate microcapsules/ E. coli growth inhibition

Table of Contents

List of Figures

List of Tables

List of Abbreviations, Initials and Acronymes

ACS	American chemical society
AIDS	Acquired immune deficiency syndrome
BSA	Bovine serum albumin
CBM	Cellulose-binding module
CLSM	Confocal laser scanning microscopy
DNA	Deoxyribonucleic acid
DPSS	Diode-pumped solid state
E. coli	*Escherichia coli*
EDC	N-ethyl-N'-(3-dimethylaminopropyl) carbodiimide
EDS	Energy-dispersive X-ray spectra
Enz	Enzyme
FAB	Fast atom bombardment
FAD	Flavine adenine dinucleotide (quinone form)
$FADH_2$	Flavine adenine dinucleotide (hyrdoquinone form)
FD	Field desorption
FITC	Fluorescein isothiocyanate
G	α-L-guluronic acid
GOx	Glucose oxidase
HRP	Hydrogen peroxidase
IgG	Immunoglobulin G
IR	Infra-red
LB	Luria-Bertani
LDI	Laser desorption/ ionization
M	β-D-mannuronic acid
MALDI	Matrix assisted laser desorption/ionization
MC-LR	Microcystin-LR
MS	Mass spectrometry

MUA	Mercaptoundecanoinc acid
MW	Molecular weight
NHS	N-hydroxy-succinimide
NPs	Nanoparticles
NSERC	Natural Sciences and Engineering Research Council of Canada
O.D.	Optical density
***o*-dia**	*o*-dianisidine
***o*-dia (ox)**	*o*-dianisidine oxidized form
PD	Plasma desorption
PE	Polyethylene
PLGA	Poly(lactic-co-glycolic) acid
PMT	Photomultiplier tube
POC	Point-of-care
RDS	Rate-determining step
RNA	Ribonucleic acid
SARS	Severe acute respiratory syndrome
SD	Standard deviation
SPR	Surface plasmon resonance
SWNTs	Single-walled carbon nanotubes
TEM	Transmission electron microscopy
TFA	Trifluoroacetic acid
TOF	Time of flight
UV	Ultra violet
Vis	Visible
w/o/w	Water-in-oil-in- water
µPCAD	Microfluidic paper-based chemiluminescence analytical device

I dedicate this dissertation to my family; especially, to my dearest:

my Mother.

Mamani, I know you'd always be happy to see my accomplishments. This one's to you. Cheers!

Acknowledgements

I would like to express my deepest appreciation and sincere gratitude to my supervisor, Prof. Dominic Rochefort for giving me the opportunity to pursue my studies in his group and for providing me with his invaluable scientific guidance during this research and most importantly his constant patience and encouragement throughout this tedious path. Also, I gratefully acknowledge SENTINEL Bioactive Paper Network for granting the financial support to this project.

Moreover, I would like to thank Prof. Joelle Pelletier and Dr. David Charbonneau for their collaboration in this research and also their comments and ideas which enlightened my understanding regarding bacterial growth.

Very special thanks to Prof. Karen Waldron for her advice and support whenever I needed her knowledge or access to her laboratories. Many appreciations to all faculty and staff of the Chemistry department at Université de Montréal specially, Prof. Jean-François Masson, Prof. Pierre Chaurand, Prof. Kevin Wilkinson and Prof. Andreea Schmitzer for granting access to their laboratories and instruments and also Dr. Hélène Yockell-Lelièvre in Prof. Masson's research group for the preparation of gold nanoparticles.

I would like to thank my committee members Prof. Jean-François Masson and Prof. Karen Waldron for their expertise, precious time and extensive comments on the thesis.

I wish to thank all current and previous members in Prof. Rochefort and Prof. Waldron's research group, Bruno Gélinas, Han-Jin Xie, Valentyn Skrypik, Soumia El Khakani, Imène Benrazek, Dr. Cedric Lousteau, Dr. Ahmad Zohrevand, Solmaz Taghavikani, Dr. David Lepage, Dr. Yvon Dougassa, Dr. Golfam Ghafourifar, Vincent Dumont, etc. for their friendship, sympathy and for creating a lovely atmosphere to work in. Also I would like to thank my friend and companion, Rehda Chérif, for his contributions to this project.

On a more personal note, I would like to express my deepest feelings to my parents, my sister, Azin and my brother-in-law, Saviz, for their love, encouragement, moral support, for believing in my capabilities and for being around in my moments of joy and sorrow.

Chapter 1. Introduction

1.1. Project design and objectives

The objective of the project, as a part of Canada's SENTINEL Bioactive Paper Network, is to develop a generic platform that can be applied to current paper production processes to prepare antibacterial bioactive paper that has the ability to capture pathogens on its surface and to deactivate them by producing an anti-pathogenic agent. As schematically demonstrated in *Figure 1*, this platform is based on alginate microcapsules carrying an active enzyme, glucose oxidase (GOx). While the enzyme is active inside microcapsules, in the presence of the substrate (glucose), a constant production of hydrogen peroxide occurs which can be used as an anti-pathogenic agent. The pathogen capturing agent is an antibody specific to a given pathogen. The antibody needs to be covalently conjugated to the external surface of microcapsules to be able to capture the pathogens and with the production of hydrogen peroxide diffusing out of microcapsules, the pathogens are decomposed and therefore deactivated. The proposed microcapsule-based platform (which carries the enzymes inside and the antibody on its surface) will possess antibacterial properties and can be applied easily to industrial conventional paper production processes, either by coating the paper or by incorporating it into the paper pulp.

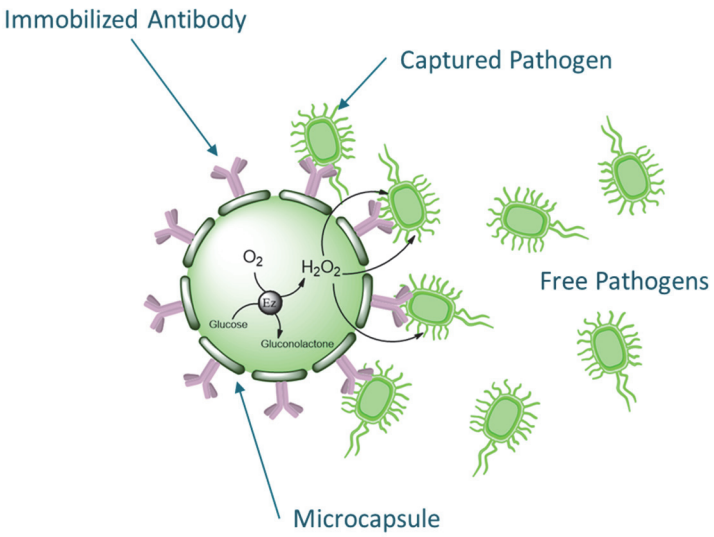

Figure 1. Schematic view of the proposed antibacterial platform.

The specific steps in this project are as follows and the activity of the enzyme was measured after each step to evaluate possible losses;

- Encapsulation of GOx in alginate microcapsules to prepare an enzymatically active platform.
- Surface preparation and functionalization of alginate microcapsules using chitosan to add $–NH_2$ functional groups on microcapsules.
- Immobilization of IgG on the external surface of the alginate-chitosan microcapsules.
- Testing the bacterial growth in the presence of the prepared system to verify its antibacterial properties and to determine the optimal conditions and the durability of the system.
- GOx was immobilized on gold nanoparticles (NPs) and the effect of this immobilization on enzymatic activity was studied.

1.2. Bioactive papers

In modern times, mankind's wellbeing is subject to various biological threats. Susceptibility against severe acute respiratory syndrome (SARS), water quality problems and incidents of tainted beef, for instance, underscore our vulnerability to biological hazards which is why we, as everyday water and food consumers, demand a safe and hygienic intake. Providing reliable food products and safety of the citizens have always been a concern for food production companies and regulatory authorities. To achieve such goals, paper-based sterile packaging, food wrap, face masks and protective clothing have been produced employing novel technologies and playing an important role in protecting us from pathogens[1].

Bioactive paper is a broad term used to define paper-based, portable, disposable and inexpensive biosensors aimed at capturing, detecting and in some cases deactivating pathogens. The research on bioactive paper is quite multidisciplinary as it lies at the interface of bioanalytical chemistry, paper chemistry and nanobiotechnology[2]. The history of bioactive paper dates back to 1952 when Martin and Syne won the Noble Prize in chemistry for the invention of paper chromatography[3]. Then in 1957, for the first time a paper-based bio assay was introduced by Free *et al.*[4] for detection of glucose in urine samples. This paper based bio

assay was made by the incorporation of an enzyme, GOx, using a simple dipping procedure. Work has also been done to prepare a bacteria-based biosensor to detect low amounts of arsenic in potable water[5]. The color change in such biosensors indicated the presence of arsenic and it is visually detectable. The application then spread to Point-Of-Care (POC) tests, some quick and easy to do clinical tests which are used to diagnose diabetes, pregnancy and the presence of pathogens and infectious diseases such as AIDS, Malaria and Syphilis[6]. The incorporation of single-walled carbon nanotubes (SWNTs) and antibodies on to paper was described by Wang *et al*.[7] to detect a water contaminant, microcystin-LR (MC-LR). Dip-coating of a strip of paper with carbon nanotubes and the antibody to MC-LR renders it conductive, and the change in conductivity of the paper strip was correlated to the presence of MC-LR in water samples. The possibility of printing antibodies on paper strips for blood type determination was demonstrated by Khan *et al*.[8] and developed for inexpensive and portable blood-typing purposes. Savolainen *et al*.[9] fabricated bioactive papers using three techniques, namely screen printing, rod coating, and flexo-printing. These methods were used to coat a paper with polyethylene (PE) microcapsules containing laccase. This bioactive paper, which contains laccase, was further improved by Virtanen *et al*[10]. Yu *et al*.[11] have also designed a microfluidic paper-based chemiluminescence analytical device (μPCAD) for simultaneous detection of glucose and uric acid in urine samples. This lab-on-paper biosensor implements some enzymatically catalyzed oxidation reactions (GOx and urate oxidase) as well as the chemiluminescence reaction between a rhodanine derivative and generated hydrogen peroxide. In recent years some bioactive paper strips were invented for rapid detection of pathogens like *E. coli* based on intracellular enzyme (β-galactosidase or β-glucuronidase) activity[12]. Similarly, for rapid self-diagnosis of bacterial vaginosis Zhang and Rochefort[13] developed an effective paper-based spot assay technique emphasizing its fast response and long-term storage stability. At the same time, some sensing platforms were designed for detection of phenols[14] and pesticides[15,16] which can potentially be used in the preparation of paper-based sensors. Another platform based on gold NPs, suitable for point-of-care applications, was developed to detect food-borne pathogens based on sensing of RNA markers[17].

1.2.1. Functionality

Certain advantages are found in using paper instead of plastic to prepare a bioactive surface. Biodegradability is an important characteristic of paper since it is made from naturally abundant cellulose and also it is more energy efficient. Its cellulosic structure is proven to be more compatible with proteins and biomolecules. The porous structure of paper facilitates a lateral flow assay and plays both roles of filtering and pumping by capillary forces and therefore, even in more complex paper-based microfluidic devices, there is no need to use an external power source to exert an interaction between the sample and the bioactive agent immobilized on the paper. Moreover, such paper substrates are inexpensive so they can be used to decrease the cost of diagnostic devices that are handy for on-site detection and can easily get to market since they are a proven technology to control the bacterial contamination in food samples.[2]

1.3. Immobilization of biomolecules on paper

There are certain structural and surface chemical properties of paper that affect the immobilization of biomolecules. Structural properties such as the porosity, mass distribution, the degree of crystallinity of fibers, their preferred orientation and accessible area of paper for immobilization influence the maximum quantity of biomolecules that can be immobilized. Surface chemical properties of paper such as the surface energy, surface sizing additives, cellulose grafting additives and plasma treatments of paper surface are factors that influence the facility of biomolecule immobilization and the reporting strategies[2]. Functionalization of paper is feasible either during the paper making process or on the finished paper. The goal in biomolecule immobilization on paper is to retain active biomolecules with maximal density and minimal leaching. In general, there are four methods available for this purpose: physical immobilization, covalent and affinity-based attachment, immobilization on carriers and entrapment[18].

1.3.1. Physical immobilization

In the physical immobilization method, the biomolecule adheres to the surface of the paper spontaneously via van der Waals and electrostatic interactions. This method is extensively

used in contact printing or non-contact paper printing (*i.e.* inkjet printing). These interactions can be improved by pre-coating of paper with cationic polymers, which graft well onto cellulose and render the surface highly cationic. Or in cases of neutral biomolecules, pre-coatings with a layer of hydrophobic molecules will enhance such interactions[19]. One of the potential problems of this method arises in certain cases of biomolecules that are not highly cationic thus their interaction with the paper surface (which is weakly anionic) is rather weak and results in the leaching of those biomolecules during assays in which the ionic strength of the media is high or the pH values are above 7. Another challenge would be the orientation of adhered biomolecules, which is essential to maintain their bioactivity. For instance, in the case of immobilizing bacteriophages on paper, a polyvinylamine pre-coating is required to render the surface of the paper positively charged so that the bacteriophage's head (with a net negative charge) can be attached to the paper surface while the tail (with a net positive charge) remains still active to interact with the bacteria[20]. One drawback in using such modifications to increase electrostatic or hydrophobic interactions is that there is a high chance of encountering some non-specific binding onto paper which can be reduced by using blocking agents such as Tween 20 surfactant or bovine serum albumin (BSA) after the adsorption of the species of interest, but adding another step to the manufacturing process can be costly and in some cases difficult[21].

1.3.2. Covalent and affinity-based attachment

In this approach a direct covalent bond acts as a bridge between biomolecules and paper. Since cellulose does not contain a significant chemically active group on its structure, some chemical modifications are needed to activate the surface of paper. These chemical modifications usually involve multiple steps, which adds to the manufacturing cost of the final product. One of the proposed solutions to resolve such difficulty is to fuse a cellulose-binding module (CBM) – generally a protein– to the biomolecule and then immobilize the biomolecule via such CBMs which attach to cellulose spontaneously. But seemingly, to synthesize such CBMs requires extra protein engineering which limits the versatility in large scale productions.[18]

1.3.3. Immobilization on carriers

In the method using carriers, the biomolecules are first attached to a carrier molecule which is then printed onto paper surface. For instance, it was demonstrated that antibodies and DNA aptamers can be covalently attached to carboxylic poly(N-isopropylacrylamide) microgels and then printed on paper stripes to be used for paper chromatography[22]. The microgels are mechanically entrapped on paper and those biomolecules retain their recognition capabilities. After applying the microgels on paper strips it is necessary to let them dry before rewetting the paper. The drying will force the microgels to penetrate the fiber network of the paper as a result of capillary forces[22]. Using water-soluble carriers provides the possibility to incorporate them into water-based inks, but this method still suffers from the added complexity to the manufacturing process[18].

1.3.4. Entrapment

Entrapment of biomolecules is carried out by entangling them in a network of cross linked polymers through a sol-gel process while maintaining the activity of the biomolecule. This network should be tight enough to prevent the leaching of biomolecules and at the same time it has to be porous enough to let smaller molecules such as reactants, substrates and target species pass through the gel and have access to active sites of biomolecules. Among all polymers, sol-gel based silica and alginate-silica sol-gel hybrid are the most popular matrices for entrapment of biomolecules.[23]

Encapsulation of biomolecules and microorganisms is another type of entrapment. In fact, this general term refers to a class of technologies which forms a polymeric matrix or shell around solids, liquids or gases, which traps them inside. The formation of encapsulated species is usually done is a single step and the particle size that is created using the encapsulation technique usually ranges from 1μm to 1000 μm; therefore, the particles are called “microcapsules” and the process is termed “microencapsulation”. Microcapsules have extensive applications as drug delivery systems in pharmaceutical and medical technology to protect the drug from environmental adverse effects, to eliminate incompatibilities, to stabilize sensitive drugs and also to mask their bad taste[24]. Apart from medical and pharmaceutical industries, microcapsules

have vast applications in other fields like in cosmetics, electronics, waste treatments, detergents, photography, graphics and paint industry, agriculture and food industry, etc[25].

1.4. Enzyme encapsulation

As mentioned in Section 1.3, the biomolecule should maintain a high activity after the immobilization process. In the case of enzyme encapsulation, often the enzymatic activity is reduced during the encapsulation process[26] (*i.e.* once it is trapped inside a microcapsule). There could be losses in enzyme quantity during the encapsulation process. Also, the heterogeneous confined space inside a microcapsule imposes some conformational changes in the structure of the enzyme resulting from interactions between the protein and the cross linked polymeric network of the microcapsule. These interactions, such as Lifshitz-van der Waals forces, dipolar or hydrogen bonding, conformational entropy, electrostatic forces, coulomb and hydrophobic dehydrations may stabilize certain conformations of the enzyme that are not favorable for the enzymatic activity. Also the diffusion rate of the substrate and other reactants across the microcapsules' wall, which is controlled by the porosity, is a limiting factor for enzymatic activity because it reduces the access of the substrates to the enzyme's active site[26]. However, in a very few reported cases, researchers were able to maintain the enzymatic activity. As demonstrated by Montalvo-Ortiz *et al*.[27] the use of hydrogen peroxidase (HRP) NPs instead of a lyophilized protein formulation encapsulated in poly(lactic-co-glycolic) acid (PLGA) microspheres through the standard water-in-oil-in- water (w/o/w) methods, will enhance the encapsulation efficiency as well as reducing burst release and enhancing the enzymatic activity during release from PLGA microspheres.

In recent years, biopolymers such as polysaccharides, proteins and lipids have been widely used as the matrix of microcapsules in microencapsulation process. There are five criteria that limit our choice of biopolymers for a given application: being a natural emulsifier for proteins and lipids, permeability for gases, the chemical composition and existing functional groups, the possibility of surface modification and finally its large scale availability in market with a reasonable price. A combination of all these criteria allows us to choose a compatible biopolymer for a certain application by granting them favorable properties such as mechanical

stability for storage, elasticity, biocompatibility, biodegradability and non-toxicity, etc[28]. A list of such biopolymers conventionally used as the matrix of microcapsules is given in *Table 1*.

Table 1. Commonly used biopolymers in microencapsulation process (reproduced from reference 28).

Source	Polysaccharide-based	Protein-based	Lipid-based
Plants	Starch, Cyclodextrine, Pectine, etc.	Gluten, Protein extracts from green beans, soy beans, lupine, etc.	Hydrogenated palm oil, Vax, Lecithin (soy), etc.
Aquatics	Carrageenans, Alginate, Agarose.		
Animals or microbes	Xanthan, Dextrose, Chitosan, Gellan.	Gelatin, Collagen, Caseins, Albumins	Lecithin (egg)
Genetics		Recombination proteins	

1.4.1. Alginate-chitosan microcapsules

Among all biopolymers commonly employed as the membrane material and the matrix for encapsulation, alginate is the most conventional and successful one because of its biocompatibility. It is also common to cover negatively charged polyamino acid polylysine microcapsules with an extra layer of alginate in order to improve biocompatibility of such membranes[29]. Alginate is the anion of alginic acid, which is a linear copolymer of β-D-mannuronic acid (M) and α-L-guluronic acid (G) covalently linked together in different sequences or blocks. The M and G monomers are arranged in the alginate chain, to form three different sequences namely M-block (two M monomers attached together), G-block (two G monomers attached together) and alternating GM-block (a G monomer and an M monomer attached to each other). These different blocks composing the alginate linear body are illustrated in *Figure 2*. This anionic biopolymer is extensively found in cell walls of brown algae.[30]

Divalent cations, such as calcium can crosslink alginate chains to form an “egg box model” structure. The formation of such structures is a result of an interaction between the divalent cation and the G-blocks of alginate, which creates a gel network (*Figure 3*)[31,32]. The ratio

between the monomers and their sequential composition is the factor that determines the physical properties of the gel such as strength and the porosity of the gel[33]. To prepare calcium-alginate microcapsules, a solution of alginate is poured in the form of tiny droplets into a bath of calcium chloride. When each droplet arrives into the calcium chloride bath the gelation process happens and the droplet will be solidified while maintaining its spherical shape and thus becomes a microcapsule[34].

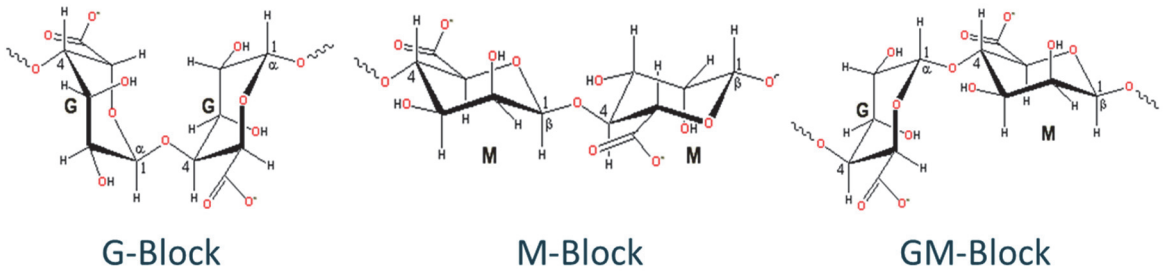

Figure 2. Different sequences (blocks) found in a linear chain of Alginic Acid. M = β-D-mannuronic acid. G = α-L-guluronic acid.

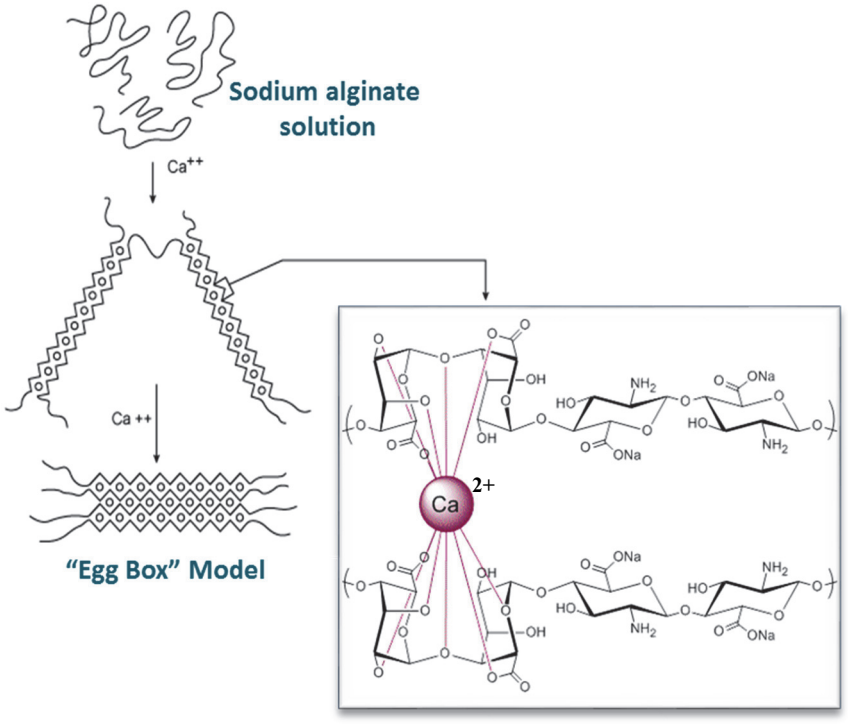

Figure 3. "Egg box" model of gel formation resulting from the crosslinking of alginate chains using calcium ion (adapted from references 31 and 32).

The encapsulation method using calcium alginate gels was chosen in our research because of its mild encapsulation conditions for biomolecules, non-toxicity, low cost and its ease of use. The characteristics of microcapsules such as permeability and wall thickness can also be easily controlled by changing the encapsulation parameters. Some of the drawbacks associated with this method are low stability in the presence of citrate, lactate and phosphate (most likely because of their affinity for calcium ion) and also high porosity of the membrane which may result in leakage of the immobilized biomolecule[35]. The porosity of such microcapsules allows low molecular weight substrates such as glucose and oxygen molecule (in this study) to pass through the microcapsule's wall; therefore, they can diffuse in and out of the microcapsule.

Chitosan is a linear polysaccharide composed of β-(1-4)-linked D-glucosamine (de-acetylated unit) and N-acetyl-D-glucosamine (acetylated unit). Chitosan is derived from its natural source, chitin, which is a long-chain polymer of a N-acetylglucosamine abundantly found in exoskeletons of crabs, lobsters, shrimps and insects[36]. The structure of these two biopolymers are shown in *Figure 4*.

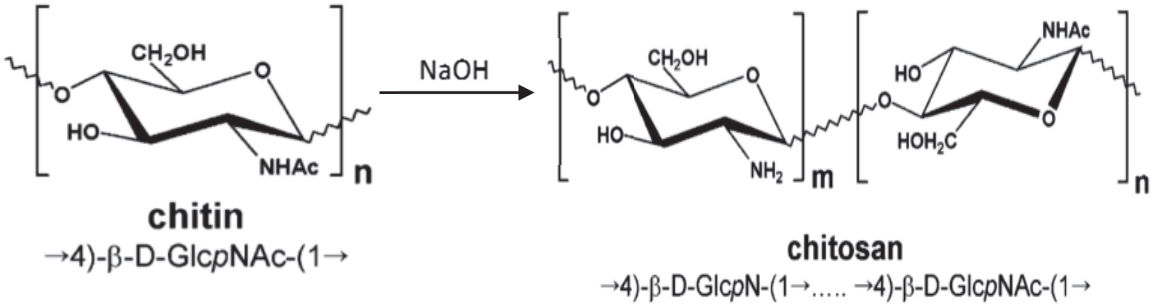

Figure 4. Chitosan formation from the deacetylation of its natural source, chitin.

There are several methods to prepare alginate-chitosan microcapsules. Basically chitosan has an ionotropic affinity for alginate (*Figure 5*). A one-stage preparation process involves droplet addition of alginate solution into an aqueous solution of chitosan which results in microcapsule formation comprising an alginate core and a chitosan layer. The opposite process is also possible to prepare chitosan core microcapsules with an alginate layer by pouring chitosan solution in the form of small droplets into an alginate bath[33]. In a two-stage procedure,

calcium-alginate microcapsules are prepared (Section 2.1) followed by incubation in a solution of chitosan to cover them with an extra chitosan layer for which the procedure will be discussed in Section 2.2.

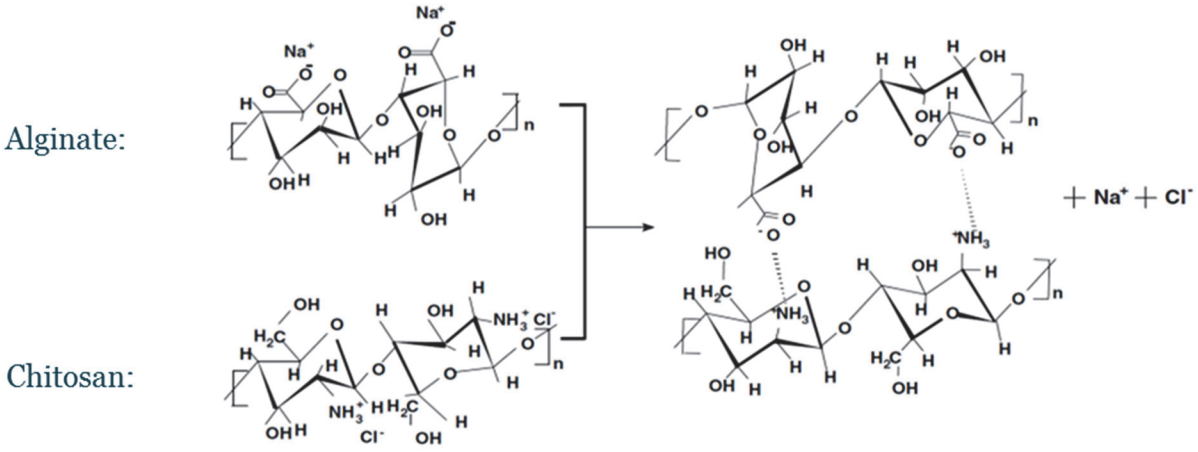

Figure 5. Ionotropic affinity between alginate and chitosan.

1.4.2. Encapsulation methods

In general microencapsulation procedures are performed in three steps[37]. The first step is the addition of the biomolecule, or the species which is to be encapsulated, to the encapsulation matrix. This step normally involves the dissolution of the species to be encapsulated into the matrix. The second step includes liquid/liquid or liquid/air mechanical dispersion of encapsulation matrix and the third step is to stabilize microcapsules either by chemical methods such as polymerization or by physical methods such as evaporation, solidification, coalescence or by physicochemical methods such as gelification or coacervation.

1.4.2.1. Dispersion methods

The common event in all dispersion methods is that the encapsulation matrix containing the target species (which are meant to be encapsulated) must be dispersed in the form of droplets in the stabilizing media to form microcapsules. Prilling, nebulization, emulsification and micro-dispersion are different methods of dispersion, which are explained briefly in the following sections.

1.4.2.1.1. Prilling methods

Basically, in prilling methods, a laminar flow of the encapsulating matrix and the biomolecule target is created by passing it through a narrow nozzle and this flow is broken up in to small droplets having a relatively small dispersion in size (*i.e.* with a maximum standard deviation of 10 % of the average particle size). The breaking up of such laminar flow is done by applying an electrostatic potential that reduces the surface tension of the flow (having flow rates of a few milliliters per hour) resulting in formation of small droplets. A schematic operating view of such nozzle is shown in *Figure 6*a[38]. It can also be performed using a vibrating nozzle which works well with low viscosity solutions and higher flow rates (a few liters per hour). Other prilling methods involve cutting off the laminar jet using a rapidly rotating disk (*Figure 6*b[38]) or grid, which are effective for higher viscosities (more than 200 mPa·s).

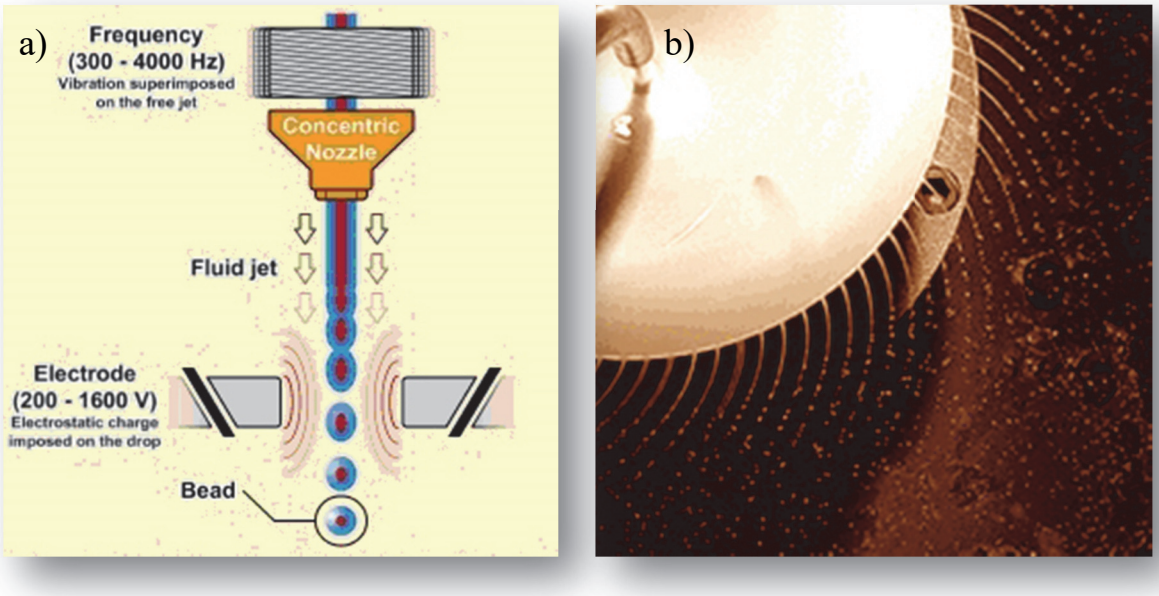

Figure 6. a) Schematic operation view of a laminar flow breaking up using an electrostatic potential. b) Laminar flow breaking up using a rotating disk. (reproduced from reference 38)

In our study we used the vibrating nozzle prilling method because it gives narrow size dispersion of the beads and also because of its compatibility to operate with the viscosity of sodium alginate solutions.

1.4.2.1.2. Nebulization

Nebulization or *spray-drying*, is a technique in which a flow of the encapsulation matrix is passed through a liquid/air nozzle or sometimes it is jetted to the surface of a spinning disk at high speed. The droplets formed using this method normally have a relatively wide dispersion, *i.e.* standard deviation of 30 – 50 % of the average particle size. The source of such a wide dispersion is the use of turbulent flow instead of a laminar flow in comparison with prilling methods. The advantage of this method is the availability of its commercialized equipment in industry for large scale productions.

1.4.2.1.3. Emulsification

In this method the encapsulation matrix containing the target species is dispersed in another immiscible liquid and the small droplets are formed with the help of violent agitation using a turbine or stirrer. The droplets may have a wide particle size dispersion (standard deviation of 30-50 %) with the high level of agitation there is a possibility of denaturing the target species; for instance, in case of living cells, they may get disrupted under strong agitation. For industrial large scale productions (tons per hour), a system of continuous flow has been designed using static mixers.

1.4.2.1.4. Microdispersion

The principle of microdispersion is the same as emulsification, which is described in Section 1.4.2.1.3, but the dispersion of two immiscible liquids is done with the help of a surfactant. The average droplet size is relatively small (less that one micrometer) and thermodynamically speaking, such micro-emulsions are generally more stable than normal emulsions.

1.4.2.2. Stabilization methods

After creating small droplets of the encapsulation matrix in the previous dispersion step, a stabilization method is required so that they are solidified to form microcapsules while trapping the target species inside them. The *solidification* of hot matrices (previously melted)

can easily be achieved by cooling them to the temperature where they become solid once more. Sometimes it is possible to evaporate the solvent of the encapsulation matrix using dry hot air and the technique is therefore called *evaporation*. Many of the polymers used as the matrix of encapsulation can be jellified in a *jellification* process either by using low temperature or certain chelating ions. For instance, agarose can be jellified by lowering the temperature and alginate can be crosslinked using calcium ions. In the *polymerization* method, a polymeric network is formed by the polymerization of the monomeric units in the presence of the agent to be encapsulated. For instance, in an emulsion we may incorporate two different monomers, one in each phase. These two monomers can react with each other to create a polymer at the interface of the two phases *i.e.* around each droplet. In the *coacervation* method, the precipitation of a polymer is induced by changing the physico-chemical parameters of the media such as acidity, ionic strength, etc.

In our study we used the jellification process of alginate using calcium ions because of the mild conditions for stabilization of microcapsules in the presence of biomolecule targets (GOx in this case) without adding a reactive agent or altering the temperature, which could be devastating to the biomolecule and its functionality.

1.5. Enzymatic activity

Enzymes are catalysts in biochemical reactions essential to the functionality of living systems. Each enzyme has an active site that interacts with a substrate to catalyze the latter's transformation to the products. Despite the similarity of the catalysis principles between the enzymes and non-protein based catalysts, enzymes have unique properties in their performance. An enzymatically catalyzed reaction rate is usually enhanced to the order of 10^6 to 10^{12} times[39]. The condition for optimal activity of most of enzymes is quite moderate, *i.e.* operating temperature of below 100˚C, atmospheric pressure and a pH value almost neutral. The substrates and the reactants of each enzyme are specific to a great extent. The activity of an enzyme is tunable by adjusting the regulatory parameters such as allosteric control (modification of an enzyme to induce a change in the shape of the enzyme to change the interaction of the active site with the substrate)[39] and covalent modification of the enzyme, for instance covalent bioconjugation of the enzyme and silver NPs[40]. The choice of GOx in this study was based on

the fact that this enzyme is well known and characterized to a high extent and also it catalyzes a reaction whose product (hydrogen peroxide) has antibacterial properties.

1.5.1. Glucose oxidase overview

GOx (β-D-glucose: oxygen 1-oxireductase) is a flavoprotein that catalyzes the oxidation reaction of β-D-glucose. This enzyme can be produced and purified from different fungi among which *Aspergillus niger (Figure 7a[41])* and *Penicillium* species (*Figure 7*b[42]) are the most common sources of this enzyme. Perhaps *Aspergillus niger* is the most conventional source of GOx meanwhile the enzyme produced from *Penicillium* species has a more efficient enzymatic activity. Different types of GOx from different sources have different detailed compositions but all of them have in common a co-factor, flavine adenine dinucleotide (FAD), which is tightly entangled in the polypeptide chain but not covalently attached to the protein. This unit plays an important role in the activity of GOx[43].

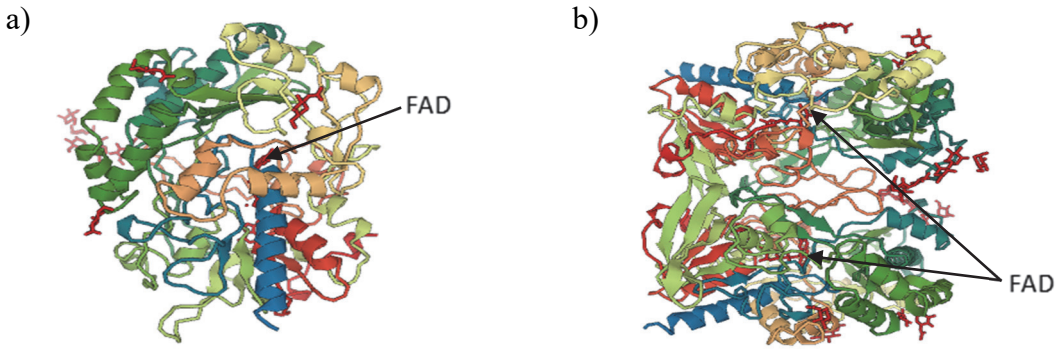

Figure 7. a) GOx from Aspergillus niger (adapted from reference 41) and b) GOx from Penicillium amagasakiense (adapted from reference 42).

As mentioned before, GOx catalyzes the oxidation reaction of β-D-glucose to D-glucono-δ-lactone using molecular oxygen as an electron acceptor (*Equation 1*). As shown in *Figure 8*[44], the FAD co-factor plays an important role in the catalytic activity of the enzyme by participating in the oxidation-reduction reaction. In the reductive half-reaction, glucose is oxidized to glucono-lactone (which is subsequently hydrolyzed to gluconic acid) while FAD is reduced to

$FADH_2$. In the oxidative half-reaction, $FADH_2$ transforms back to FAD while giving an electron to molecular oxygen and reducing it to hydrogen peroxide.

Equation 1 $$\beta - D - glucose + O_2 \xrightarrow{GOx} D - gluconeδlactone + H_2O_2$$

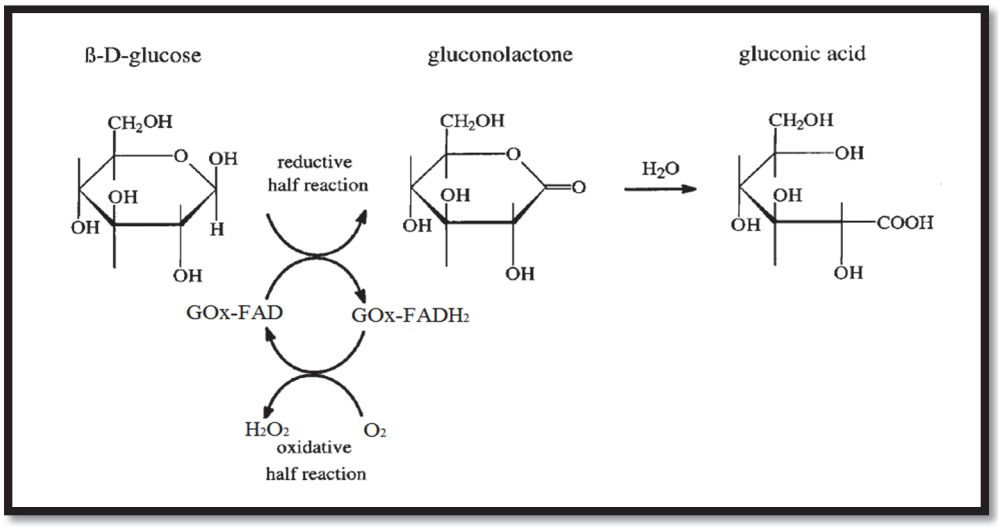

Figure 8. Details of the oxidation reaction of glucose (adapted from reference 44).

1.5.2. Glucose oxidase applications

GOx has been widely used in biotechnology and the pharmaceutical, food and beverage, electronics and textile industries[43]. In pharmaceutical and clinical chemistry, GOx is the enzyme used in nearly all types of glucose biosensors. The glucose biosensor for diabetes monitoring is an important field of application for this enzyme and it is even in some cases lifesaving. These biosensors are extensively used to monitor and detect the blood sugar fluctuations for patients having diabetes who are prone to hyperglycemia (high blood glucose content) or to hypoglycemia (low blood glucose content). This enzyme also can be used to prepare oral care products thanks to bacteriocide properties of H_2O_2 which is produced during the oxidation reaction.[43]

Also the presence of glucose in some food may boost the growth of harmful microorganisms which reduces the food's shelf time and produces unwanted bad taste and

inconvenient color. Therefore, in food and beverage industry GOx is successfully used to remove the residual glucose content from food or beverages to increase their durability and shelf time. To remove the H_2O_2 produced in food products, the use of catalase is favorable to transform H_2O_2 to water and oxygen. For instance, during the production of egg powder, using the combination of the two enzymes, GOx and catalase, during the drying process prevents the appearance of the brown color. Also it is used to remove the oxygen from the top of the bottled beverages and food packing. Moreover, the gluconic acid (produced form hydrolysis of D-glucono-δ-lactone) can act as a food additive for acidity regulation purposes.[43]

In the electronics industry, bio-electronic devices need biofuel cells as a power supply. GOx is one of the biocatalysts that is used in biofuel cells to convert biochemical energy to electrical energy. In one of the approaches, enzymatically catalyzed oxidation reaction of glucose can be used in anode, coupled with the enzymatically catalyzed reduction of dioxygen in cathode using dioxygen-reducing enzyme such as laccase. All material used in such biofuel cells are biocompatible and biodegradable.[43]

In textile industry, the produced H_2O_2 can be used as the bleaching agent for scoured woven cotton fabric also the gluronic acid can act as the stabilizer in the process so there is no need to use a stabilizing agent. Also the combination GOx/ hydrogen peroxidase (HRP) can be used to oxidize the colored components since H_2O_2 is produced and then it is rapidly consumed to oxidize and subsequently bleaches the natural fibers.[43]

In this project, the production of H_2O_2 from the reaction of glucose with oxygen will be used to deactivate pathogens.

1.5.3. Enzyme kinetics

As mentioned before, enzymes are biological catalysts but their function is much more complicated than normal catalysts. Some enzymes conduct a reaction on a single substrate while others may act on two or more substrates[39]. In the simplest case where the enzyme deals with one single substrate, it has been found that in low concentrations of the substrate, the rate of the reaction varies linearly with the initial concentration of the substrate which means the reaction is following first-order kinetics while at high concentrations of the substrate, the reaction rate

becomes independent of the initial substrate concentration which means the kinetics of the reaction has a zero-order pattern. The change in the concentrations of the different species involved in a single substrate enzymatic reaction is demonstrated in *Figure 9*[45].

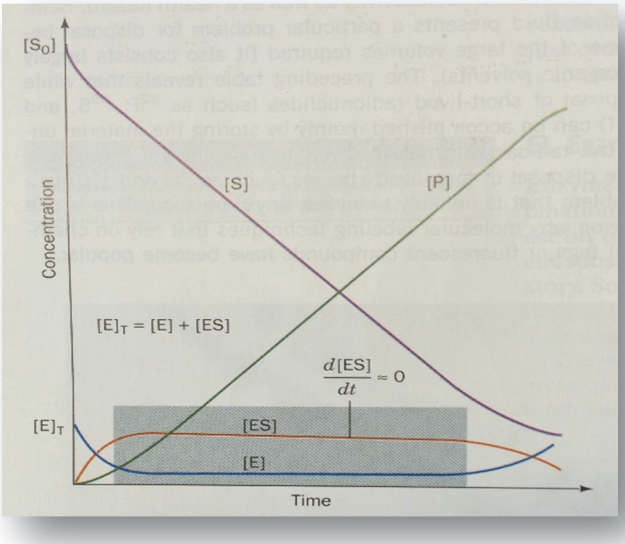

Figure 9. Concentration change of the species in a single substrate enzymatic reaction. S: substrate, E: enzyme, P: product, ES: enzyme-substrate complex (reproduced from reference 45).

The behavior of the enzymes was first studied and defined in 1913 by Leonor Michaelis (1875-1949) and Maud L. Menten (1879-1960) as *Equation 2*[46]:

Equation 2
$$E + S \underset{k_{-1}}{\overset{k_1}{\rightleftarrows}} ES \xrightarrow{k_2} E + P$$

where E, S and P are the enzyme, substrate and the product, respectively and ES is the enzyme-substrate complex, *k* values are rate constants for each reaction. In *Equation 2*, when the concentration of the substrate is much bigger than the concentration of the enzyme, it can be assumed that all the enzyme is transformed to the enzyme-substrate complex so the second step of the reaction is the *rate-determining step (RDS)* so the rate of the reaction (υ) can be expressed as:

Equation 3
$$\upsilon = \frac{d[P]}{dt} = -\frac{d[S]}{dt} = k_2[ES]$$

The steady state assumption which allows us to assume that the change in the concentration of ES in time equals zero, provides an estimation for the concentration of the enzyme-substrate complex:

Equation 4 $$[ES] = \frac{k_1[E]_0[S]}{k_{-1}+k_2+k_1[S]}$$

Where $[E]_0$ is the initial concentration of the enzyme and at any time point and it equals the concentration of free enzyme plus the concentration of the enzyme in the form of the complex with substrate ($[E]_0 = [E] + [ES]$). By substitution of *Equation 4* in *Equation 3* and also considering the fact that the maximum rate of the reaction occurs when the substrate exists at high concentrations which converts all of the enzyme to ES (*i.e.* $V_{max}=k_2[E]_0$), further rearrangement of the *Equation 3* results in:

Equation 5 $$\upsilon = \frac{V_{max}[S]}{[{}^{(k_{-1}+k_2)}/_{k_1}]+[S]}$$

By defining $K_m = \frac{k_{-1}+k_2}{k_1}$ as *Michealis-Menten constant*, *Equation 5* can be written as:

Equation 6 $$\upsilon = \frac{V_{max}[S]}{K_m+[S]}$$

Two boundaries of substrate concentration can be imagined, one where [S] is much bigger than K_m, as can be seen in *Figure 10*[45], the rate of the reaction reaches its maximum value and independent of [S] which means it is zero-order. The other extreme is met when [S] is much lower than K_m, so the rate of the reaction becomes first-order (*Equation 7*) and it is preferably said that no rate determining step exists in the kinetics of the reaction[46].

Equation 7 $$\upsilon = \frac{k_2}{K_m}[E]_0[S]$$

It can be easily perceived from *Equation 6*, when the rate of reaction is at one-half of V_{max}, the value of [S] equals the value of K_m. Smaller values of K_m indicates that the saturation of the enzyme (total conversion of the enzyme to enzyme-substrate complex) occurs at lower substrate concentrations and thus, the affinity of the enzyme for its substrate is relatively high. Greater values of K_m, similarly means that the affinity of the enzyme for the substrate in relatively low

so higher concentrations of the substrate are needed to saturate the enzyme. In our study, we will make sure to operate at V_{max} to be able to measure the enzymatic activity of GOx.

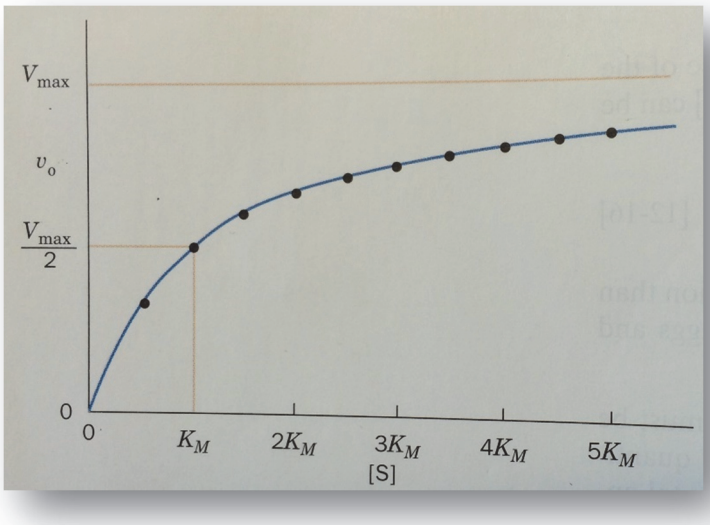

Figure 10. The plot of the initial rate of the reaction versus the concentration of substrate (reproduced from reference 45).

1.6. *Escherichia coli (E. coli)*

In our study, *E. coli* was selected as a representative model of pathogens. *E. coli* is an abbreviation for *Escherichia coli* (*Figure 11*)[47] that is attributed to a group of bacteria that reside in the intestines of humans and animals. They are mostly found in contaminated food or water so disinfecting processes on food and water such as proper cooking of meat and raw vegetables, water treatments, pasteurization of dairy products and juices as well as controlled contact with animals in petting zoos and farms can highly reduce the risk of spreading such bacteria. Infections of *E. coli* are both gastrointestinal and extraintestinal. Severe stomach cramps, diarrhea, vomiting, a mild fever for certain strand of bacteria kidney failure are the symptoms and adverse effects of *E. coli* on human body[48]. Since the term biotechnology first emerged during a meeting at a Hawaiian delicatessen in 1972, *E. coli* has been extensively used for research purposes in microbiology and biological engineering research specially as a host for propagating and cloning engineered plasmids[49]. In our study, *E. coli* K-12 was used as a

representative pathogen because there are non-pathogenic strains of this bacteria which can be safely manipulated in laboratories for research purposes.

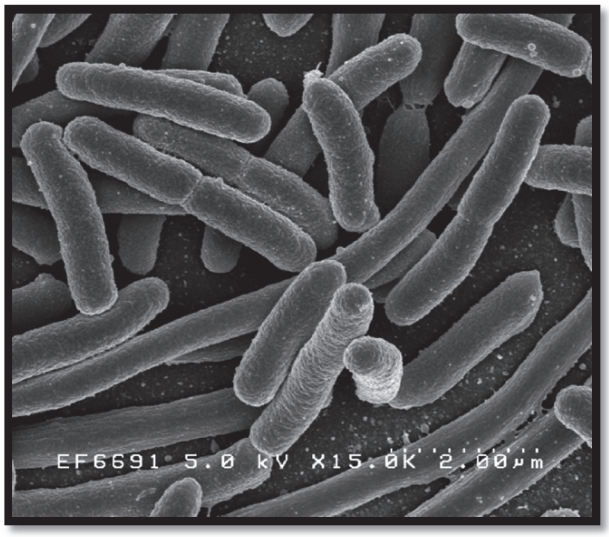

Figure 11. Scanning electron micrograph of Escherichia coli, grown in culture and adhered to a cover slip (reproduced from reference 47).

1.6.1. Bacterial growth

Growth is a characteristic of all living organisms and is a general definition used when a living organism increases its cellular mass or the number of cells. About half a century ago (or even earlier), researchers were able to understand the general laws of bacterial growth[50]. This growth is greatly affected by environmental factors such as pH, temperature, osmotic pressure, the content of nutrients, etc. Bacteria are unicellular microorganisms and in favorable conditions for their growth, they start consuming the nutrients in the media and attain certain size and consequently, they divide into two cells through a binary fission process. In this process a parent bacteria cell is divided into two new daughter cells while its genetic material (DNA) duplicates and each daughter cell receives one copy of DNA[51]. Different steps of such reproduction process for an *E. coli* bacteria cell is schematically illustrated in *Figure 12*[52]. Generally, prokaryotic organisms have chosen binary fission as their primary method of reproduction.

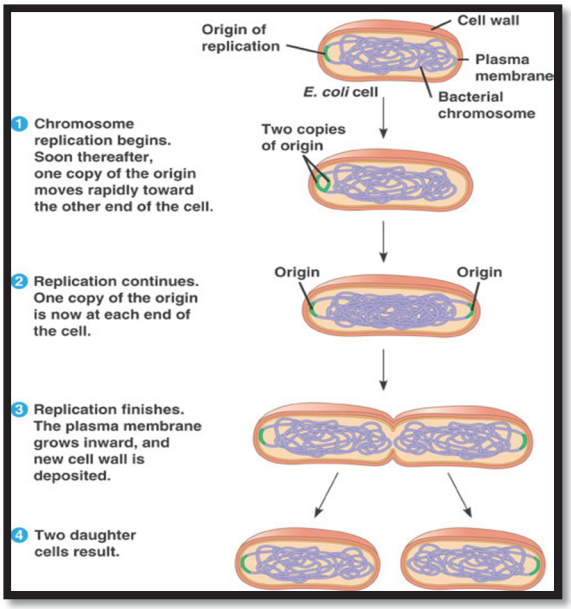

Figure 12. Different steps of a binary fission process in E. coli cell (reproduced from reference 52).

The growth pattern for each bacteria is varied in different ecological conditions. The number of cells (N_t) after a certain time (t) can be predicted from *Equation 8* where N_0 is the initial number of bacteria cells and τ is the time required for a single cell to grow and duplicate[53].

Equation 8 $$N_t = N_0 2^{t/\tau}$$

The bacterial growth curve is an indication of a bacteria's population by plotting the binary logarithmic scale of the number of cells at each time point versus time. The resulting graph is illustrated in *Figure 13*[52]. This graph exhibits four distinctive stages of the bacterial life cycle provided that bacteria are cultured in an isolated culture media where no additional nutrients or space are added and also no waste or dead cells are removed from the culture media. The first stage is the *lag phase* which occurs after the bacteria are added to the culture medium. In fact, this time elapse before the growth phase (second stage) is the period of time required for the organisms to adapt themselves to the new environment so the population growth at this period close to 0. The second stage is the *growth phase* and the binary logarithm of the number of cells grows linearly with time according to *Equation 9* obtained by rearranging *Equation 8*.

Equation 9 $$log_2\left(N_t/N_0\right) = t/\tau$$

This *growth phase* which also called *log phase* is the period of optimal population growth depending of the growth conditions. Eventually, however, when the growing population approaches the upper limit, the media runs out of nutrients and space. At this point, the bacterial population levels off and population growth becomes nearly 0 again. This stage, called the *stationary phase* and may last for a long period of time. The last stage of this life cycle is called the *death phase*. The waste and dead cells begin to accumulate and the population declines because of the lack of nutrients. Some species that are able to form spores can persist beyond this stage and can regenerate a population if conditions once again become favorable. In this study, the effect of H_2O_2 generated by the enzymatically catalyzed reaction of glucose on the lag phase of the bacterial growth were studied.

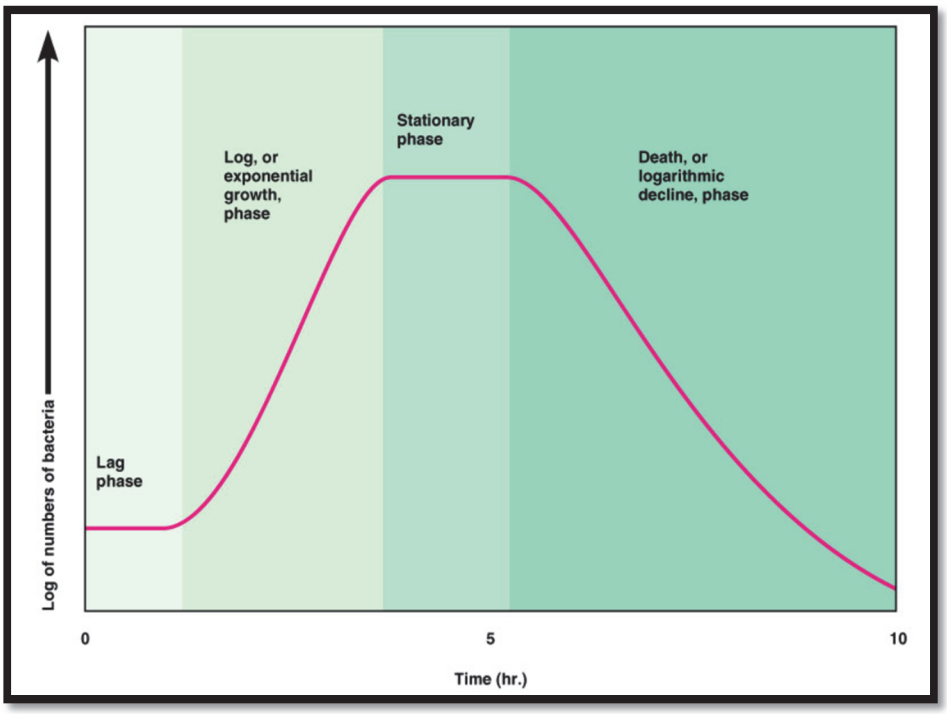

Figure 13. Life cycle of a bacterial growth (reproduced from reference 52).

1.7. Structure of the thesis

As mentioned in Section 1.1, the goal of this research is to develop a generic antibacterial platform that relies on the use of immobilized enzymes and can be applied to current paper production processes. The design, preparation and characterization of such a platform and its impact on the enzymatic activity is presented in the current study. This antibacterial platform was designed to trap GOx in microcapsules consisting of an alginate-calcium matrix. The enzymatic activity of GOx in the presence of its substrates (glucose and O_2) produces an antibacterial agent, H_2O_2, which leaches out of the microcapsules and decomposes pathogens in the media. In this regard, non-pathogenic bacteria, *E. coli* K-12, was proposed as a model. Since this platform is destined to be used in a laboratorial papermaking process (in future research) and it will be incorporated onto paper, it has to be structurally robust against mechanical stress. Therefore, a layer of chitosan was used to cover the surface of alginate microcapsules. Also, to be able to capture low amounts of pathogens on the surface of microcapsules and to increase the efficiency of the system, the immobilization of a given antibody (selective to a certain pathogen) was considered. Since antibodies against *E. coli* are expensive and available only in small amounts, human Immunoglobulin G (human IgG) was selected as a model antibody. It was assumed that developing a successful immobilization method for this model antibody, while maintaining the enzymatic activity of encapsulated GOx, could be applied to other antibodies with similar structure. After the preparation of this platform, its antibacterial properties against our model pathogen were investigated. It is important to note that the application of this antibacterial platform onto paper was not pursued in this research and will be the subject of the future studies.

As will be presented in following sections of this research, the encapsulation of GOx resulted in a reduction in its enzymatic activity. Therefore, we came up with the idea that immobilization of GOx on gold nanoparticles (NPs), before encapsulation, could possibly increase its enzymatic activity. The goal of this sub-project (Chapter 5) was to compensate the enzymatic activity loss during the encapsulation process and also to increase the encapsulation efficiency.

This thesis is composed of seven chapters. The current chapter includes an introduction to the scientific notions of this research and provides background knowledge for readers to be able to understand this project. The second chapter presents the detailed description of all materials, protocols, methods and the instruments with which the research was carried out. All the observations, measurements and data regarding the preparation of encapsulated GOx are brought to the reader in chapter three. The results and discussion regarding the study on antibacterial properties of our microcapsules are presented in chapter four along with the interpretations and discussions to justify those obtained results. Chapter five contains the data regarding the immobilization of GOx on gold NPs and the effect of this immobilization on the enzymatic activity. Since this part of the project is considered as a sub-project (additional to the main stream of the project), the introduction and experimental procedures for this part of the study are presented in the same chapter as the corresponding results and discussion. The sixth chapter presents the conclusion of this project and opens a window to the future possible works which lie ahead. Finally, the seventh chapter of this thesis provides all the implemented bibliographic references to support the ideas discussed in the thesis.

Chapter 2. Instruments and experimental methods

2.1. Enzyme encapsulation

The encapsulation of enzyme is achieved by ionotropic jellification of small droplets of alginate solution, which contain GOx. This process also involves laminar jet break-up of the solution. The encapsulation efficiency is then determined to evaluate the amount of encapsulated enzyme.

2.1.1. Laminar jet break-up encapsulation

2.1.1.1. Method

For the preparation of encapsulated enzyme, a laminar jet break-up[54] with a vibrational nozzle method of dispersion was used in combination with a further gelification of the encapsulation matrix as a stabilization method using the *Inotech Encapsulator® IE-50 R* (*Figure 14*) which is a semi-automated instrument for encapsulation of biomolecules and pharmaceutics. Setting different instrumental parameters helps us to control and determine the size of microcapsules (beads). The bead size varies from 100 µm to > 1000 µm in diameter according to the encapsulation parameters and the size of the nozzle with size dispersion of about 5 % in

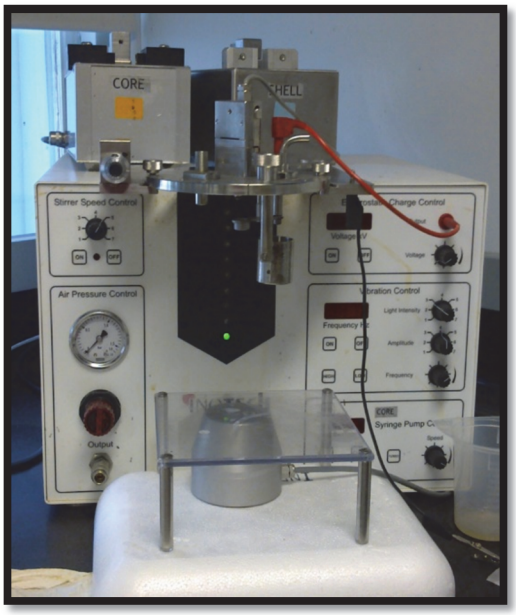

Figure 14. Inotech Encapsulator® IE-50 R.

terms of relative standard deviation. Bead production rate is rather high *i.e.* 50-3000 beads per second depending on the bead size and viscosity of the encapsulation-product mixture. This technique possesses low sheer stress which results in high cell viability when microorganisms undergo encapsulation. The schematic view of the *Inotech Encapsulator® IE-50 R*[54] is shown in *Figure 15*[54] along with presentation of different parts of the instrument. The encapsulation

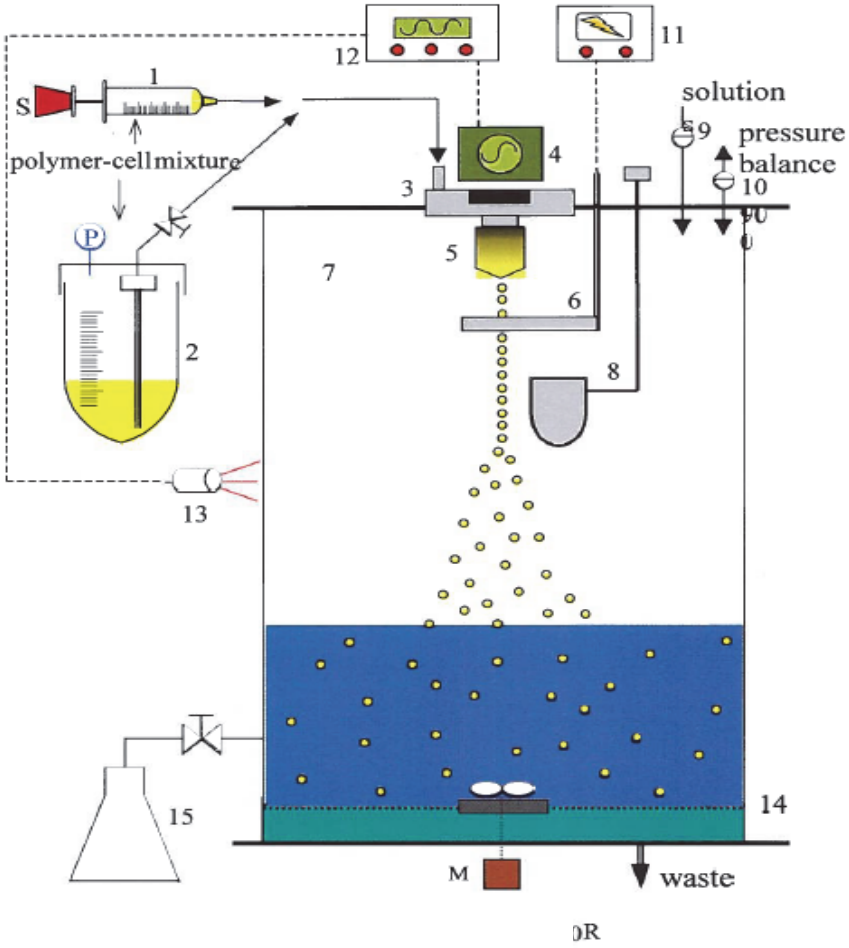

Legend:

1.	Syringe	2.	Product delivery bottle	3.	Pulsation chamber
4.	Vibration system	5.	Nozzle	6.	Electrode
7.	Reaction vessel	8.	Bypass-cup	9.	Liquid filter
10.	Air filter	11.	Electrostatic charge generator	12.	Frequency generator
13.	Stroboscope	14.	Filtration grid	15.	Bead collection flask
M.	Magnetic stirrer	P.	Pressure control system	S.	Syringe pump

Figure 15. Schematic representation of Inotech Encapsulator® IE-50 R (reproduced from reference 54).

solution is introduced into the system via a syringe pump with laminar flow before it reaches the vibrating nozzle the laminar flow is created. Thus, the flow is broken up resulting in the formation of microscopic droplets. Then these micro droplets are dispersed using an electrostatic field and incubated in the gelification bath (containing Ca^{2+} ions).

2.1.1.2. Materials

Alginic acid sodium salt from brown algae (low viscosity) and GOx from *Aspergillus niger* were purchased from Sigma-Aldrich and were used to prepare encapsulation matrix-enzyme mixture. Calcium chloride dihydrate ($CaCl_2.2H_2O$) from Sigma-Aldrich was used to prepare the jellification solution (bath). The water used in all procedures was purified by a MilliQ system to a resistivity of 18 MΩ.cm.

2.1.1.3. Protocol

A solution of alginate (0.7 m/v %) was prepared by dissolving sodium alginate in water along with stirring and heating under the boiling point to minimize evaporative losses. The encapsulation matrix-enzyme mixture was prepared by adding a weighed amount of GOx powder to alginate solution and then completing the solution to volume with water. The final concentration of enzyme in the mixture was set to be approximately 0.5 mg/ml (the exact concentration of the enzyme was measured in the encapsulation efficiency evaluation step). This mixture was then filtered using a Whatman nylon 5 µm filter before introduction to the Encapsulator instrument. The encapsulation parameters, which were optimized for the quality of beads and their dispersion, are given in *Table 2*. After the formation of microcapsule in calcium chloride bath, they were incubated for 30 minutes then they were simply filtered out using a vacuum Buchner funnel and filter paper followed by several rinsing steps using the calcium chloride solution (0.1 M).

Table 2. Glucose oxidase encapsulation parameters.

Encapsulation Parameter	**Value**	**Encapsulation Parameter**	**Value**
Syringe pump flow rate	2.6 ml/min	Electrostatic charge voltage	1.41 kV
Frequency	1376 Hz	Calcium chloride bath concentration	0.1 M

2.1.2. Encapsulation Efficiency

To evaluate the encapsulation efficiency, we needed to measure how much enzyme is encapsulated. Therefore, the Bio-Rad protein assay was used to analyze the protein content of the calcium chloride bath which is an indicator of the amount of GOx lost during the encapsulation process. Knowing the total amount of the enzyme introduced to *Inotech Encapsulator*®, we were able to calculate indirectly the encapsulation efficiency.

2.1.2.1. Method for protein assay

The Bio-Rad protein assay is a method for the determination of solubilized protein based on the method of Bradford[55] that involves the addition of an acidic dye to the protein solution and the formation of protein-dye complex that absorbs light maximally at a different wavelength than its unbound form. The absorbance of light is linearly proportional to the concentration of the complex, which correlates to the concentration of protein in a given solution. In this case, the complex forming dye is Coomassie® Brilliant Blue G-250 (*Figure 16*) and its maximum absorbance wavelength shifts from 465nm to 595 nm once it is bound to proteins. The unbound form of the dye has three charge states: cationic form (red), neutral form (green) and anionic form (blue). However, when it binds to protein, it is converted to a stable un-protonated anionic blue form (λ_{max}=595 nm). It has been found that Coomassie blue primarily binds to aromatic and basic amino acid residues especially arginine[56]. In this method the calibration curve can be obtained using Bovine Serum Albumin (BSA) and provides us with a linear range of 0.04 to 0.2

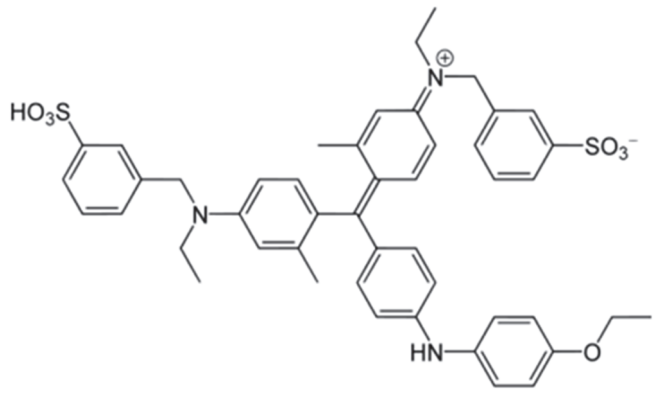

Figure 16. Coomassie® Brilliant Blue G-250. The protein complexation dye in Bradford protein assay.

mg/ml or using Bovine Gamma Globulin with a linearity ranging from 0.04 to 0.3 mg/ml[57]. These concentrations refer to the final concentration of the protein in the spectrophotometric cell. In our study since no standard solution is commercially available for GOx, we chose BSA as the protein standard for the calibration curve.

2.1.2.2. Materials

Protein assay dye reagent concentrate was purchased from Bio-Rad Laboratories, Inc. and BSA protein micro standards (1 mg/ml) from Sigma-Aldrich.

2.1.2.3. Protocol

Dye reagent was prepared by diluting 1part dye reagent concentrate with 4 parts MilliQ water. Three to five diluted stock solutions of BSA standard were prepared ranging from 0.2 to 0.9 mg/ml and 100 µl of each standard solution is added to 5.0 ml of the dye reagent and then vortexed for a few seconds. These solutions were incubated at room temperature for at least 5 minutes (but not for more than one hour) and their absorbance was measured using a Varian Cary 100 Bio UV-Vis Spectrophotometer at λ=595 nm. Sample preparation was carried out similarly and to prepare the blank sample 100 µl of calcium chloride (0.1 M) was added to dye reagent to represent the matrix of calcium bath.

2.2. Modification of alginate microcapsules with chitosan

2.2.1.1. Method

Taking the affinity of chitosan for alginate to our advantage, we were able to cover microcapsules with an extra layer of chitosan. Different methods are available for such modification. One of these methods is simple incubation of microcapsules in a solution of chitosan (0.15 % w/v) in acetate buffer (50 mM) pH 5.0 containing calcium chloride (0.1 M)[33]. The high concentration of calcium cations in the incubation solution stabilizes microcapsules and prevents their rupture resulting from diffusion of calcium from microcapsules out to the solution.

2.2.1.2. Materials

Acetate buffer was prepared using sodium acetate trihydrate ($CH_3COONa.3H_2O$) that was purchased from American Chemicals Ltd. and glacial acetic acid A.C.S. reagent from J.T.Baker. Chitosan, medium molecular weight (deacetylation degree of 75-85 %) was purchased from Sigma-Aldrich.

2.2.1.3. Protocol

A solution of chitosan (0.15 % w/v) in acetate buffer (50 mM) pH 5.0 containing calcium chloride (0.1 M) was prepared by dissolving chitosan and calcium chloride in acetate buffer with vigorous shaking for at least 45 minutes. Then approximately 6.0 g of microcapsules were added to 200 ml chitosan solution and allowed to incubate overnight. Microcapsules were then recovered on filter paper using a vacuum Buchner funnel and washed with calcium chloride solution (0.1 M) and stored at 4˚C for further analysis.

2.3. Microcapsule characterization

Confocal laser scanning microscopy (CLSM) was used to take fluorescent images of the microcapsules. To do so, chitosan must be labeled with fluorescein isothiocyanate (FITC), a very common fluorophore that can easily react with amino groups on chitosan structure (*Figure 17*). Also to determine the presence of nitrogen that originates from chitosan in the composition of alginate-chitosan microcapsules (without encapsulated GOx), Elemental Analysis technique was used.

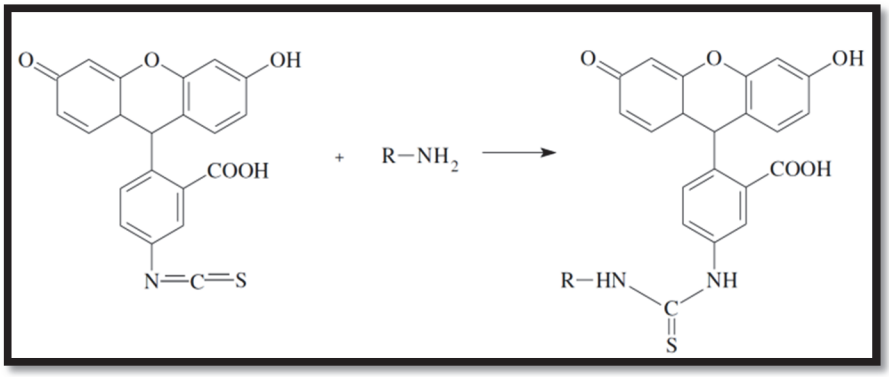

Figure 17. Fluorescein isothiocyanate (FITC) reaction with amino groups.

2.3.1. Imaging methods

2.3.1.1. Optical imaging

Traditional optical transmission images were taken using a MOTIC BA310 optical microscope.

2.3.1.2. Confocal laser scanning microscopy imaging

Confocal laser scanning microscopy (CLSM) is a useful imaging technique that has the ability to produce images from different depths of a thick sample. The images are taken point by point and out-of-focus information is eliminated resulting in high resolution 3D images. The CLSM technique was developed by Marvin Minsky in 1957[58] and grew in popularity over the proceeding decades thanks to advances in laser technology and computer science. The fluorescence signal is greatly improved since an intense laser or arc-discharge source is usually used for excitation which improves fluorescence emission intensity. The detector for such devices is usually a photomultiplier tube (PMT) which has high quantum efficiency in the near-UV, visible and near IR.

2.3.1.2.1. Materials

Fluorescein isothiocyanate (FITC) Isomer I was purchased from EMD Chemicals.

2.3.1.2.2. Method

In our research, a Leica TCS SP5 II CLSM[58] equipped with three point laser sources controlled by high speed acousto-optic tunable filters was used which is schematically shown in *Figure 18*[58] . The excitation laser sources for this device include helium neon (λ=633 nm), diode-pumped solid state (DPSS: λ=561 nm), and argon ion (λ=458/488/514 nm). The source that we used for our study was the 488 nm argon ion line and the emission signal was captured at 500 nm. These excitation and emission wavelengths are standard for fluorescein isothiocyanate (FITC), which was our fluorophore label.

In order to label chitosan with fluorescein isothiocyanate (FITC), a certain amount of chitosan was dissolved in acetic acid 0.1 M to reach the final chitosan concentration of 1 % m/v. The use of acetic acid allowed us to dissolve chitosan in an aqueous solution. FITC was dissolved in anhydrous methanol (2 mg/ml) and in order to react FITC with chitosan, 50 ml of FITC in methanol solution was added to 100 ml of the aforementioned chitosan solution along with addition of an extra 100 ml of anhydrous methanol. This mixture was agitated in the dark for three hours. Precipitation of FITC- tagged chitosan was done using a 1 L of NaOH solution (0.1 M) then dissolved in acetate buffer (5mM at pH 5.0) followed by a dialysis process in the same buffer during three days at 4˚C and by changing the dialysis solution twice per day to remove the excess amount of FITC .The recovered FITC-labeled chitosan solution was used to cover our microcapsules through procedure described in Section 2.2.1.1.

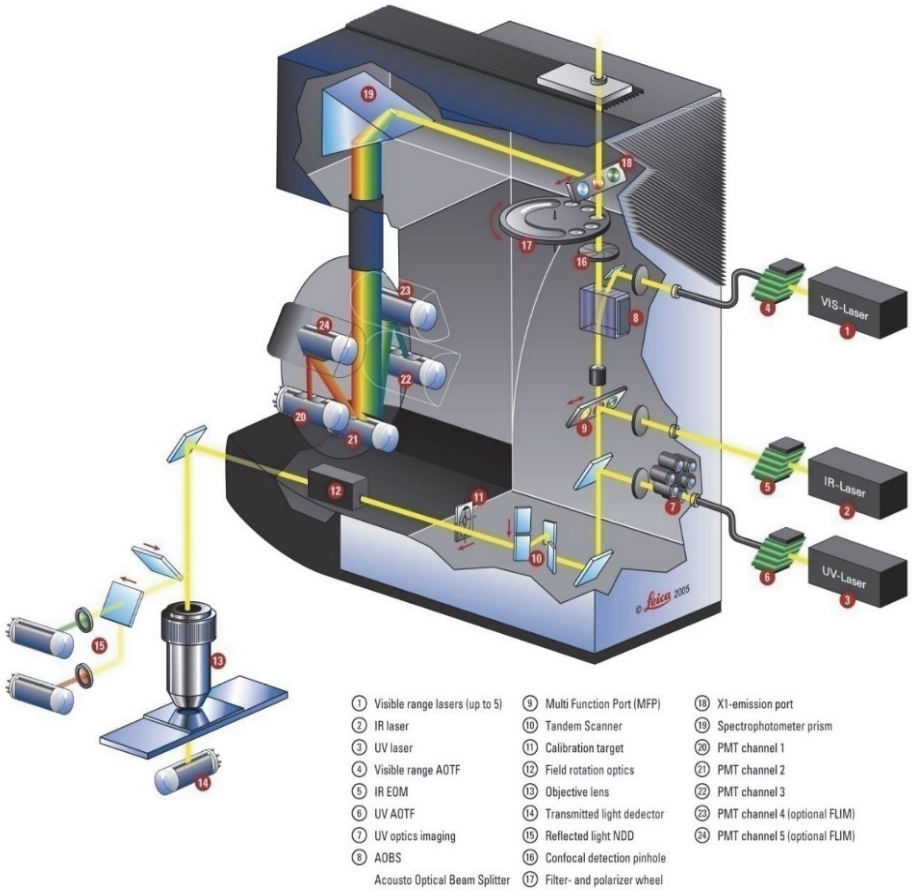

Figure 18. Confocal laser scanning microscope Leica TCS SP5(reproduced from reference 58).

2.3.2. Elemental analysis

Elemental analysis was used to determine the elemental composition of a substance which can provide us the percentage of the elements, C/H/N/S, with a good precision. The analysis was performed at Laboratory *of elemental analysis, Département de chimie, Université de Montréal* using EAS1180, Fisons instruments S.p.A.[59]

2.4. Antibody Immobilization

In this study, human immunoglobulin G (IgG) was used as a model antibody to verify the possibility of antibody immobilization onto the external surface of the designed microcapsule-based platform. The choice of this model antibody was made according to its availability and cost since an IgG specific for our model pathogen, *E. coli*, was not available in large quantities with a reasonable cost. The chosen immobilization method is a covalent coupling reaction using glutaraldehyde.

2.4.1. Method

Glutaraldehyde covalent coupling method could be used to immobilize antibodies on alginate-chitosan microcapsules. Glutaraldehyde (Pentane-1, 5-dial) is one of the most well-known and easy to handle agents for protein cross linking that has been used in many fields of research and science. The reactivity of glutaraldehyde toward protein originates from the reaction between glutaraldehyde's single linear molecular form (because in an aqueous solution, glutaraldehyde can form a cyclic hemiacetal as well as dimers, trimers, etc.) and several reactive functional groups residues on the body of protein. In fact, glutaraldehyde can react with amine, thiol, phenol and imidazole groups on amino acid side-chains[60]. It is also a simple and mild coupling agent to immobilize biomolecules (enzymes and antibodies) on water insoluble carriers because the reaction happens in aqueous buffer solution under conditions close to physiological pH. Different possible reactions between proteins and glutaraldehyde are summarized in *Figure 19*[60].

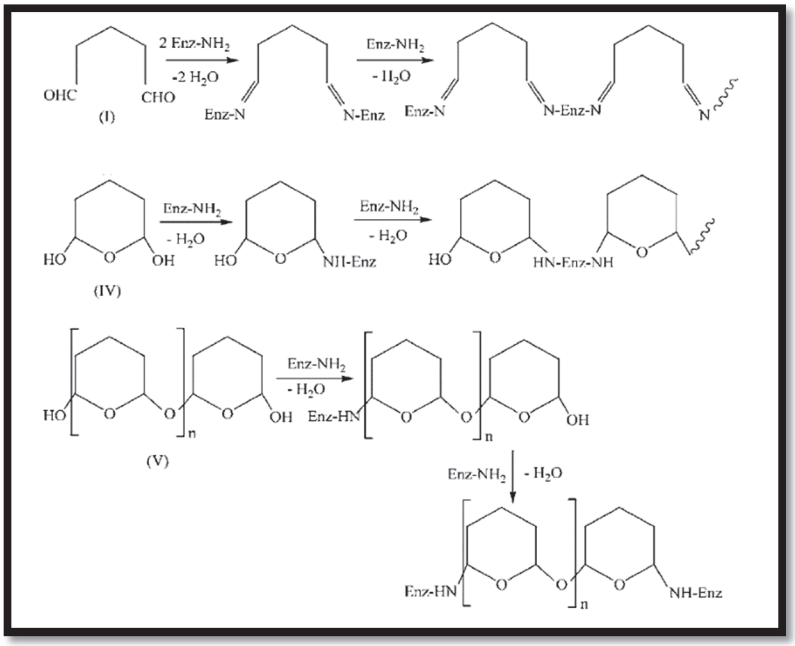

Figure 19. Reactions of glutaraldehyde with proteins under acidic or neutral conditions. The labels I, IV and V refer to different forms of glutaraldehyde in the original document. I: Monomer (single molecular from). IV: Cyclic hemiacetal form. V: Polymeric species of cyclic hemiacetal form (reproduced from reference 60).

The glutaraldehyde coupling reaction has three different main steps[61]. In the first step our alginate-chitosan microcapsules are incubated with glutaraldehyde to activate the amino groups of chitosan. Ideally glutaraldehyde molecules are attached to the surface of microcapsules via one of its formyl group (formation of imine bond) while the other end is free for the next step of immobilization process. The second step includes the incubation of glutaraldehyde-activated microcapsules with human IgG as a model antibody. In this step the incubation solution must contain calcium ions to prevent the swelling of microcapsules as a result of calcium ions removal from microcapsules by the antibody because calcium ion tends to bind to the antibody while reducing its immunoaffinity. Adding 5 mM as the maximum concentration of calcium ion in the reaction buffer prevents stability loss of microcapsules but maintains the affinity of the antibody[61]. In the final step, unreacted free ends of glutaraldehyde are end-capped with glycine to reduce the risk of unwanted crosslinking reactions. A schematic presentation of these steps are shown in *Figure 20*.

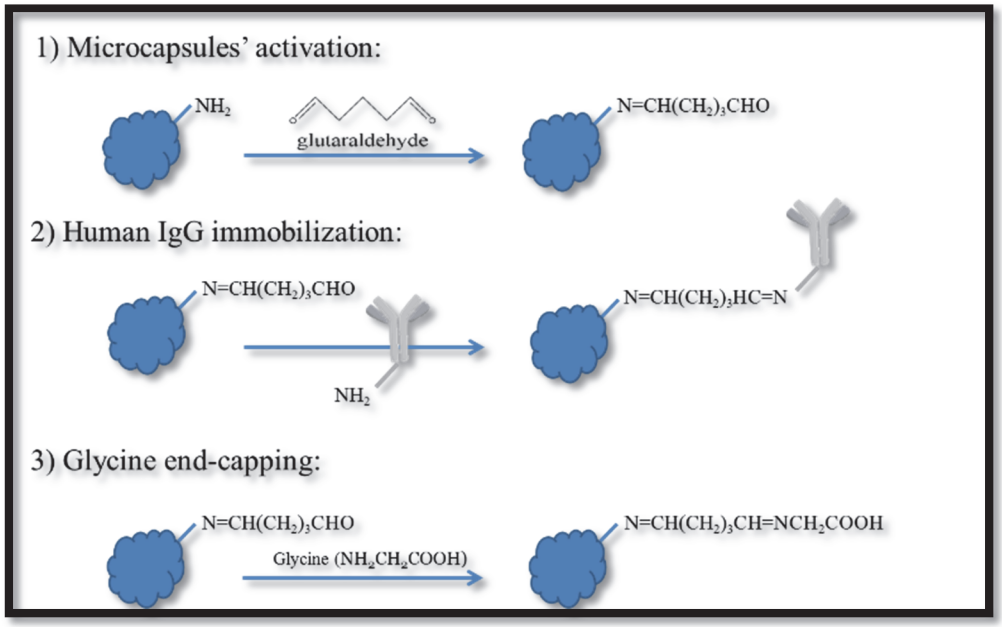

Figure 20. Different steps of antibody immobilization on alginate-chitosan microcapsules.

2.4.2. Materials

Anhydrous sodium tetraborate ($Na_2B_4O_7$), sodium chloride, glycine ($C_2H_5NO_2$), glutaraldehyde solution grade I, 50 % ($C_5H_8O_2$) were all supplied by Sigma-Aldrich. IgG from human plasma (MW=150 kDa) was purchased from Athens Research & Technology, Inc.

2.4.3. Protocol

A mass of 0.50 g of microcapsules (previously dried on filter paper) was added to 2 ml of borate buffer (0.1 M) pH 7.2 containing $CaCl_2$ (5 mM) and glutaraldehyde (0.25 % w/v) and stirred at room temperature for 60 min. Microcapsules were then filtered out on filter paper using a Buchner funnel and rinsed 4 times with 3 ml of borate buffer (0.1 M) pH 7.2 containing $CaCl_2$ (5 mM) to remove the excess amount of glutaraldehyde completely. Glutaraldehyde-activated microcapsules were added to a solution of the same buffer containing $CaCl_2$ (5 mM) and human IgG (0.2 mg/ml) and stirred at 4˚C. After 60 min, 0.05 ml of glycine solution (1 M) was added and incubated for another 60 min. Finally, microcapsules were filtered out and rinsed once with NaCl (0.5M) and three times with 3 ml borate buffer (0.1 M) pH 7.2.

2.5. Antibody immobilization confirmation

2.5.1. Method

To check if covalent binding of the antibody was successful, the Matrix Assisted Laser Desorption/Ionization-Time of Flight Mass Spectrometry (MALDI-TOF-MS) technique was used. Laser desorption/ ionization (LDI) technique was invented half a century ago. It is a technique in which the dry sample is hit by a high intensity laser beam that results in desorption and ionization of the sample for further analysis by the analyzer component of the mass spectrometer. Its drawback in comparison with other similar desorption techniques such as field desorption (FD), plasma desorption (PD) and fast atom bombardment (FAB) is that its application is limited to low-mass organic salts and light-absorbing organic molecules and a tremendous effort was needed to desorb and ionize biomolecules especially when their mass exceeds 2000 Da. To fix this problem, large biomolecules were co-crystallized with an organic compound (differs for the type of biomolecule) which facilitates the desorption process and increases the rate of ionization. This laser desorption technique assisted by an organic matrix, MALDI along with a time of flight mass analyzer is capable of producing mass spectra of biomolecules and polymers of a few 100,000 Da.[62]

2.5.2. Protocol

A solution of sinapinic acid (20 mg/ml) in 1:1 acetonitrile: 0.2 % v/v trifluoroacetic acid (TFA) in water was prepared and used as the matrix material. On the MALDI plate, microcapsules were sandwiched between two layers of matrix since they were not soluble. First the surface of the allocated place on the plate was covered with the matrix (approximately a few microliters). After letting it dry for a couple of minutes, microcapsules were added on to the dried matrix. The amount of added microcapsules was not necessarily known. After drying, a few more small droplets of the matrix were added on top of microcapsules. The MALDI-TOF-MS experiment was carried out using Burker's Ultraflex TOF/TOF instrument with laser intensity of 70 %. Data acquisition was made in the m/z range of 20,000 to 350,000 Da, all in positive polarity mode with 7500-20000 laser pulses at each shot. At least 30 shots were made randomly on the surface of the samples, for each analysis. The samples analyzed by this

experiment were microcapsules with and without immobilized human IgG, all without encapsulated GOx.

2.6. Activity measurements

The enzymatic activity can be calculated by measuring the initial rate of oxidation reaction of glucose which is catalyzed by GOx enzyme. The oxygen content of a solution in a closed system decreases in the presence of GOx and its substrate, glucose. This diminution of oxygen content can be followed by various techniques, one of which is the oxygen electroanalytical technique.

2.6.1. Method

To measure GOx activity, the oxygen electroanalysis technique was used by plotting the percentage of dissolved oxygen content versus time in a closed *Clark-Cell* oxygen electrode containing glucose and encapsulated GOx. This electrochemical sensor for oxygen is based on the reduction of O_2 on a Pt electrode and it is named after his inventor Leyland C. Clark (1959). To measure the partial pressure of oxygen in gas phase or in dissolved form, this electrochemical sensor has widely been used in environmental studies, in bacterial attack progression monitoring in sewage water treatments, in monitoring and controlling the O_2 level in fermentation of alcoholic beverages as well as in medicine in monitoring of physiological analytes[63]. The detection range of dissolved O_2 for this device varies from 2.84 µM (*i.e.* 0.01 %) to 284 µM (*i.e.* 100 %) at 25˚C. The main advantage of *Clark-Cell* oxygen electrode for O_2 detection is that its membrane is gas-permeable but not ion-impermeable which separates the system from the sensing platinum electrode (cathode). This important role of the membrane prevents electrode passivation and poisoning resulting from a direct contact in cases where the sensing electrode is placed inside the system[64].

The different parts of the *Clark-Cell*[64] device are schematically shown in *Figure 21*. The device is comprised of two electrodes. The working electrode (cathode) is a platinum disc, 2 mm in diameter covered with a membrane. O_2 diffuses through the membrane and is reduced at the surface of this electrode. The counter and reference electrode is a silver ring with a surface

ten times larger than that of the platinum electrode and the conduction between these two electrodes is achieved with a solution of NaCl (3 M) which saturates a tissue paper covering the two electrodes. The gas-permeable membrane is made of Teflon with a thickness of 12.7 µm. By applying a potential to the cathode, diffused O_2 is reduced (*Equation 10*) at the surface of platinum and a current flows between two electrodes which is proportional to the partial pressure of O_2 in the system. The oxidation reaction on silver anode and the overall electrochemical reaction is given in *Equation 11* and *Equation 12*, respectively.

Equation 10 $$O_2 + 2H_2O + 4e^- \rightarrow 4OH^-$$

Equation 11 $$Ag + Cl^- \rightarrow AgCl + e^-$$

Equation 12 $$4Ag + O_2 + 2H_2O + 4Cl^- \rightarrow 4AgCl + 4OH^-$$

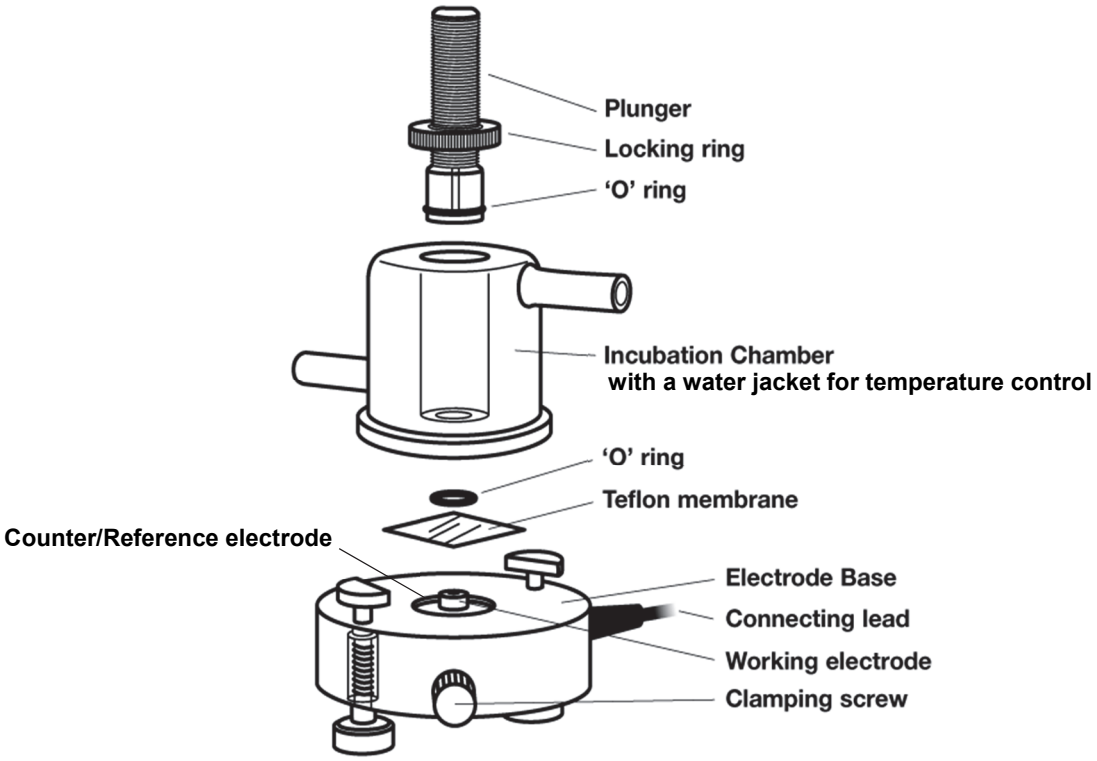

Figure 21. Schematic view of Clark-Cell oxygen electrode (adapted from reference 64).

2.6.2. Materials

D-(+)-Glucose ($C_6H_{12}O_6$), ACS grade reagent was purchased from Sigma-Aldrich. The same materials were used to prepare acetate buffer as described in Section 2.2.1.2.

2.6.3. Protocol

A solution of glucose (100 mg/ml), the substrate for GOx, was prepared in acetate buffer (50 mM) pH 5.0. For each activity measurement, either for free enzyme or encapsulated enzyme, 2.0 ml of the glucose solution was diluted with 3.0 ml of acetate buffer in *Clark-Cell* oxygen electrode then the enzyme was also added to the solution chamber. The percentage of oxygen was plotted versus time and the slope of the liner region of the plot was taken in to consideration as the initial rate of the oxidation reaction. Throughout this thesis, the uncertainty for each measured data is reported as ± standard deviation (SD).

2.7. Bacterial growth inhibition

Preliminary studies on bacterial growth inhibition properties of the designed platform were carried out using *E. coli* K-12 as a model pathogen and cultivating them on a petri dish. Then the effect of enzymatic activity on the bacterial growth was studies in more detail by measuring the optical density of the bacteria culture media.

2.7.1. Bacterial growth on petri dish

2.7.1.1. Method

The bacteria were spread uniformly on Luria-Bertani (LB) broth culture media[65] containing agar gel in a petri dish and any antibacterial agent which is to be tested is placed on the central spot on a paper disc. In such a culture system, bacteria will grow on the surface of the gel while making the gel turbid except over the regions in which there exists some antibacterial effect. So anti-bacterial region stays more transparent comparing with the turbid surface of the agar gel.

2.7.1.2. Materials

All materials needed to prepare bacteria's culture media were used at bacteriological grade and purchased from Bioshop Canada Inc.

2.7.1.3. Protocol

The LB broth culture media is made by adding tryptone (10 g), yeast extract (5 g) and NaCl (10 g) to some MilliQ water followed by pH adjustment to 7.0 with NaOH (5 M) and volume adjustment to 1 L. Then the broth was autoclaved at 121 ˚C for 25 minutes.

Sterilized warm LB broth culture media containing 2 % agar gel and 10% glucose was poured in a petri dish and cooled to room temperature. Then 100 µl of a saturated solution of *E. coli* K-12 (made by adding some bacteria to LB broth culture media and incubating at 37 ˚C for 16 hours) was added on to the gel and spread uniformly to create a carpet-like layer of bacteria. A certain mass of microcapsules with encapsulated GOx (and microcapsules without encapsulated GOx for the control sample) was spread on a piece of sterilized paper disc (d=1.6 cm). This paper was placed in the center of the petri dish and subsequently, the petri dish was incubated at 37 ˚C for 16 hours.

2.7.2. Optical density measurements for bacterial growth in Luria-Bertani broth

2.7.2.1. Method

LB broth culture media is one of the richest culture media for bacteria and provides essential nutrients for them to grow fast and also with a good growth yield. This culture medium is commonly used in steady-state bacterial growth researches and exhibits a high level of reproducibility. During steady-state growth studies (the middle linear section of the second stage of the bacteria life cycle as presented in Section 1.6.1), it is assumed that all intrinsic properties of the cells such as the mean volume, mass, density and the macromolecular composition of the cells remain constant and all extrinsic parameters such as optical density of the culture medium, the number of cells per milliliter, the protein content per milliliter, etc. increase doubly at the

same doubling time for reproduction of cells for instance, the doubling time for *E. coli* K-12 in LB broth culture media is 20 minutes. The ambient parameters such as temperature, pH and the composition of the medium also need to be kept constant.[66]

2.7.2.2. Materials

All materials needed to prepare bacteria's culture media were used at bacteriological grade and purchased from Bioshop Canada Inc.

2.7.2.3. Protocol

Each bacteria culture was done in a sterilized 250 ml- Erlenmeyer flask by adding 95 ml of LB broth culture media, 5 ml of glucose (40 % w/v) in addition to the desired amount of GOx or microcapsules and the number of *E. coli* K-12 to initiate the bacterial growth. Then the Erlenmeyer flask was sealed and incubated at 37 ˚C under agitation. The optical density of each batch was measured by transferring 1 ml of the culture media in to a disposable cuvette and reading the absorbance (turbidity measurements) at λ=600 nm by Cary 100 Bio UV-Vis Spectrophotometer. All manipulations were done in the vicinity of a flame to ensure the absence of other bacterial contaminations.

Chapter 3. Enzyme encapsulation

3.1. General objectives

As previously mentioned in Section 1.1, the goal of the project is to develop an antibacterial platform that can be applied to current paper production processes, which has the ability to capture pathogens on its surface and to deactivate them by producing an anti-pathogenic agent. To achieve this goal, the first phase of this research included the preparation of alginate microcapsules and the encapsulation of GOx at the same time. Then the surface of these microcapsules had to be functionalized by chitosan. Finally, the possibility of immobilizing human IgG (our model antibody) on the external surface of the alginate-chitosan microcapsules was evaluated. Control experiments were performed to confirm the successful modification of microcapsules after each step and the activity of GOx was also monitored after each modification to ensure that the enzyme is still active. So this chapter contains the result and discussion regarding all aforementioned steps.

3.2. Size distribution of microcapsules

Alginate microcapsules were transferred onto a microscope slide and were observed using conventional light microscopy (*Figure 22*). A sample of 234 microcapsules were examined statistically to find their size distribution. The size distribution, which was manually measured using the scale provided by the microscope, is presented in *Figure 23* and an average diameter

Figure 22. Optical microscopy image of alginate microcapsules.

of 120±20 µm was found for microcapsules prepared using the microencapsulation conditions described in Section 2.1.1.3. In *Figure 22* microcapsules appear to be collapsed, which is due to the mechanical pressure of the microscope slide cover.

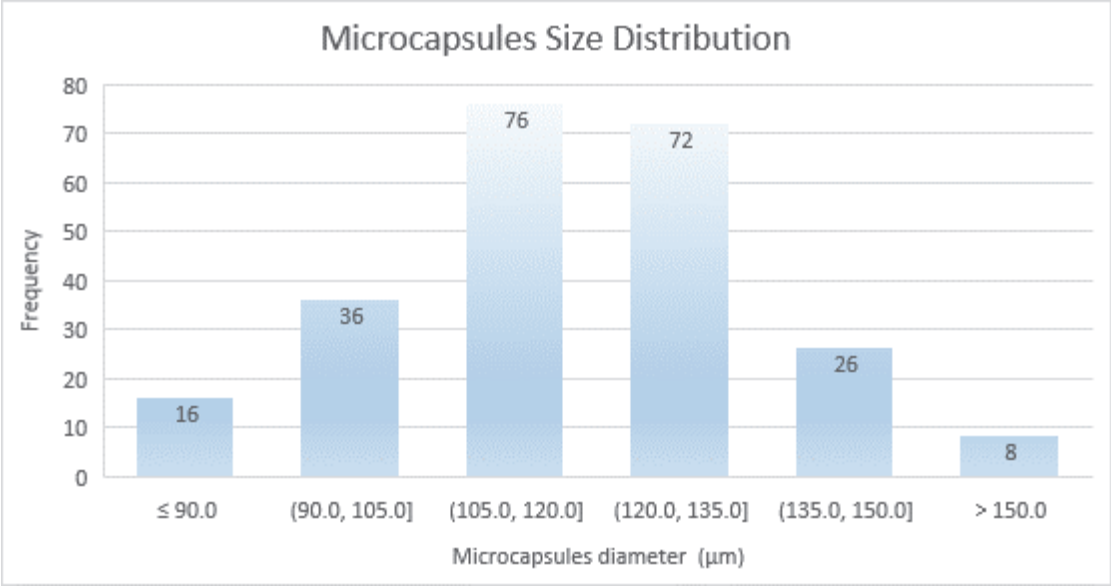

Figure 23. Histogram of microcapsules size distribution.

3.3. Encapsulation efficiency

The encapsulation efficiency in our study is defined as the percentage of enzyme encapsulated in comparison with the total amount of enzyme introduced to the Encapsulator (see Section 2.1.1.1). For each preparation of a batch of microcapsules, the total amount of the enzyme (GOx) was obtained be measuring the flow rate and the time during which the encapsulation solution (GOx in aqueous sodium alginate) was poured into the calcium chloride bath. From this total amount of enzyme, inevitably, some of it is dispersed in calcium chloride bath once each small droplet reached the bath. Another portion of the enzyme diffused out of microcapsules in early stages of encapsulation process where the wall thickness of microcapsules was not thick enough to prevent the diffusion of enzyme molecules due to the time required for calcium ions to get incorporated into microcapsules' wall network. Therefore, until the wall thickness reached its maximum, some of the enzyme passed through the pores of

microcapsules' wall. To determine the loss of enzyme in the calcium chloride bath, a Bradford protein assay was used to quantify the protein content of the bath. A typical calibration curve using BSA (bovine serum albumin) as the standard is shown in *Figure 24*. The amount of encapsulated enzyme was simply calculated by subtracting the amount of enzyme found in calcium chloride bath from the total amount of the enzyme introduced to the system. Using the aforementioned approach, the encapsulation efficiency was found to be 47 % in optimal conditions *i.e.* for a solution of GOx (0.5 mg/ml) in sodium alginate (7 % w/v) and formation of microcapsules in calcium ion bath (0.1 M)*.

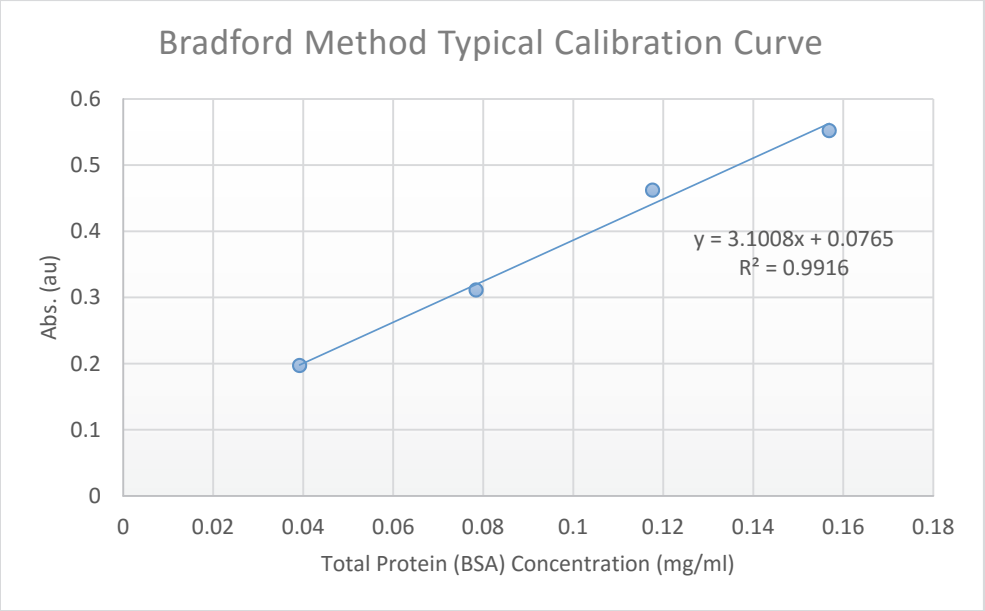

Figure 24. A typical Bradford assay calibration curve using BSA as the standard. The concentration values refer to the total protein concentrations in spectrophotometric cell.

3.4. Chitosan modification

Alginate, the main component in the structure of microcapsules, does not contain a significantly active functional group that can easily serve for further modification of microcapsules *i.e.* immobilization of antibody. That is why we decided to cover our microcapsules with a layer of chitosan. As described in Section 1.4.1, chitosan possesses amino

* The Data was obtained previously in Dr. Rochefort's group by a summer intern.

groups that can be protonated at acidic pH. Thus these amino groups carry positive charges which creates an ionotropic affinity for negatively charged carboxyl groups of alginate. Simple incubation of microcapsules in chitosan will form a layer of chitosan on the surface of alginate microcapsules. Another advantage of this extra layer is that the rigidity of microcapsules increases and they become more resistant in the presence of mechanical stress however, the porosity of microcapsules is reduced after the addition of chitosan layer[67].

To confirm a successful chitosan coverage of microcapsules, elemental analysis was carried out on empty alginate-chitosan microcapsules. The result of this analysis is given in *Table 3*. The presence of 0.54 % nitrogen is a confirmation of successful chitosan coverage because the only substance which contains nitrogen is chitosan because alginate does not have any nitrogen in its structure.

Table 3. Elemental analysis result on alginate and alginate-chitosan microcapsules.

Sample	**Nitrogen (%w/w)**	**Carbon (%w/w)**	**Hydrogen (%w/w)**
Alginate microcapsules	0	40.91	4.54
Alginate-chitosan microcapsules	0.54	29.07	4.75

To further confirm the coverage of alginate microcapsules by chitosan, it was suggested that chitosan be labeled with the fluorophore, fluorescein isothiocyanate (FITC). Therefore, chitosan was first derivatized with FITC and consequently used to cover alginate microcapsules. Apparently, despite FITC reacted the amino groups on the structure of chitosan, there existed some unreacted amino groups that could interact with alginate on the body of microcapsule. Both transmission and fluorescent images were taken using confocal laser scanning microscopy (CLSM) (see Section 2.3.1.2.2) and the images are presented in *Figure 25*. The fluorescent signal from FITC-labeled chitosan in *Figure 25b* is a confirmation of the attained chitosan coverage. However, microcapsules appeared to be collapsed due to the mechanical pressure of the microscope slide cover.

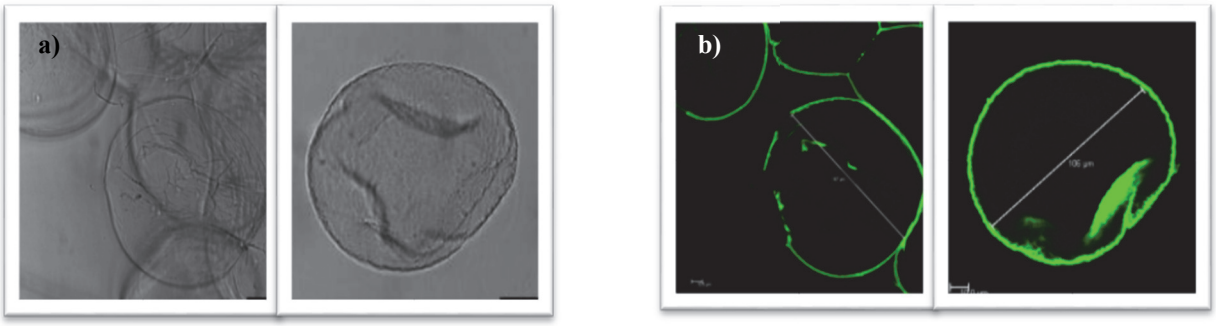

Figure 25. CLSM transmission images (a) and fluorescent images (b) of alginate microcapsules covered with FITC-labeled chitosan.

3.5. Antibody immobilization

To investigate the possibility of antibody immobilization on microcapsules, human immunoglobulin (IgG) was chosen as a model antibody with glutaraldehyde as the coupling agent as mentioned in Section 2.4.1. Keeping the concentration of calcium ion at 5 mM in these steps was needed to prevent the disassembly of microcapsules caused by the loss of calcium ions that bind the alginate chains together. According to the literature, this amount of calcium ions is low enough not to reduce the immunoaffinity of IgG[61].

The immobilization of human IgG was tested using MALDI-TOF-MS. First, analysis was carried out on a sample of pure human IgG and the mass spectra is shown in *Figure 26*. Two characteristic peaks, one at ~150 kDa attributed to m/z of singly charged protonated IgG $[M+H]^+$, and another one at ~75 kDa attributed to m/z of doubly protonated IgG $[M+2H]^{2+}$ (*Figure 26a*). The very small peak observed at ~100 kDa remains unidentified. The same analysis on underivatized microcapsules shows a broad peak, typical for polysaccharides resulting from different polymeric chains of alginate with different lengths, which appear at many different and overlapping values of m/z (*Figure 26b*). The analysis of microcapsules with human IgG immobilized on their outer surface with MALDI-TOF-MS is shown in *Figure 26c* and depicted the presence of both characteristic peaks (the broad peaks for alginate and the pair of narrow peaks for the IgG) in the spectrum. It was quite important that MALDI-TOF-MS signal come from the antibody that is covalently attached to microcapsules and not those bound

non-specifically via adsorption which could possibly give a false positive signal. To make sure of the absence of non-covalently bound antibody on the surface of microcapsules, a control sample experiment was carried out by omitting the linking agent (glutaraldehyde) from the

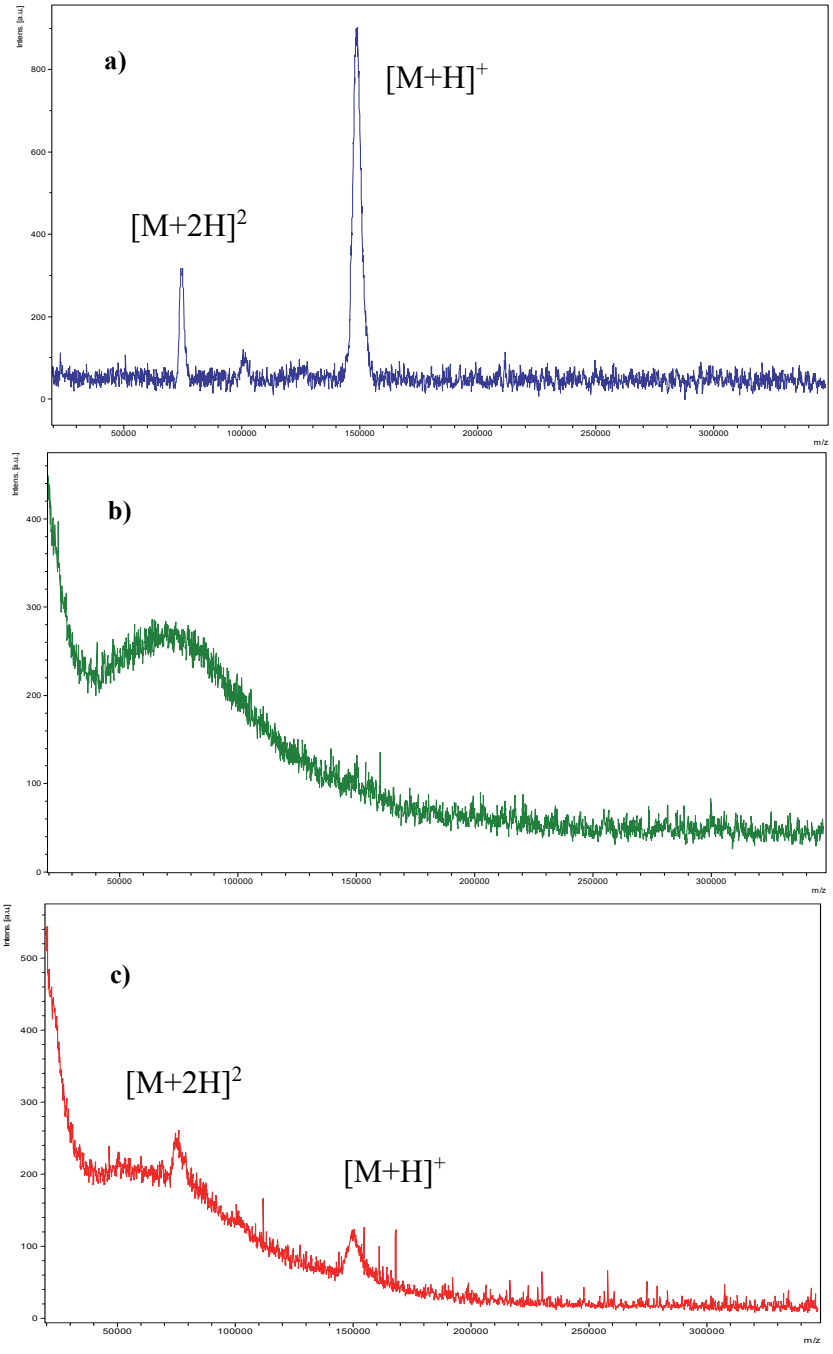

Figure 26. MALDI-TOF-MS spectra of human IgG (a), alginate microcapsules (b) and human IgG immobilized on alginate microcapsules (c).

immobilization reaction process. The obtained MALDI-TOF-MS spectrum was identical to that of bare microcapsules confirming that the antibody is attached covalently (results not shown).

3.6. Activity measurements

Our goal is to maintain the activity of the enzyme after encapsulation of GOx and also after each modification step. By definition, the activity of an enzyme in terms of a "Unit (U)" is defined as the μmoles of substrate consumed in one minute. "The specific activity" is defined as the activity of the enzyme in units per one gram of enzyme's protein content, *i.e.* U/g. The activity measurements were carried out using the oxygen electro-analysis technique described in Section 2.6. So for each activity measurement, a certain amount of microcapsules was carefully weighed and transferred to the oxygen electrode cell. It was assumed that all our solutions were naturally saturated with oxygen, *i.e.* 284 μM at 25˚C . The solution in the cell was buffered with acetate buffer (50 mM, pH 5.0) and an excess amount of glucose (50 mg/ml) was added. The *Clark-Cell* electrode monitors the percentage of oxygen as a function of time. As predicted, the amount of oxygen stayed constant before the addition of glucose which is a proof that the signal is stable and also that the instrument works well. The oxygen content started to decrease after the addition of glucose and the initial slope of this curve, where the substrate (oxygen) existed in a high concentration, indicated the initial rate of the reaction. According to the notions explained in Section 1.5.3, the initial rate of the reaction has the maximum value of reaction rate that is also proportional to the concentration of the enzyme. The slope of the curve (% of oxygen versus time) stays constant as long as the reaction rate stays constant. This slope, which is in fact the $\frac{d[O_2\ \%]}{dt}$, can easily be converted to the $\frac{d(\mu mol\ of\ glucose)}{dt}$ by knowing the stoichiometry of the reaction and also knowing the total amount of dissolved oxygen at 100 % of saturation at the temperature of the experiment as follows. According to the stoichiometry of the glucose oxidation reaction, the glucose to O_2 ratio is 1:1; therefore, the enzymatic activity in terms of consumed μmoles of glucose is equal to that for μmoles of O_2. Also knowing that at 25˚C, the concentration of dissolved O_2 in a saturated solution is 284 μM, the slope can be transformed in to the $\frac{d(\mu mol\ of\ O_2)}{dt}$ as shown in *Equation 13*, where V is the total volume of the solution in the oxygen electrode cell in milliliters. A typical curve showing the rate of oxygen

consumption is given in *Figure 27*. Control experiments were conducted with empty microcapsules (*i.e.* without GOx) and no reduction in oxygen content was observed, confirming that the presence of GOx is needed to reduce the O_2 content.

Equation 13

$$\frac{d(\mu mol\ of\ O_2)}{dt} = \frac{284V}{1000} \times \frac{d(\%O_2)}{dt}$$

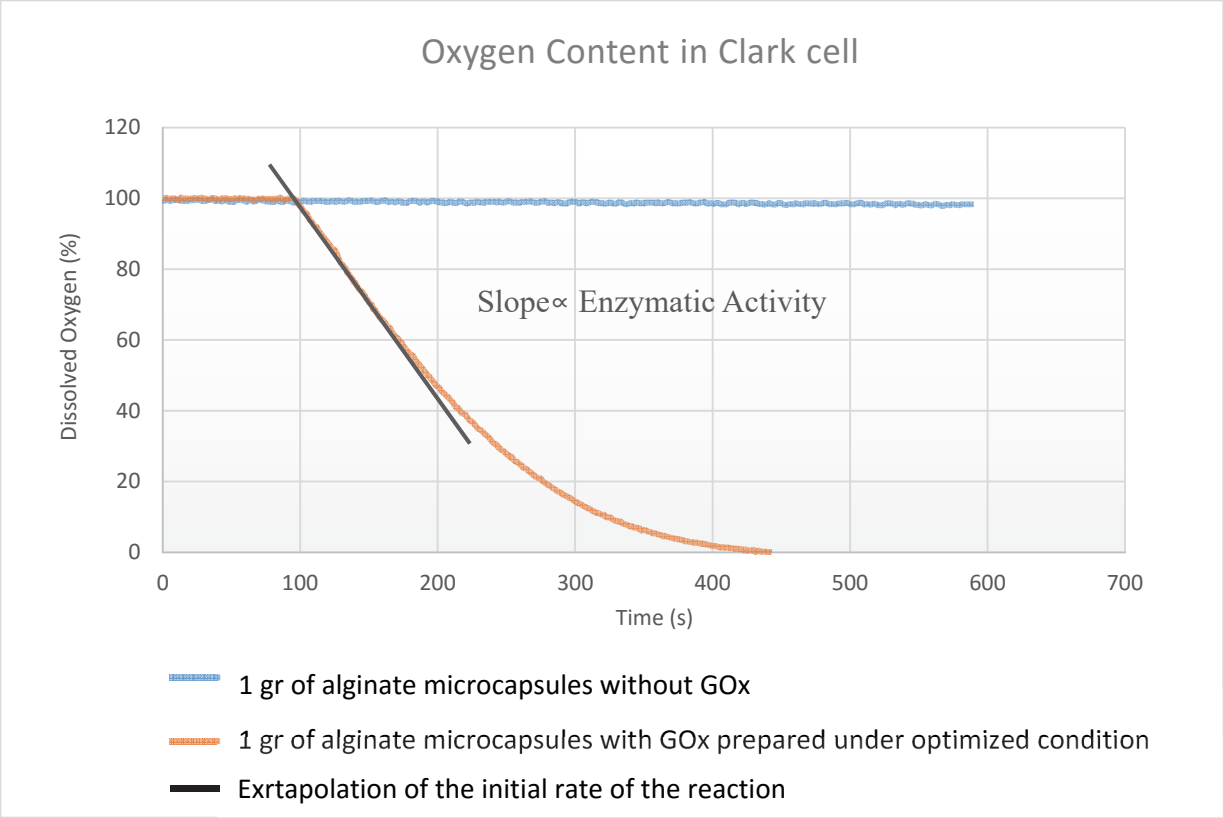

Figure 27. The oxygen content evolution in Clark-Cell oxygen electrode in the presence of alginate microcapsules.

To find the activity per gram of enzyme it was necessary to find out the total amount of the enzyme per unit of mass of microcapsules. In this regard, using the encapsulation efficiency, the total mass of encapsulated enzyme was divided by the total mass of obtained microcapsules in the same encapsulation batch. Performing the aforementioned method on five separate batches showed that with the applied encapsulation conditions, the amount of encapsulated enzyme is 0.82 ± 0.04 mg of enzyme per each gram of microcapsules.

The results of enzymatic activity measurements on free enzyme and on microcapsules after each modification step are given in *Table 4*. As can be seen, the enzymatic specific activity of GOx is reduced after its encapsulation in alginate microcapsules. This reduction can be due to the imprisonment of the enzyme in a confined space and being entangled in a network of alginate chains that possibly results in stabilizing certain conformations of the enzyme that are unfavorable for enzymatic activity. Moreover, once the enzyme is encapsulated, enzymatic activity is not merely dependent on the activity of the enzyme itself but also depends on the diffusion rate of the substrates (glucose and oxygen) through the microcapsule's wall. The porosity and the thickness of the wall, as well as the density of the polymeric network inside the microcapsules are the factors that limit the accessibility of the substrates to the enzyme. All these unfavorable parameters have resulted in the reduction of enzymatic activity.

Table 4. Activity measurements after each modification step on microcapsules.

Sample	**Specific Activity (U/ $g_{protein}$)**
Free GOx enzyme	$(5.3\pm0.1)\times10^{4}$
Encapsulated GOx in microcapsules	$(4.3\pm0.3)\times10^{2}$
Encapsulated GOx in chitosan-modified microcapsules	$(1.3\pm0.2)\times10^{2}$
Encapsulated GOx in chitosan-modified microcapsules after antibody immobilization	$(1.2\pm0.3)\times10^{2}$

The second step of modification *i.e.* covering the microcapsules with chitosan also results in specific activity reduction. This event was also predictable since covering microcapsules with another layer will potentially decrease the porosity of the wall which as mentioned before could result in a lower diffusion rate for substrates. It was imagined that incubation of microcapsules overnight in a solution of chitosan may be accompanied by the gradual leaching of the enzyme out of microcapsules. So the incubation solution was assessed for protein by the Bradford method. The results did not show a significant leaching out of enzyme that could be detectable by Bradford method. Therefore, it was assumed that after the formation of microcapsules in

calcium chloride bath and incubation for at least 30 minutes, the microcapsule's wall becomes thick enough not to let the enzyme escape away from microcapsules.

After the last modification step (*i.e.* immobilization of an antibody on microcapsules), it was expected that a decrease in enzymatic activity might be observable, which can be explained by two possible sources. One is the addition of another complex layer of biomolecules on the surface of microcapsules and another source is the use of glutaraldehyde during the immobilization step. As a small but highly reactive molecule, some glutaraldehyde can possibly diffuse into microcapsules and crosslink or handcuff the enzyme in some ways. But the reduction in enzymatic activity was observed to be really small and below the confidence interval of the measurement since a relatively low concentration of glutaraldehyde (0.25 % w/v) is used. Also, the amino groups on the surface of the microcapsules are more accessible for glutaraldehyde to react with rather than the enzyme inside microcapsules. It is also possible that the glutaraldehyde could crosslink chitosan, making it less porous to glucose.

3.7. Summary

In this chapter, it was demonstrated that GOx can be encapsulated in alginate microcapsules. Also the surface of such microcapsules can be functionalized and covered with an extra layer of chitosan to increase the mechanical stability of the capsules and to add amino groups required to subsequently link antibodies on the capsules. A successful immobilization of human IgG as a model antibody was confirmed by MALDI-TOF-MS. The enzymatic activity of GOx was measured after each step and the results showed that the enzyme have maintained its activity during the preparation of our designed platform.

Chapter 4. Bacterial growth inhibition

4.1. General objectives

The next step of our study, after the preparation and characterization of the proposed antibacterial platform consisted in the evaluation of the antibacterial properties of the microcapsules. Therefore, in the present chapter, the effect of the enzymatic activity (originated from encapsulated GOx in alginate microcapsules) on the growth of *E. coli* K-12, our model bacteria, is studied. Also the results and discussion of the inhibition of bacterial growth are brought to the attention of the readers.

4.2. Inhibition of bacterial growth in a petri dish

In preliminary studies, to evaluate the antibacterial properties of microcapsules containing GOx, 1.007 g of microcapsules containing GOx were spread on a sterilized paper disc (d=1.6 cm) and placed at the central spot of a petri dish containing sterilized LB broth culture media with 2 % agar gel, 10 % glucose and a carpet of *E. coli* K-12 on top of the culture media (see Section 2.7.1) . For the control sample, 1.007 g of empty microcapsules (without GOx) were used on the central paper disc. In general, in the absence of any antibacterial activity, the bacteria will grow on the petri dish and as the result of the bacterial growth the culture media becomes turbid due to the optical density of the bacteria. In the presence of an antibacterial agent in any region on the petri dish, no bacterial growth near the region of antibacterial activity will occur thus, no turbid area is observable, which means the culture media stays transparent. In our experiment, after 16 hours of incubation at 37˚C, both petri dishes were observed visually to see the possible bacterial growth inhibition. The result is shown in *Figure 28* and as can be seen, on petri dish with microcapsules containing GOx (*Figure 28-right*), a transparent halo had appeared around the paper disc showing that the bacteria was inhibited to grow in the region where there was some GOx. Apparently glucose (present in the culture media) was able to diffuse into microcapsules where it is engaged in the oxidation reaction thus producing some hydrogen peroxide that could diffuse away from the microcapsules. This amount of hydrogen peroxide was enough to prevent the bacterial growth in the vicinity of treated paper disc. While for the control experiment (*Figure 28-left*), since there was no GOx in the system and therefore no hydrogen peroxide production occurring, the bacteria were able to grow freely.

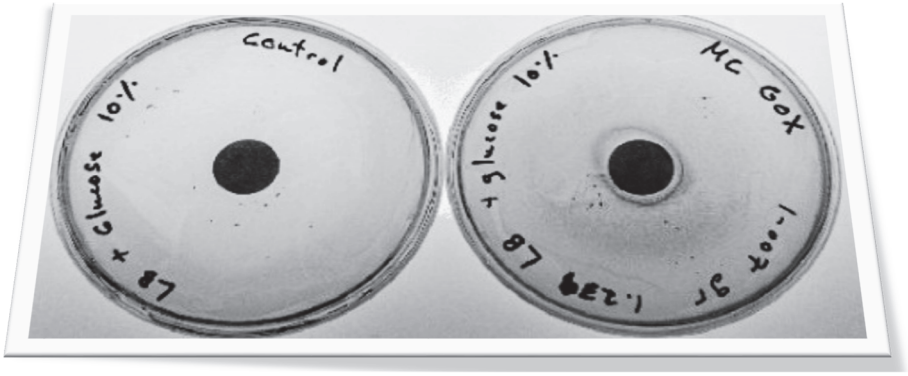

Figure 28. Bacterial Growth inhibition on petri dish with microcapsules containing glucose oxidase (right) and microcapsules without glucose oxidase (left) applied to a 2 cm^2 paper disc placed at the centre of the petri dish.

4.3. Growth inhibition threshold

For further understanding of the antibacterial activity of our designed microcapsule-based platform we decided to analyze the inhibition of bacterial growth at a scale larger than a petri dish. Therefore, the growth inhibition was studied by monitoring the optical density of *E. coli* K-12 at 600 nm approximately once every 30 min during a time window of 24 hours. In this regard microcapsules containing GOx (providing a known amount of enzymatic activity) were added to the LB broth culture media according to the procedure described in Section 2.7.2.

Since hydrogen peroxide is the antibacterial agent in our system and it is produced gradually in the media and on the other hand *E. coli* growth is a dynamic process of living cells, in presence of some enzymatic activity, the bacterial growth is assumed to be a function of different factors. The bacteria are growing while consuming the glucose as a nutrient, and on the opposite side while the enzyme is still active, we will have a constant consumption of glucose and a constant production of hydrogen peroxide which is then consumed to decompose the bacteria. Since the bacteria are living cells, they are trying to grow; therefore, at each certain time-point the total population of the bacteria is a function of their growth rate and their decomposition rate.

It was obviously assumed that there would be a threshold for the amount of enzymatic activity in the system that can effectively inhibit the bacterial growth of a certain initial number of bacteria. To find the optimized enzymatic activity or in other words, to find the threshold which can also be defined as the "optimal effective enzymatic activity", different concentrations (as U/ml) of free GOx were tested while keeping the initial concentration of *E. coli* cells constant. In a set of parallel experiments, 100 µl of a saturated solution of *E. coli* K-12 (previously cultivated in LB broth culture media and incubated in 37˚C for 16 hours) was added to LB broth culture media through the experimental set up and conditions as described in Section 2.7.2.3. Knowing that the saturated cellular concentration of *E. coli* in LB broth culture media is approximately 6.7×10^{9} cells/ml[66], the 100 µl amount of bacteria in our experiment provides 6.7×10^{8} cells/ml of *E. coli*. The enzymatic activity was created by adding GOx ranging from 0 to 1.9×10^{-2} U/ml in different culture batches while keeping the initial amount of bacteria constant. The bacterial growth in all batches was observed and plotted as shown in *Figure 29*.

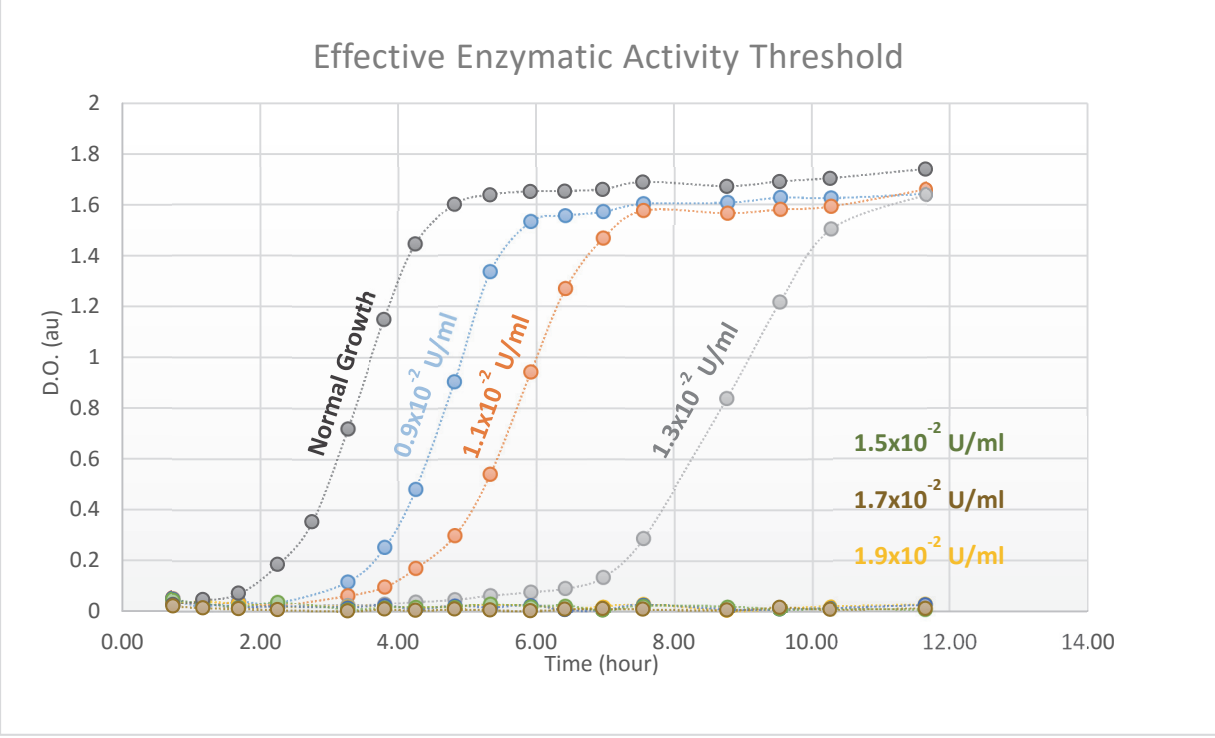

Figure 29. Effective enzymatic activity threshold inhibiting bacterial growth for six different concentrations (in U/ml) of free GOx.

The sample containing 0 U/ml, is considered as the control sample which demonstrate the normal growth of *E. coli*. and reached the stationary phase of bacteria's life cycle in about 4.8 hours after the incubation at 37˚C. As can be seen in *Figure 29*, normal bacterial growth exponential phase faces a difficulty to initiate and therefore a relatively large lag phase was observed in presence of enzymatic activity or more precisely, the production of hydrogen peroxide in culture media. Consequently, at 0.9×10^{-2} U/ml of free GOx, the stationary phase was attained after approximately 6.5 hours. Similarly, 1.1×10^{-2} U/ml of free GOx activity will delay the growth even more and the stationary phase appeared 7.5 hours after the start of incubation. Surprisingly, at 1.3×10^{-2} U/ml the bacteria had a real problem for growth and with a relatively large delay (in comparison with lower amounts of enzymatic activity in the culture media), the stationary phase appeared after 12 hours of incubation. For the samples containing higher enzymatic activity *i.e.* for the samples containing 1.5×10^{-2}, 1.7×10^{-2} and 1.9×10^{-2} U/ml no growth was observed which means apparently the bacteria's decomposition rate is larger than their growth rate. In this case either the bacteria decomposed totally at earlier stages or the population is kept so low that it could not enter the exponential growth phase. Therefore, 1.3×10^{-2} U/ml was considered as the maximum enzymatic activity that *E. coli* K-12 could tolerate and grow, although with relative difficulty.

Moreover, besides exerting a lag in bacterial growth, the presence of enzyme with a certain activity was observed to have an adverse effect on the growth rate during the exponential growth phase of the bacteria's life cycle. To evaluate this, the slope of growth was calculated by linear regression for each exponential growth phase and the trend lines are presented in *Figure 30*. As can be seen from the slopes, the rate of growth is another factor that can be affected by the presence of some enzymatic activity in the culture media. With an increase in the enzymatic GOx activity from 0 to 1.3×10^{-2} U/ml, the slope decreases consequently showing that the decomposition rate exceeds the growth rate accordingly.

To summarize this part of the study, we can conclude that the presence of enzymatic activity on bacterial growth showed a total inhibition effect for concentrations of GOx corresponding to activity of more than 1.3×10^{-2} U/ml and also showed a delaying effect that increased with GOx. This delay on the time the bacteria's life cycle reaches its stationary state

was observed to be partly as a result of elongation in the bacteria's lag phase and also as a decrease in the slope of the exponential growth phase. It should be mentioned that the optical densities of the culture media for all batches were checked after 24 hours and the condition of all samples had stayed the same as what had been measured after 12 hours.

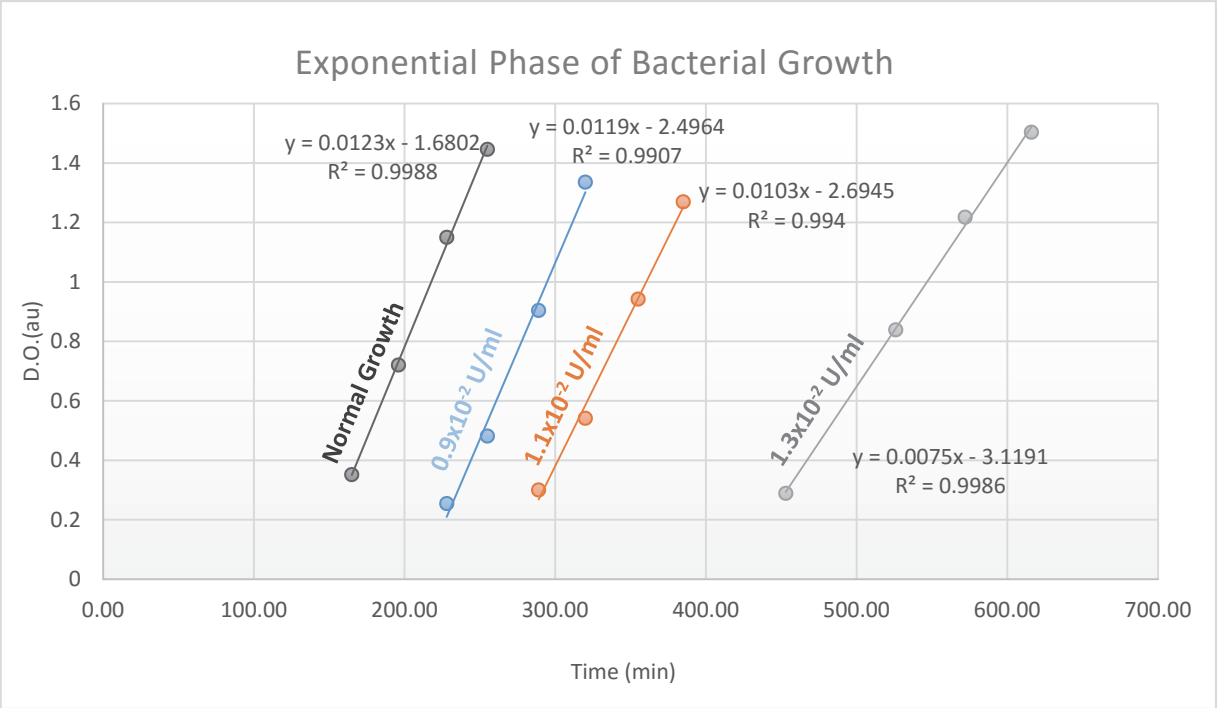

Figure 30. Linear regression of the exponential growth phase from the graphs in Figure 29 for free GOx.

To check the reproducibility of the system and also to see if our antibacterial microcapsules behave in the same manner as free enzyme, the following four different samples (each repeated in triplicate) were prepared and analyzed: i) a control sample with zero enzymatic activity *i.e.* no free GOx; ii) a sample containing 1.3×10^{-2} U/ml generating from free GOx; iii) a sample containing 1.3×10^{-2} U/ml generating from our antibacterial microcapsules; and iv) a sample containing 1.9×10^{-2} U/ml generating from our antibacterial microcapsules. All twelve samples were incubated with *E. coli* K-12 under the same conditions as previously mentioned in the current section. The result of optical density monitoring at different time points for all four samples including their error bars (SD, n=3) are presented in *Figure 31*. As was expected for the first sample, normal growth was observed because no enzymatic activity and thus no

hydrogen peroxide was present to meddle with bacterial growth. The bacteria in the second sample (containing free GOx with enzymatic activity equal to the determined threshold) succeeded to grow after approximately 12 hours. Although the third sample contained the threshold amount of enzymatic activity, the encapsulated enzyme showed slightly less inhibition than the free enzyme for the equivalent enzymatic activity. Such behavior could be possibly due to the imperfection of experimental conditions. It was observed that through the incubation and strong agitation of the incubation vessel (an Erlenmeyer), some of the microcapsules adhere to the inner wall of the vessel therefore these microcapsules may not contribute to the total enzymatic activity of the solution. For the forth series of samples containing encapsulated GOx at 1.9×10^{-2} U/ml, since the enzymatic activity in the culture media is higher than the threshold determined in *Figure 29* for inhibition, no bacterial growth was observed, as expected. Also, and the adhesion of microcapsules to the inner wall of the vessel, is not effective enough to reduce the enzymatic activity inside the solution to a level below threshold. Thus, our designed microcapsules have depicted the expected antibacterial properties above the aforementioned threshold.

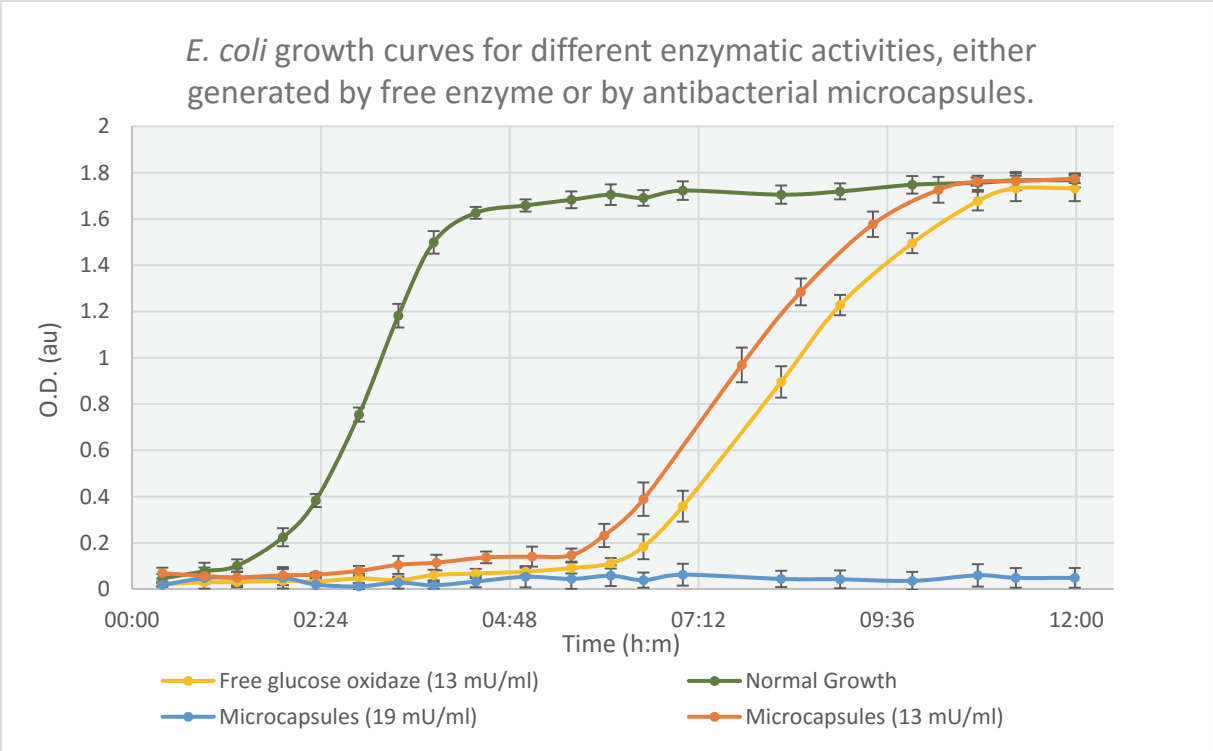

Figure 31. Reproducibility and comparison between antibacterial microcapsules (orange) and free glucose oxidase (yellow). The error bars show SD of three measurements.

Another step for optimizing the bacterial growth inhibition is to find the initial number of bacteria that could not grow in the presence of a certain level of enzymatic activity and thus the generated hydrogen peroxide. Therefore, in another series of experiments, the enzymatic activity was kept at constant value of 1.9×10^{-2} U/ml and different initial amounts of *E. coli* K-12 ranging from 0.67×10^{9} to 3.0×10^{9} cells/ml were tested for growth. The results, which are given in *Figure 32* demonstrate that a population of 0.67×10^{9} cells/ml *E. coli* bacteria sample could not grow in the presence of 19 mU/ml GOx whereas a larger initial population were able to grow. However, a relative delay in bacterial growth was observed proportional to the initial amount of the bacteria.

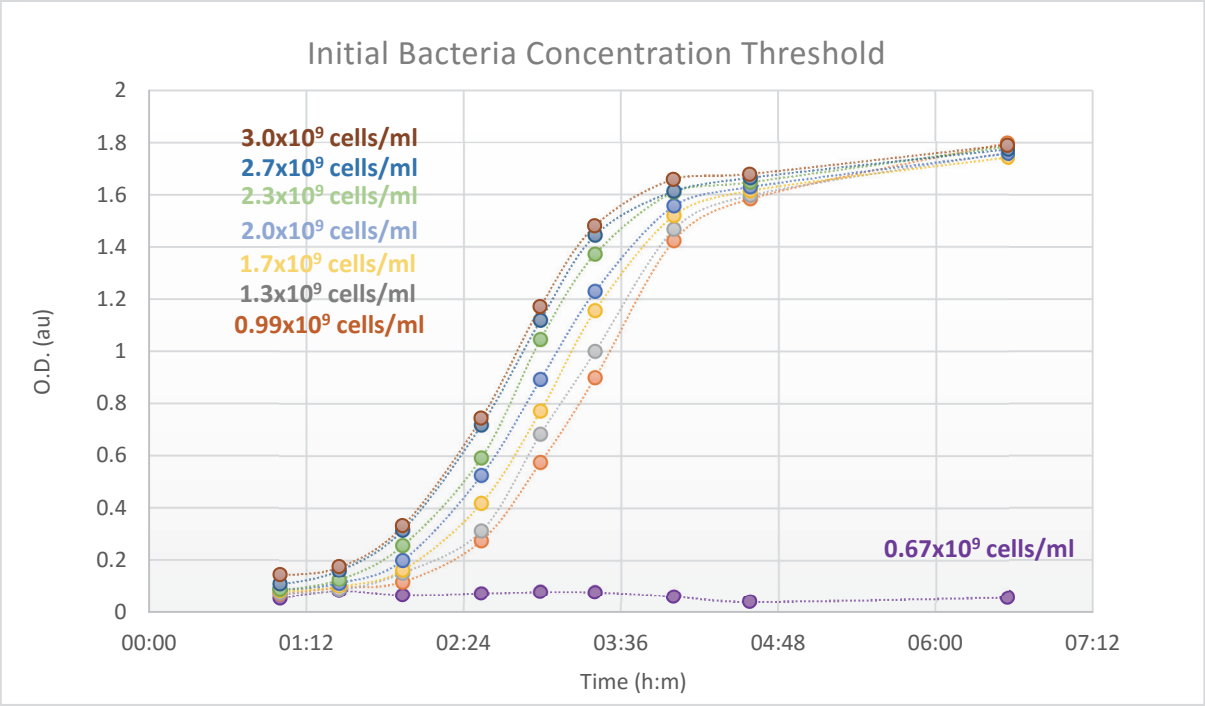

Figure 32. Initial concentration of bacteria threshold for a constant level of free GOx of 1.9×10^{-2} U/ml enzymatic activity.

4.4. Summary

In this chapter, the antibacterial properties of our designed platform was verified against *E. coli* K-12 as a model pathogen. Preliminarily, a successful inhibition of bacterial growth was observed in a petri dish. furthermore, the detail of this bacterial growth inhibition was studied

by monitoring the optical density of the culture media which represented the number of bacteria at different time points of bacterial growth. In this regard a threshold of enzymatic activity in the media was found to be effective to prevent certain initial amount of bacteria from growing. Similarly, the minimum initial amount of bacteria that could grow at certain amount of enzymatic activity was also determined.

Chapter 5. Immobilization of glucose oxidase on gold nanoparticles

5.1. General objectives

Since the encapsulation of GOx in alginate microcapsules results in reduction of its activity and losses in enzyme during the encapsulation procedure (see Section 3.6), we evaluated the immobilization of the GOx on gold NPs prior to its encapsulation. Our hypothesis is that enzyme immobilization on gold NPs could possibly increase the enzymatic activity and potentially compensate the activity loss in the microcapsules. This idea is based on the assumption that immobilization of enzyme molecules on massive gold NPs could possibly reduce the mobility of the enzyme and thus could reduce the diffusion of the enzyme at early stages of encapsulation while the thickness of the microcapsules' wall is not large enough to prevent the loss of enzyme in the calcium chloride bath. Another advantage could be an increase in the enzyme's shelf life and thermostability that can be considered as an asset in preparation of a durable antibacterial paper that maintains its properties on larger time scales as well as being operative in wider range of temperatures.

5.2. Introduction

Recently, metal NPs, especially gold NPs, have played an extensive role in biochemistry and biomedical research because of their high reactivity to living cells (in terms of translocation into the cells) , their large surface area to volume ratio, their various sizes and shapes and most importantly their stability at high temperatures[68]. In comparison with other metals, gold NPs are most preferable for applications such as drug and gene delivery, due to their inertness and lower cytotoxicity. All these applications are feasible through a bioconjugation process in which biomolecules are attached to gold NPs via a bifunctional ligand[68]. In the case of GOx, a bioconjugation method was proposed in which gold NPs are functionalized by carboxyl terminated thiol groups (HS—R—COOH) *i.e.* using mercaptoundecanoic acid (MUA). It has also been shown that thermostability of the enzyme is enhanced once it is immobilized on gold NPs (d=20 nm)[69]. Meanwhile, another study showed the same immobilization process of GOx on gold NPs (d=5 nm) will enhance the enzymatic activity greatly as well as its shelf life[70]. The same study showed a lower value of *Michealis-Menten constant* (K_m) for the immobilized enzyme compared to that of the free enzyme and an enhancement of 1.56-fold in the enzymatic

affinity was found. The enhancement in thermostability of GOx was also shown using bioconjugation of this enzyme on gold nanorods[71]. However, a very recent study yielded completely different results, showing that the immobilization of GOx on gold NPs (d=37 nm) has an adverse effect on enzymatic activity. This decrease was explained by a decrease in the percentage of the enzyme's α-helix conformation, which contributes to its enzymatic activity once it is attached to the surface of gold NPs. It seems that the closer to the surface of the nanoparticle the enzyme is, the lower the activity becomes[72].

5.3. Methods

5.3.1. Preparation of thiol-modified gold nanoparticles

The synthesis of gold NPs was carried out using the conventional Turkevich method[73] which includes the reduction of hydrogen tetrachloroaurate (III) ($HAuCl_4.3H_2O$, Sigma-Aldrich) using trisodium citrate dihydrate (Sigma-Aldrich) through reaction presented in *Equation 14* and heating the solution to the boiling point. Citrate ions also act as the stabilizing agent for gold NPs which prevents them from forming aggregates. All glassware was rinsed with *Aqua Regia* (a 1:3-mixture of nitric acid and hydrochloric acid) followed by rinsing with MilliQ water to remove all traces of metallic contaminations. These NPs were then incubated overnight in a solution of MUA in ethanol to undergo a process of ligand exchange during which citrate is replaced with MUA to give thiol-modified gold NPs for further reactions. NPs were removed from the solution by centrifugation followed by several washes with ethanol and re-dispersion in phosphate buffer (10mM, pH 6.8 with 0.2 mg/ml Tween-20).

Equation 14
$$2\,HAuCl_4 + 4\,Na_3C_3H_5O_7 \rightarrow H_2 + 2\,Au^0 + 4\,CO_2 + 4\,NaC_5H_5O_5 + 8\,NaCl$$

5.3.2. Immobilization of glucose oxidase on gold nanoparticles

Immobilization of GOx on thiol-modified gold NPs was carried out based on a coupling reaction using N-ethyl-N'-(3-dimethylaminopropyl) carbodiimide (EDC) activation and N-hydroxy-succinimide (NHS). A summary of the whole process is schematically illustrated in *Figure 33* [69]. A sample of 1.0 mg of the NPs were reacted with a freshly prepared solution of 50

mM NHS and 200mM EDC for 10 min. Then, NHS-terminated gold NPs were separated from the reaction solution by centrifugation (at 8000 rpm for 10 min) and washed with phosphate buffer (10 mM, pH 6.8, with 0.2 mg/ml Tween-20) several times. The NHS-terminated gold NPs were then incubated with 0.8 mg/ml GOx in phosphate buffer (10 mM, pH 6.8) overnight under argon atmosphere. The mixture was then centrifuged to discard free GOx which remains in the supernatant and washed by phosphate buffer, and re-dispersed in the same buffer for further analysis. The detail of this series of reactions is given in *Figure 34*.

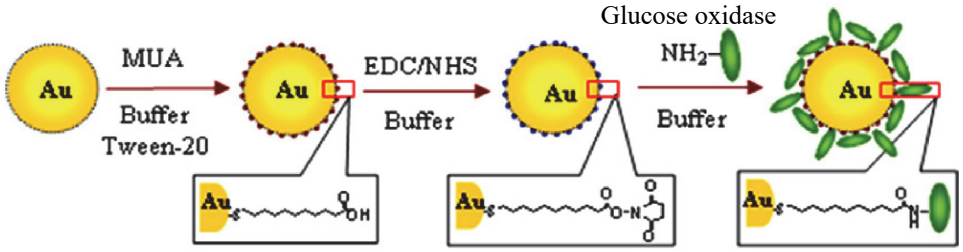

Figure 33. Schematic illustration of enzyme immobilization on gold nanoparticles (adapted from reference 69).

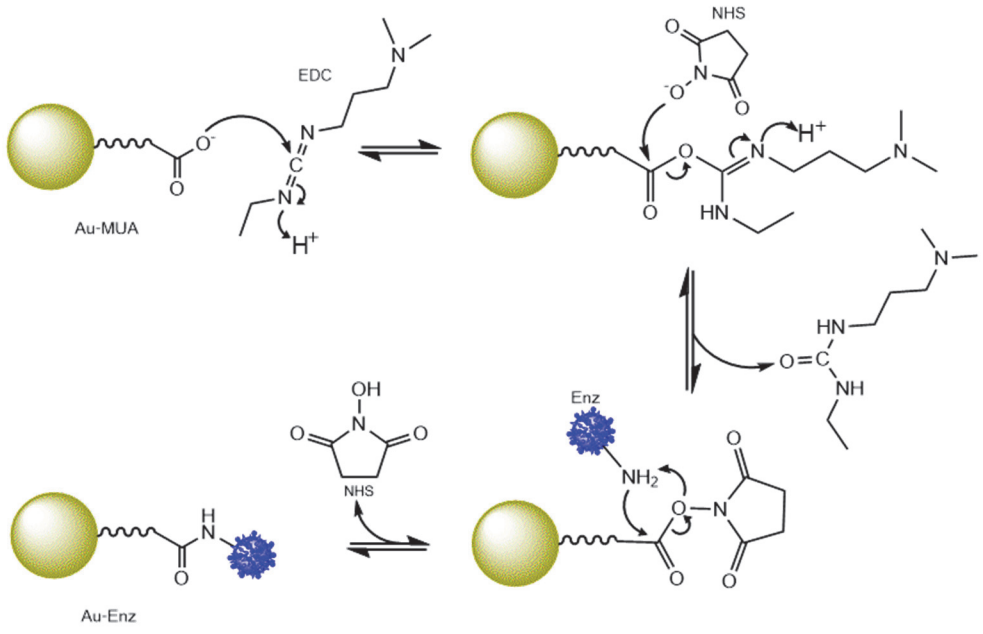

Figure 34. Mechanism of the reactions resulting in immobilization of glucose oxidase on thiol-modified gold nanoparticles.

5.4. Enzymatic activity measurements

Several attempts were made to measure the enzymatic activity of GOx immobilized on gold NPs using the oxygen electroanalysis method described in Section 2.6.1. This method was found to be practically impossible as a result of the strong aggregation of NPs observed in the *Clark-Cell* and also due to relatively low sensitivity of this technique. We therefore, used the spectrophotometric method of horseradish peroxidase (HRP) and its substrate, 3,3′-dimethoxybenzidine (*o*-dianisidine). In this method, glucose is oxidized in the presence of GOx which produces hydrogen peroxide (*Equation 1*). Then, hydrogen peroxide is used rapidly to oxidize *o*-dianisidine through an enzymatically catalyzed reaction using HRP to form the oxidized dimer form of *o*-dianisidine which absorbs visible light at λ_{max}= 455 nm, as shown in *Equation 15*. The details of this reaction are schematically illustrated in *Figure 35*[74]. Typically, to measure the enzymatic activity, 2.5 ml of a solution of 0.33mM of *o*-dianisidine in phosphate buffer (0.1 M pH 6.8), 0.1 ml of a solution of 0.02 % HRP and 0.3 ml of 18 % glucose solution were mixed in a spectrophotometric cell and then a certain amount of GOx bound to gold NPs solution was added and the absorbance evolution was observed as a function of time at 455 nm.

Equation 15 $$H_2O_2 + o-dianisidine\ (reduced) \rightarrow H_2O + o-dianisidine\ (oxidized)$$

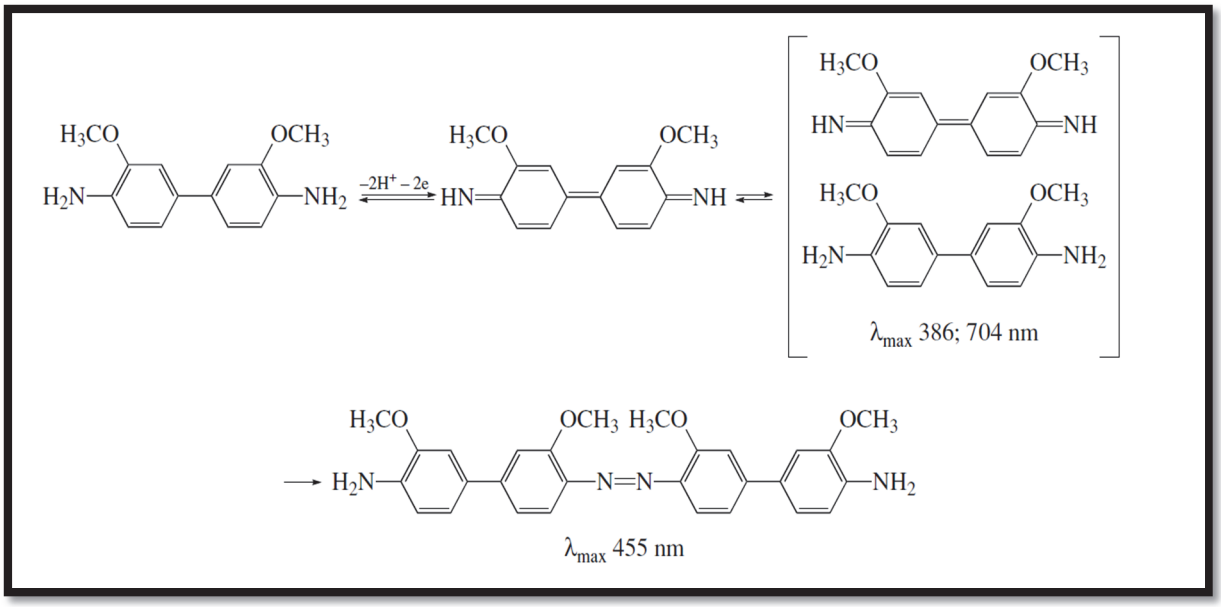

Figure 35. The reaction scheme of peroxidase oxidation of o-dianisidine (reproduced from reference 74).

To calculate the enzymatic activity, after plotting the evolution of absorbance (A) versus time as shown in *Figure 36*, the slope of the linear part of the curve (at early stages of the reaction) is determined which corresponds to the enzymatic activity of GOx as follows: the slope of the curve corresponds to $\frac{\Delta A_{o-dia\,(ox)}}{\Delta t}\,(min^{-1})$, knowing that ε, the extinction coefficient for the oxidized form of *o*-dianisidine at 455 nm equals to 11300 ($M^{-1}cm^{-1}$)[75] and the thickness of the spectrophotometric cell which represents the light path (b) equals 1 cm, on the basis of the Beer-Lambert law (A= ε.b.C) the slope can easily be converted to $\frac{\Delta[o-dia\,(ox)]}{\Delta t}\,(M\,min^{-1})$ and by taking the stoichiometry of the reactions into consideration (*Equation 1* and *Equation 15*), we can conclude that:

Equation 16
$$\frac{\Delta[o-dia\,(ox)]}{\Delta t}\,(M\,min^{-1})=-\frac{\Delta[H_2O_2]}{\Delta t}\,(M\,min^{-1})=-\frac{\Delta[glucose]}{\Delta t}\,(M\,min^{-1})$$

And since the total volume of the solutions in the spectrophotometric cell, V(ml) is also a known parameter, therefore, the enzymatic activity can be determined from *Equation 17* as follows:

Equation 17
$$\text{Enzymatic activity}_{\text{(µmoles of glucose/min)}} = \frac{V\Delta[glucose]}{1000\Delta t} = \frac{\Delta[\mu\,moles\,of\,glucose]}{\Delta t}$$

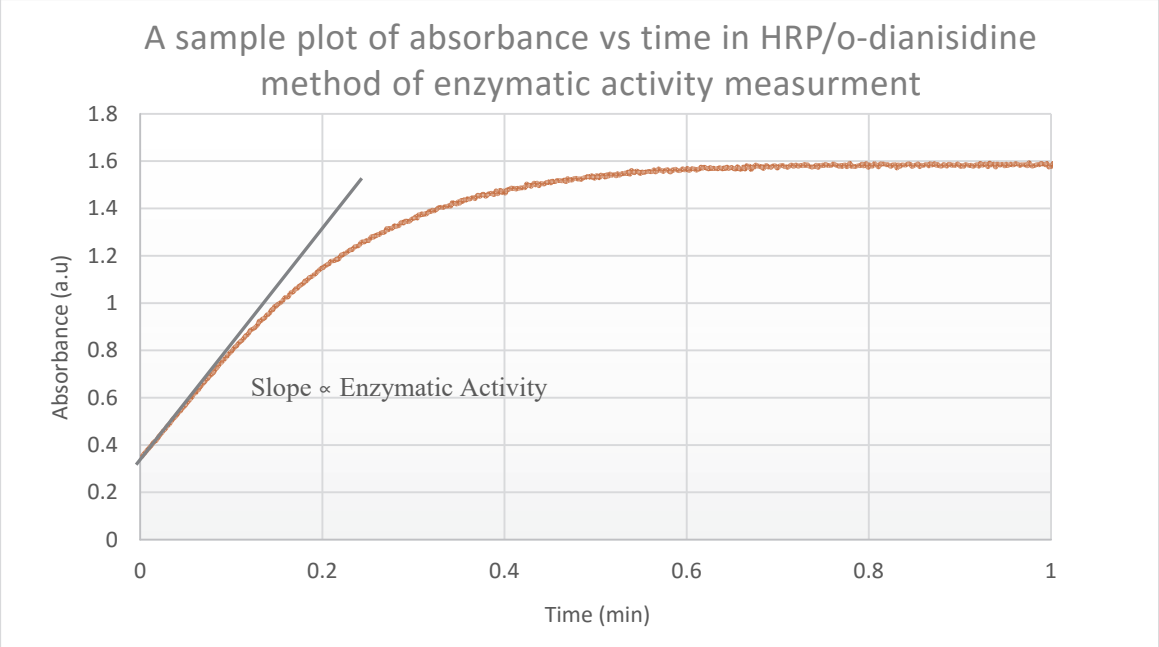

Figure 36. Enzymatic activity measurement in HRP/o-dianisidine- a sample plot.

5.5. Results and discussion

5.5.1. Preparation of gold nanoparticles

In our study, two sets of gold NPs having different sizes were tested for the GOx immobilization. The first set of gold NPs had an average diameter of 10.9±1.8 nm (*Figure 37*). The average diameter and size distribution for these gold NPs (*Figure 39*) that were prepared using the method described in Section 5.3.1 were determined using transmission electron microscopy (TEM). The UV-Vis extinction spectra is also provided in *Figure 38*. The other set was gold NPs of ~50 nm in diameter. The approximate diameter of these NPs was determined from its UV-Vis extinction spectra by finding the ratio of its absorbance value at λ_{SPR} to the absorbance value at 450 nm and by comparing the calculated ratio with the values mentioned in the literature. This method of size determination was developed by Haiss *et al.*[76] in 2007. The UV-Vis extinction spectra (*Figure 40*) of such NPs was obtained and the ratio A_{527nm}/A_{450nm} yields the value equal to 2.03 which determines the average diameter of 50 nm for this sample of gold NPs.

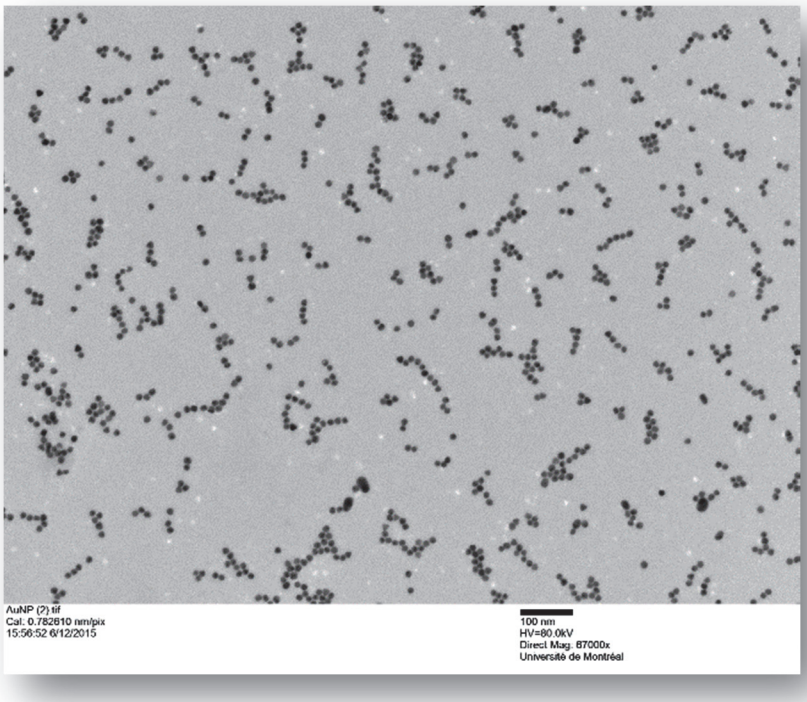

Figure 37. TEM image of gold NPs of d=10.9 nm.

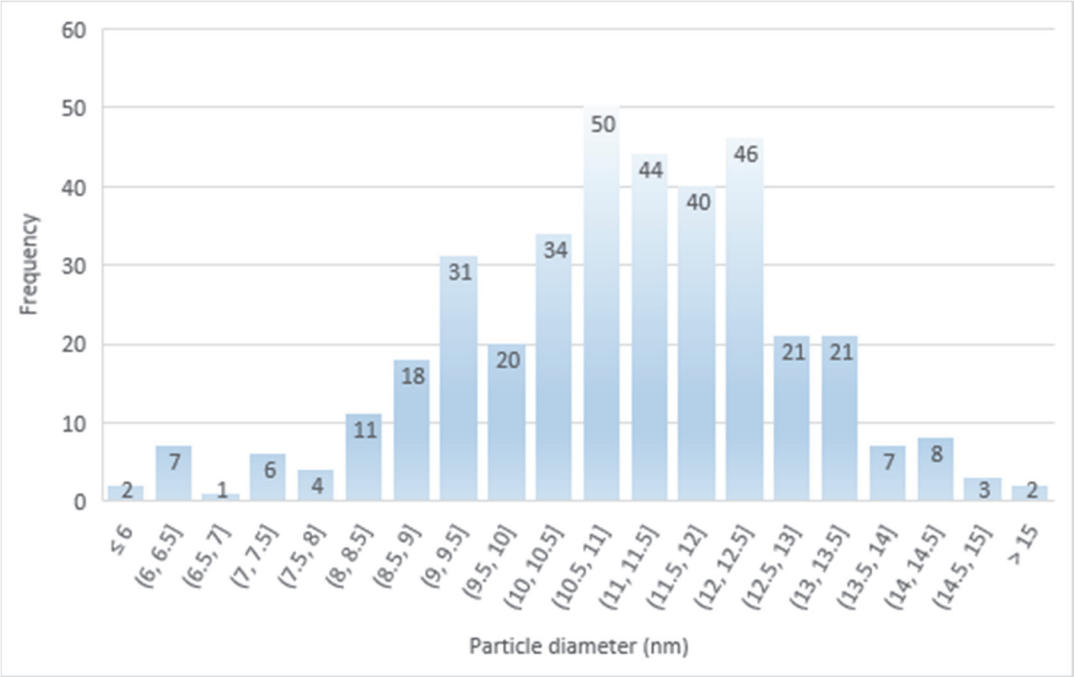

Figure 39. Histogram of gold NPs' size distribution with average diameter equal to 10.9 nm as determined by TEM image treatment.

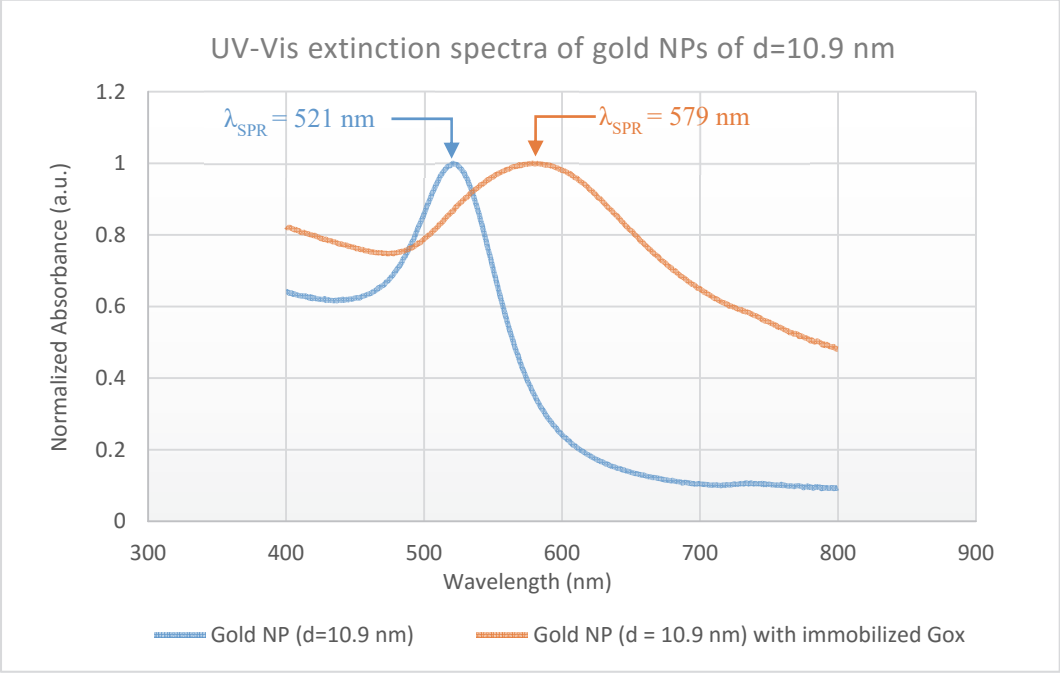

Figure 38. UV-Vis extinction spectra of gold NPs (d=10.9 nm) and GOx-immobilized-gold NPs(d=10.9 nm). The absorbance values are normalized to the value of the maximun absorbance of each curve.

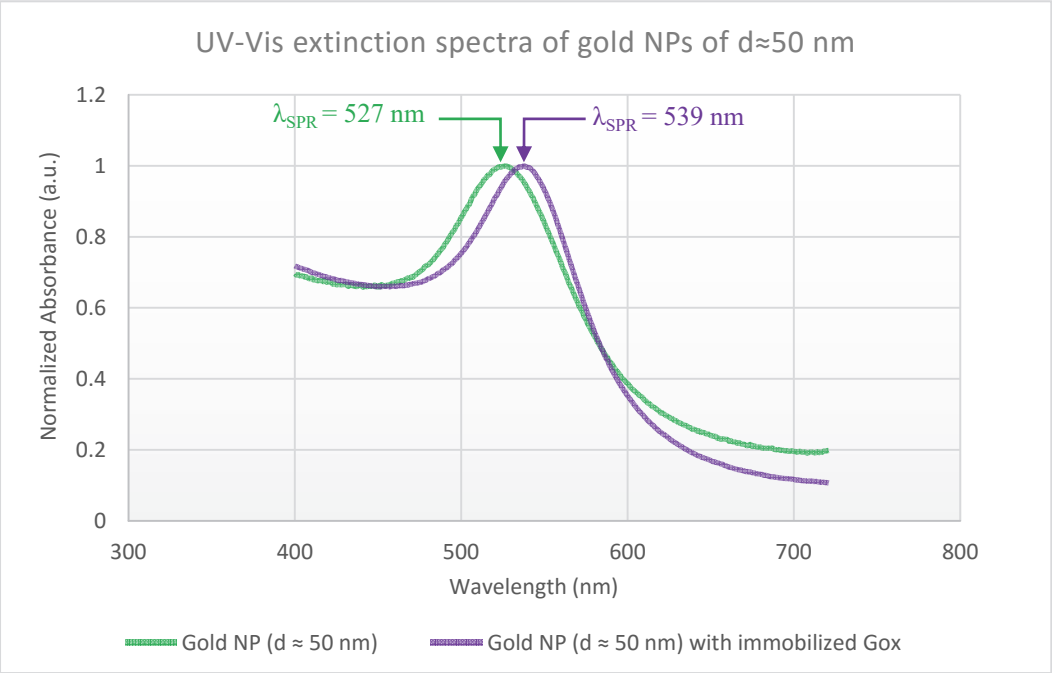

Figure 40. UV-Vis extinction spectra of gold NPs (d≈50 nm) and GOx-immobilized-gold NPs(d≈50 nm). The absorbance values are normalized to the value of the maximun absorbance of each curve.

Gold NPs with an average diameter of 10.9 nm were prepared according to the method explained in Section 5.3.1 and a batch of gold NPs with an average diameter of 50 nm was provided by Dr. Jean-François Masson's research laboratories at Université de Montréal. After functionalizing these two sets of gold NPs with MUA, we used them for GOx immobilization. To be able to calculate the enzymatic activity, it was necessary to determine the amount of enzyme that could possibly be immobilized on gold NPs. For this, a Bradford protein assay was used to analyze the enzyme solution before and after the incubation step with the NPs. After the incubation and centrifugation steps, samples were taken from the supernatant for quantification of the amount of the enzyme which stayed unreacted and free in the solution. It is evident that the difference of those two amount indicate the amount of immobilized enzyme on NPs (the results are presented and discussed in Sections 5.5.2 and 5.5.3). The NPs were then redispersed in phosphate buffer (10 mM, pH 5.8) for storage at 4˚C. These NPs were consequently observed by TEM, their zeta potential (ξ) was measured and their enzymatic activity was determined using HRP/*o*-dianisidine spectrophotometric method.

5.5.2. Immobilization of glucose oxidase on gold nanoparticles with average diameter of 10.9 nm

In the enzyme immobilization process, three samples of gold NPs (d=10.9 nm) were tested including a control sample for which the linking reactants (EDC/NHS) were eliminated to see if the enzyme could be physically adsorbed on the surface of gold NPs. The details of these samples are given in *Table 5* along with the amount of the enzyme immobilized as determined by performing the Bradford protein assay on the enzyme solution before and after incubation with gold NPs. Although it could be expected that a sample with more NPs provides more surface available for the enzyme to be immobilized, it was observed that lower amounts of protein were immobilized. This observation suggests that a single enzyme molecule is possibly attached to more than one nanoparticle when high concentrations of NPs were used in the incubation step. As we will see, this results in a deactivation of the enzyme.

Table 5. Immobilized enzyme content on gold NPs of d=10.9 nm.

Sample	Description	Enzyme content in solution (mg), n=3		Total immobilized enzyme (mg)	Efficiency (%)
		Before incubation	After incubation		
1	• 0.46 mg of gold NPs	18.16±0.06	17.19±0.02	1.01±0.08	5.6±0.5
2	• 0.10 mg of gold NPs	15.84±0.04	9.44±0.02	6.42±0.06	40.5±0.5
3	• 0.10 mg of gold NPs • Control without EDC/NHS	17.01±0.02	17.03±0.02	-	-

The results from activity measurements, which were obtained using HRP/*o*-dianisidine spectrophotometric method are given in *Table 6*. Surprisingly, a very low specific activity was observed for the enzyme immobilized on gold NPs of d=10.9 nm compared to free enzyme. Moreover, the specific activity (U/g of protein) for the sample using larger amount of NPs was higher than that of the sample with smaller amount of NPs. Regardless of this difference in specific activity, both of these two values are very much lower than the activity of free enzyme. One possible explanation for this observation could be the denaturation of the enzyme during

the immobilization process. The favorable conformation for the enzymatic activity of GOx could undergo certain changes that may have resulted in a reduction in enzymatic activity. Another possible explanation could be based on the proximity of the size of GOx (d=4.3 nm)[77] to the size of NPs (d= 10.9 nm). Since the enzyme's size is close to the nanoparticle's size, there is a chance of having a very few number of immobilized enzyme per a single nanoparticle. Also there is a possibility that a single enzyme attaches to two or more NPs, exerting some unwanted interactions that may alter the favorable conformation of the enzyme which ends up in a decrease in enzymatic activity. This hypothesis is also justified by studying the UV-Vis spectra of gold NPs before and after immobilization of GOx. As can be seen in *Figure 38*, the λ_{SPR} of gold NPs shifted to larger wavelengths and this redshift of 58 nm is accompanied by the λ_{SPR} peak broadening which can be a proof to the fact that the immobilization of the enzyme resulted in coalescence of gold NPs. The coalescence of gold NPs creates agglomerations of particles with different sizes whose size distribution contributes to the λ_{SPR} peak broadening. In fact, by attaching to two or more particles, the enzyme could act as a chemical glue for the gold NPs. In order to evaluate these possibilities, another sample of gold NPs with a larger size was used to carry out the immobilization.

Table 6. Enzymatic activity measurements for free glucose oxidase and different nanoparticle samples of d=10.9 nm.

Sample	**Description**	**Specific enzymatic activity (U/g of protein), n=3**
0	Free GOx	$(13.2\pm0.2)\times10^{4}$
1	• 0.46 mg of gold NPs	$(8.1\pm0.5)\times10^{1}$
2	• 0.10 mg of gold NPs	7.4±0.3
3	• 0.10 mg of gold NPs • Control without EDC/NHS	No activity observed

5.5.3. Immobilization of glucose oxidase on gold nanoparticles with average diameter of ≈50 nm

A set of three samples was prepared and tested with these gold NPs and the amount of the enzyme immobilized in each sample was determined by performing the Bradford protein assay on the enzyme solution before and after incubation of gold NPs (*Table 7*). Similar to the previous set, for the sample with more NPs in incubation step, it was observed that smaller amount of protein was immobilized comparing to the sample with smaller quantity of NPs. As previously observed in the study GOx immobilization on smaller gold NPs (Section 5.5.2), here again the idea that a single enzyme molecule can possibly attach to more than one NP and thus, possible coalescence of NPs could be suggested. However, the amount of coalescence is not as large as in the case of smaller gold NPs because the UV-Vis extinction spectra of such gold NPs in *Figure 40* (after immobilization of GOx) does not show a significant redshift or peak broadening in comparison with that of the gold NPs of d=10.9 nm (*Figure 38*) . No significant differences in protein content was found before and after incubation for the sample without using EDC/NHS showing that the enzyme was not immobilized without anchoring group.

Table 7. Immobilized enzyme content on gold NPs of d≈50 nm.

Sample	Description	Enzyme content in solution (mg), n=3		Total immobilized enzyme (mg)	Efficiency (%)
		Before incubation	After incubation		
1	• 0.46 mg of gold NPs	17.24±0.05	16.27±0.03	0.97±0.08	5.6±0.5
2	• 0.10 mg of gold NPs	14.45±0.05	10.30±0.04	4.15±0.09	28.7±0.7
3	• 0.10 mg of gold NPs • Control without EDC/NHS	16.64±0.03	16.68±0.07	-	-

The results of the activity measurements for these three samples are given in *Table 8*. As can be seen, sample 1 which has higher amount of NPs (and also contains smaller amount of immobilized enzyme) shows a significant value of specific enzymatic activity comparing to sample 2 that has smaller amount of NPs (and also contains more immobilized enzyme). Also in comparison with sample 1 of the previous set in Section 5.5.2 (that contains same mass of

NPs with smaller size), this sample exhibits a larger value of enzymatic activity. This observation suggests that greater coalescence phenomenon occurs in case of immobilization of GOx on smaller gold NPs. A higher coalescence results in a lower enzymatic activity due to the smaller diffusion rate of substrate to the active sites of the enzyme when the aggregation of NPs happens. But regardless of such an improved activity by just increasing the size of gold NPs, there is still a big difference between the activity of free enzyme and immobilized enzyme which is totally unfavorable to our need. Possibly in certain cases, the enhanced thermostability and increased shelf life of the GOx after immobilization on gold NPs (as stated in previous studies[69-71]) could be tempting to use this combination (nanoparticle-enzyme) in the encapsulation process. For sample 3 (the control sample without using reagents EDC/NHS in incubation step), no significant enzymatic activity was observed. Further details on the properties of gold NPs after the modification steps are required to understand the changes in the NPs' surface.

Table 8. Enzymatic activity measurements for free glucose oxidase and different nanoparticle samples of d≈50 nm.

Sample	**Description**	**Specific enzymatic activity (U/g of protein), n=3**
0	Free GOx	$(13.2\pm0.2)\times10^{4}$
1	• 0.46 mg of gold NPs • Normal reaction conditions	$(11.2\pm0.3)\times10^{2}$
2	• 0.10 mg of gold NPs • Normal reaction conditions	$(17.7\pm0.6)\times10^{1}$
3	• 0.10 mg of gold NPs • Reaction without EDC/NHS	No activity observed

The effect of immobilization of GOx on a wavelength which corresponds to the NPs' Surface Plasmon Resonance (SPR) was also observable in UV-Vis extinction spectra of NPs after the immobilization step. As can be seen in *Figure 40* the λ_{SPR} of gold NPs undergoes a red shift of 12 nm comparing to the λ_{SPR} of gold NPs stabilized by citrate and is one of the proofs that the chemistry of the surface of gold NPs have changed.

Imaging of gold NPs covered with MUA and GOx immobilized-gold NPs (*Figure 41(a)* and *(b)* respectively) were acquired using transmission electronic microscopy (TEM). As can be seen in *Figure 41(b)* , a semi-transparent layer of the enzyme covers the NPs which forms structures known as the "fried egg". For further confirmation of the presence of the enzyme attached to NPs, a few drops of silver nitrate (1 % w/v) had been added to the TEM grid in both images in *Figure 41* and as the result of reduction of silver ions to Ag^0 by oxidative amino acids present in the protein, tiny NPs of silver are formed in areas which the enzyme exists unlike for the grid containing gold NPs with MUA in *Figure 41(a)*. These Ag NPs are more visible in *Figure 42(a)*, which is a magnified image of *Figure 41(b)* and the energy-dispersive X-ray

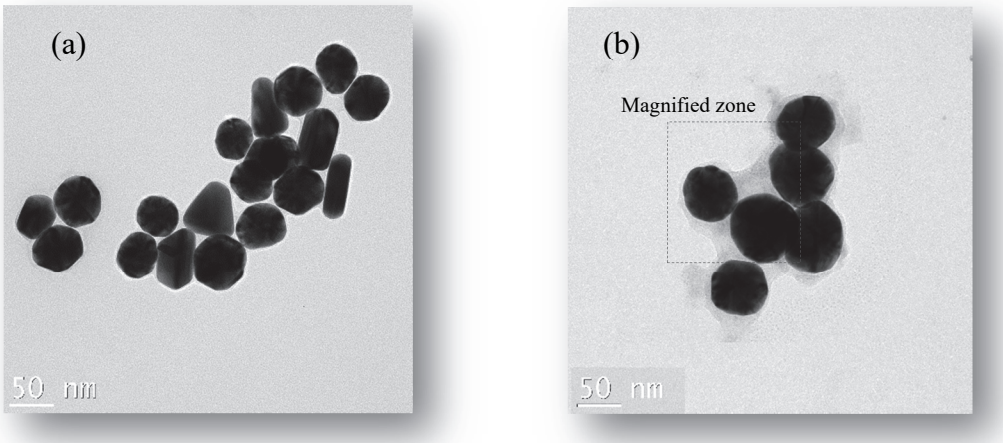

Figure 41. TEM images of gold nanoparticles with MUA (a) and gold nanoparticles with immobilized glucose oxidase (b).

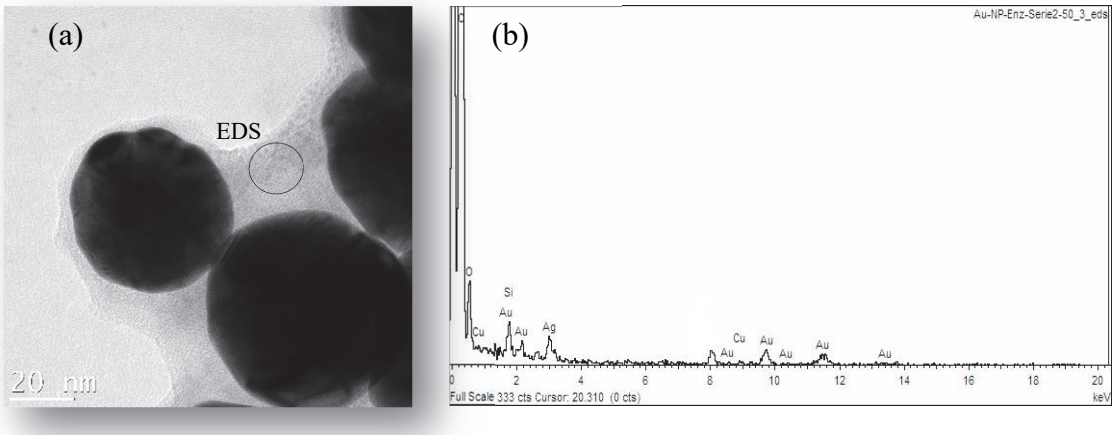

Figure 42. Magnified TEM image of glucose oxidase- immobilized gold nanoparticles (a) and EDS of the specified region (b) .

spectra (EDS) of the specified region on the photo is presented in *Figure 42(b)* confirming the presence of silver element around each gold NPs which gives a peak at ~3KeV in the spectra. It should be noted that the addition of silver nitrate solution on conventional copper-made TEM grids was impossible due to the oxidation and therefore corrosion of copper grids by silver ions. So in order to prevent this, we had to use TEM grids made of gold.

Another way to follow the surface modification of gold NPs is to measure the zeta potential (ξ) of these particles. The zeta potential for this set of gold NPs were also measured and in a DTS1070 disposable capillary cell using a Malvern Zetasizer Nano ZS instrument and the results are given in *Table 9*. The zeta potential is a parameter which shows how strongly ions of opposite charge are bound to the charged surface to form a charged layer. This layer of ions with opposite charge plays an important role to stabilize gold NPs in the solution and prevent them from aggregation and therefore precipitation because a strongly-bound charged layer will repulse other particles with the same charge and that is why the particles could never get close enough to each other to form a larger aggregate of solid that could precipitate.

Table 9. Zeta potential measurements of different gold NPs samples of d≈50 nm.

Sample	Description	Zeta potential (mV) (n=3)
0	Gold NPs-MUA (in phosphate 10mM, pH 6.8, 0.2 mg/ml Tween-20)	-35.9±0.1
1	Gold NPs-enzyme (in phosphate 10mM, pH 5.8) Immobilization conditions: • 0.46 mg of gold NPs	-4.0±0.9
2	Gold NPs-enzyme (in phosphate 10mM, pH 5.8) Immobilization conditions: • 0.10 mg of gold NPs	-5.6±0.9
3	Gold NPs-enzyme (in phosphate 10mM, pH 5.8) Immobilization conditions: • 0.10 mg of gold NPs (Control without EDC/NHS)	-9.4±0.9

In our case it was observed that gold NPs covered with MUA have a zeta potential value of -35.9 mV, which explains a relative stability of these gold NPs in a solution at pH 5.8 (10 mM phosphate, pH 6.8, 0.2 mg/ml Tween-20) compared to the samples with immobilized GOx. This stability results from the carboxyl group at the end of MUA which covers the NPs. This

carboxylic acid is a highly polar functional group and also dissociable to form carboxylate ion which is negatively charged. Another reason for this large value of zeta potential was the use of Tween-20 as a non-ionic surfactant which creates extra stability[69]. After the immobilization of the enzyme on gold NPs the zeta potential decreases to values close to zero. Such a low value for zeta potential could be another factor for a decrease in enzymatic activity. Since the particles have low stability in solution and they tend to form aggregates, the active site of the enzyme may not be easily accessible for the substrates and also the slow diffusion of the substrate on the aggregates could result in a decrease in enzymatic activity of GOx.

To study the effect of zeta potential on enzymatic activity, it was suggested that we first increase the stability of NPs. Since we were dealing with an enzyme, the use of Tween-20 as a non-ionic surfactant was not recommended since it may alter the activity of the enzyme directly by stabilizing certain conformations. Another choice was to increase the pH to increase the negative charge on GOx (knowing that the isoelectric point of this enzyme is 4.2[78]). According to the targeted application of these gold NPs, which is to use them in the encapsulation process, the maximum pH that can be reached is at pH 7.0 since calcium ions could potentially produce precipitation of calcium hydroxide at alkaline pH values. Another set of NPs was prepared using the same conditions as sample 1 in the previous set (0.46 mg of gold NPs incubated with GOx) and this time the particles were dispersed in phosphate buffer (10 mM, pH 6.8). Subsequently, the activity and zeta potential were measured at pH 6.8 as shown in *Table 10*.

Table 10. Zeta potential and enzymatic activity of glucose oxidase immobilized- gold NPs of d≈50 nm.

Sample	**Description**	**Zeta potential (mV) (n=3)**	**Enzymatic activity (U/g of enzyme) (n=3)**
1	Gold NPs-enzyme (in phosphate 10mM, pH 5.8) Immobilization conditions: • 0.46 mg of gold NPs • Normal reaction conditions	-4.0±0.9	$(11.2\pm0.3)\times10^2$
2	Gold NPs-enzyme (in phosphate 10mM, pH 6.8) Immobilization conditions: • 0.46 mg of gold NPs • Normal reaction conditions	-25.4±0.2	$(25.7\pm0.7)\times10^2$

The results, given in show that the zeta potential has increased by increasing pH to 6.8. In addition, the enzymatic activity is also nearly doubled comparing to pH 5.8. In fact, this observation supports the that the enzymatic activity decreases by increasing the chance of aggregation of NPs. It should also be noted that that the enzymatic activity itself is pH dependent. The optimum pH for GOx is 5.5 and by increasing the pH to 6.8 the enzymatic activity decreases about 10 % of the maximum activity[69]. However, apparently avoiding the aggregation is much more effective in increasing the enzymatic activity. But in a larger viewpoint, the immobilization of GOx on gold NPs under these conditions results in a significant decrease in enzymatic activity which is unfavorable for our application of encapsulation purposes. As mentioned earlier, since the previous studies have shown a better thermostability and shelf life of immobilized enzyme on gold NPs, the encapsulation of such a combination is subject to a debate, whether the increased thermostability will compensate the significant losses in enzymatic activity or not.

5.6. Summary

To conclude this section, the immobilization of GOx on gold NPs, although successful, did not provide the expected increase in activity. While it may help to increase the thermostability and shelf life of GOx, the immobilization on NPs will need to be improved to achieve high enzymatic activity before these enzyme immobilized-gold NPs can be applied to the encapsulation process. After the immobilization of GOx on gold NPs, the results of enzymatic activity measurements showed a decrease in enzymatic activity of GOx due to two main reasons. First the possible conformation change of the enzyme and second the coalescence of the gold NPs in which the enzyme acted as a chemical glue to aggregate the gold NPs. The latter's effect is more significant once the immobilization of the enzyme is done on gold NPs with a size close to the size of GOx itself.

Chapter 6. Conclusion and future work

The present research aimed at investigating the possibility of GOx encapsulation and the immobilization of antibodies on the outer surface of alginate microcapsules to construct an antibacterial platform for paper coating and finally for the preparation of bioactive paper in larger scales which has the ability to capture the pathogens and to deactivate them using the chemical anti-pathogenic agent, hydrogen peroxidase, produced inside microcapsules by GOx activity.

Throughout this study it has been demonstrated that GOx can be encapsulated in alginate microcapsules using the vibrational break up of laminar flow encapsulation technique and stabilization of microcapsules in a calcium chloride bath presenting the encapsulation efficiency of 47 % while maintaining some of the enzymatic activity. These microcapsules have an average diameter of 120±20 μm and their size distribution was obtained using traditional optical microscope. Since the surface of alginate microcapsules does not contain a significantly chemically active group, they could easily be covered with another layer composed of chitosan using the ionotropic affinity between these two polymers. Chitosan contains amino groups which can be used for further modifications. This successful coverage was monitored by elemental analysis which showed the presence of nitrogen in the structure of microcapsules that can only be found in the structure of chitosan since alginate does not contain nitrogen. Also chitosan coverage was observable by using FITC-labeled chitosan that produced a fluorescent signal in laser scanning microscopy. Human IgG was chosen as a model antibody to check the possibility of immobilization of antibodies on the outer surface of microcapsules using the glutaraldehyde coupling reaction. To demonstrate the successful immobilization, MALDI-TOF-MS was used and the superimposition of two distinctive peaks of the antibody with the broad peak resulting from the polysaccharide structure of microcapsules was observable showing the covalent immobilization of human IgG on microcapsules. To measure the enzymatic activity of our designed platform, oxygen electroanalysis was used after the enzyme encapsulation and also after each modification step. Although the results show a decrease in enzymatic activity especially after encapsulation of GOx, we were able to maintain some of its activity showing that our approach has been successful to prepare the desired immobilization platform and we expect it to be adaptable to various enzyme-antibody combinations.

To verify the antibacterial properties of our designed platform, *E. coli* K-12 was chosen as a model pathogen. Preliminary observation of bacterial growth inhibition was made by its cultivation in LB broth culture media in a petri dish and the emergence of transparent halo around the central spot where the microcapsules were placed depicted successful bacterial growth inhibition. The detail of this bacterial growth inhibition was studied using optical density measurements of the culture media at different time points in order to determine a threshold of enzymatic activity with which we are able to inhibit bacterial growth. This threshold was found to be 1.3×10^{-2} U/ml for *E. coli* K-12 growth inhibition of 6.7×10^{8} cells/ml. Similarly, the minimum initial amount of bacteria that could grow at an enzymatic activity equal to 1.9×10^{-2} U/ml was found to be 6.7×10^{8} cells/ml. At this enzymatic activity threshold, the behavior of antibacterial microcapsules was also compared to the behavior of free GOx. The immobilization of GOx on gold NPs did not show a significant enhancement and instead, a decrease in enzymatic activity.

For the future work of this study, since we already demonstrated that human IgG can be immobilized on our microcapsules, some quantitative analysis is be required to determine the immobilization efficiency. Also it may be needed to immobilize a specific antibody which has an affinity for a specific pathogen in order to check if the antibody stays active after immobilization so that we can possibly observe the efficiency of the system in capturing and deactivation of the pathogen. Moreover, since so far we checked and monitored the antibacterial properties of the microcapsules during a period of 24 hours, it is suggested that complementary studies be done to monitor this characteristic over a larger time windows (*i.e.* ranging from a few weeks to a few months). Finally, these antibacterial microcapsules are to be introduced to the laboratorial paper coating process in order to check the efficiency of the system once it is coated on paper. This process can be done *using* a cylindrical laboratory coater (*Figure 43*) as previously performed in Dr. Rochefort's research group for a combination of the enzyme laccase encapsulated in poly(ethyleneimine) microcapsules[79]. In the related study, it was demonstrated that the encapsulated enzyme maintains its activity once the microcapsules are coated on paper surface. Therefore, we expect that our hydrogen peroxide producing microcapsules, once modified with antibodies could be used to make an efficient bioactive paper with antibacterial properties at large scales.

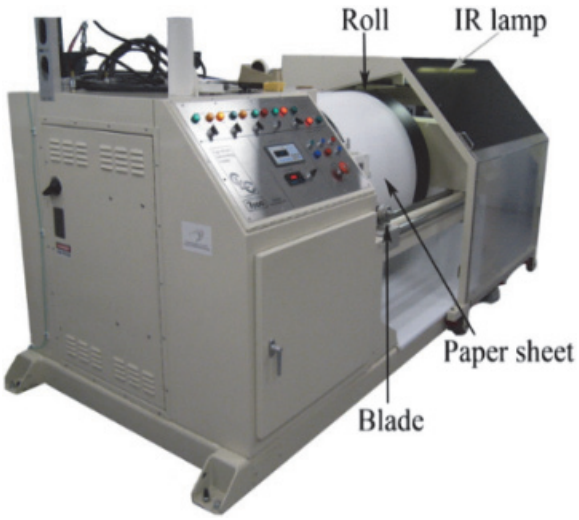

Figure 43. Cylindrical laboratory coater -CLC 7000 (reproduced from reference 79).

Chapter 7. References

1. Bioactive Paper Network Sentinel. "About us". http://www.bioactivepaper.com/about-us/ (accessed 29 May 2015).

2. Kong F.; Hu Y., Biomolecule immobilization techniques for bioactive paper fabrication. *Analytical and Bioanalytical Chemistry* **2012,** *403* (1), 7-13.

3. Comer J. P., Semiquantitative Specific Test Paper for Glucose in Urine. *Analytical Chemistry* **1956,** *28* (11), 1748-1750.

4. Free A. H.; Adams E. C.; Kercher M. L.; Free H. M.; Cook M. H., Simple Specific Test for Urine Glucose. *Clinical Chemistry* **1957,** *3* (3), 163-168.

5. Stocker J.; Balluch D.; Gsell M.; Harms H.; Feliciano J.; Daunert S.; Malik K. A.; van der Meer J. R., Development of a Set of Simple Bacterial Biosensors for Quantitative and Rapid Measurements of Arsenite and Arsenate in Potable Water. *Environmental Science & Technology* **2003,** *37* (20), 4743-4750.

6. Mabey D.; Peeling R. W.; Ustianowski A.; Perkins M. D., Tropical infectious diseases: Diagnostics for the developing world. *Nature Reviews/Microbiology* **2004,** *2* (3), 231-240.

7. Wang L.; Chen W.; Xu D.; Shim B. S.; Zhu Y.; Sun F.; Liu L.; Peng C.; Jin Z.; Xu C.; Kotov N. A., Simple, Rapid, Sensitive, and Versatile SWNT−Paper Sensor for Environmental Toxin Detection Competitive with ELISA. *Nano Letters* **2009,** *9* (12), 4147-4152.

8. Khan M. S.; Thouas G.; Shen W.; Whyte G.; Garnier G., Paper Diagnostic for Instantaneous Blood Typing. *Analytical Chemistry* **2010,** *82* (10), 4158-4164.

9. Savolainen A.; Zhang Y.; Rochefort D.; Holopainen U.; Erho T.; Virtanen J.; Smolander M., Printing of Polymer Microcapsules for Enzyme Immobilization on Paper Substrate. *Biomacromolecules* **2011,** *12* (6), 2008-2015.

10. Virtanen H.; Orelma H.; Erho T.; Smolander M., Development of printable bioactive paper containing laccase. *Process Biochemistry* **2012,** *47* (10), 1496-1502.

11. Yu J.; Ge L.; Huang J.; Wang S.; Ge S., Microfluidic paper-based chemiluminescence biosensor for simultaneous determination of glucose and uric acid. *Lab on a Chip* **2011,** *11* (7), 1286-1291.

12. Hossain S. M. Z.; Ozimok C.; Sicard C.; Aguirre S.; Ali M. M.; Li Y.; Brennan J., Multiplexed paper test strip for quantitative bacterial detection. *Analytical and Bioanalytical Chemistry* **2012,** *403* (6), 1567-1576.

13. Zhang Y.; Rochefort D., Fast and effective paper based sensor for self-diagnosis of bacterial vaginosis. *Analytica Chimica Acta* **2013,** *800*, 87-94.

14. Arciuli M.; Palazzo G.; Gallone A.; Mallardi A., Bioactive paper platform for colorimetric phenols detection. *Sensors and Actuators B: Chemical* **2013,** *186*, 557-562.

15. Kavruk M.; Ozalp V. C.; Oktem H. A., Portable Bioactive Paper-Based Sensor for Quantification of Pesticides. *Journal of Analytical Methods in Chemistry* **2013,** *2013*, Article ID 932946.

16. Badawy M. E. I.; El-Aswad A. F., Bioactive Paper Sensor Based on the Acetylcholinesterase for the Rapid Detection of Organophosphate and Carbamate Pesticides. *International Journal of Analytical Chemistry* **2014,** *2014*, Article ID 536823.

17. Liu H.; Zhan F.; Liu F.; Zhu M.; Zhou X.; Xing D., Visual and sensitive detection of viable pathogenic bacteria by sensing of RNA markers in gold nanoparticles based paper platform. *Biosensors and Bioelectronics* **2014,** *62*, 38-46.

18. Sicard C.; Brennan J. D., Bioactive paper: Biomolecule immobilization methods and applications in environmental monitoring. *MRS Bulletin* **2013,** *38* (04), 331-334.

19. Di Risio S.; Yan N., Adsorption and inactivation behavior of horseradish peroxidase on cellulosic fiber surfaces. *Journal of Colloid and Interface Science* **2009,** *338* (2), 410-419.

20. Anany H.; Chen W.; Pelton R.; Griffiths M. W., Biocontrol of Listeria monocytogenes and Escherichia coli O157:H7 in Meat by Using Phages Immobilized on Modified Cellulose Membranes. *Applied and Environmental Microbiology* **2011,** *77* (18), 6379-6387.

21. Cheng C.-M.; Martinez A. W.; Gong J.; Mace C. R.; Phillips S. T.; Carrilho E.; Mirica K. A.; Whitesides G. M., Paper-Based ELISA. *Angewandte Chemie International Edition* **2010,** *49* (28), 4771-4774.

22. Su S.; Ali M. M.; Filipe C. D. M.; Li Y.; Pelton R., Microgel-Based Inks for Paper-Supported Biosensing Applications. *Biomacromolecules* **2008,** *9* (3), 935-941.

23. Avnir D.; Coradin T.; Lev O.; Livage J., Recent bio-applications of sol-gel materials. *Journal of Materials Chemistry* **2006,** *16* (11), 1013-1030.

24. Kissel T.; Maretschek S.; Packhauser C.; Schneiders J.; Seidel N., *Microencapsulation Techiniques for Parenteral Depot Systems and Their Application in the Pharmaceutical Industry*; In Benita S. (Ed.), *Microencapsulation : Methods and Industrial Applications*, 2nd ed.; Taylor & Francis: New York, **2006**; 756 p., Chapter 4.

25. Poncelet D.; Dreffier C.; Subra-Paternault P.; Vandamme T., *Introduction aux techniques de microencapsulation*; In Vandamme T.; Poncelet D.; Subra-Paternault P. (Eds.), *Microencapsulation : des sciences aux technologies*, Éditions Tec & Doc: Paris, **2007**; 355 p., Chapter 1.

26. Zhang Y. Development of an enzyme immobilization platform based on microencapsulation for paper-based biosensors, Ph.D. Thesis. Université de Montréal, Montreal, **2011**.

27. Montalvo-Ortiz B. L.; Sosa B.; Griebenow K., Improved Enzyme Activity and Stability in Polymer Microspheres by Encapsulation of Protein Nanospheres. *AAPS PharmSciTech* **2012,** *13* (2), 632-636.

28. Renard D.; Reddy T., *Polymères d'origine biologique pour la microencapsulation* In Vandamme T.; Poncelet D.; Subra-Paternault P. (Eds.), *Microencapsulation : des sciences aux technologies*, Éditions Tec & Doc: Paris, **2007**; 355 p., Chapter 12.

29. Christenson L.; Dionne K. E.; Lysaght M. J., *Biomedical Applications of Immobilized Cells*; In Goosen M. F. A. (Ed.), *Fundamentals of animal cell encapsulation and immobilization*, CRC Press: Boca Raton, Fla., **1993**; 326 p., Chapter 2.

30. Lee K. Y.; Mooney D. J., Alginate: properties and biomedical applications. *Progress in polymer science* **2012,** *37* (1), 106-126.

31. Cheeky Monkey Cream Chargers. Properties of Sodium Alginate as a Gel. http://www.creamchargers.org.uk/sodium-alginate-205-p.asp (accessed 24 July 2015).

32. USTL Université des Sciences et Technologie de Lille. Polysaccharides alimentaires. http://biochim-agro.univ-lille1.fr/polysaccharides/co/Contenu_7_2.html (accessed 24 July 2015).

33. Gåserød O.; Smidsrød O.; Skjåk-Bræk G., Microcapsules of alginate-chitosan – I: A quantitative study of the interaction between alginate and chitosan. *Biomaterials* **1998,** *19* (20), 1815-1825.

34. Mazzitelli S.; Tosi A.; Balestra C.; Nastruzzi C.; Luca G.; Mancuso F.; Calafiore R.; Calvitti M., Production and characterization of alginate microcapsules produced by a vibrational encapsulation device. *Journal of Biomaterials Applications* **2008,** *23* (2), 123-145.

35. Blandino A.; Macías M.; Cantero D., Glucose oxidase release from calcium alginate gel capsules. *Enzyme and Microbial Technology* **2000,** *27* (3–5), 319-324.

36. Rinaudo M., Chitin and chitosan: Properties and applications. *Progress in Polymer Science* **2006,** *31* (7), 603-632.

37. Poncelet D.; Dreffier C., *Les méthodes de mocroencapsulation de A à Z (ou presque)*; In Vandamme T.; Poncelet D.; Subra-Paternault P. (Eds.), *Microencapsulation : des sciences aux technologies*, Éditions Tec & Doc: Paris, **2007**; 355 p., Chapter 3.

38. Microencapsulation-Innovations c/o Burgundy Gold Ltd "Physical Microencapsulation Technologies". http://www.microencapsulationinnovations.com/Physical.html (accessed 03 July 2015).

39. Voet D.; Voet J. G.; Pratt C. W., *Enzymatic Catalysis*; In *Fundamentals of biochemistry : life at the molecular level*, 2nd ed.; John Wiley & sons: New York, **2006**; 1130, 112 p., Chapter 11.

40. Ma S.; Mu J.; Qu Y.; Jiang L., Effect of refluxed silver nanoparticles on inhibition and enhancement of enzymatic activity of glucose oxidase. *Colloids and Surfaces A: Physicochemical and Engineering Aspects* **2009,** *345* (1–3), 101-105.

41. RSCB-Protein Data Bank. "Glucose oxidase from Aspergillus niger". http://www.rcsb.org/pdb/pv/pv.do?pdbid=1CF3&bionumber=1 (accessed 07 July 2015).

42. RSCB-Protein Data Bank. "Glucose oxidase from penicillium amagasakiense". http://www.rcsb.org/pdb/pv/pv.do?pdbid=1GPE&bionumber=0 (accessed 07 July 2015).

43. Bankar S. B.; Bule M. V.; Singhal R. S.; Ananthanarayan L., Glucose oxidase — An overview. *Biotechnology Advances* **2009,** *27* (4), 489-501.

44. Witt S.; Wohlfahrt G.; Schomburg D.; Hecht H. J.; Kalisz H. M., Conserved arginine-516 of Penicillium amagasakiense glucose oxidase is essential for the efficient binding of β-d-glucose. *Biochemical Journal* **2000,** *347* (2), 553-559.

45. Voet D.; Voet J. G.; Pratt C. W., *Enzyme Kinetics, Inhibition, and Regulation*; In *Fundamentals of biochemistry : life at the molecular level*, 2nd ed.; John Wiley & sons: New York, **2006**; 1130, 112 p., Chapter 12.

46. Laidler K. J.; Meiser J. H., *Chemical Kinetics II. Compisite Mechanisms*; In *Physical chemistry*, 2nd ed.; Houghton Mifflin: Boston, **1995**; 988 p., Chapter 10.

47. National Institute of allergy and infectious diseases/ image library. http://www.niaid.nih.gov/topics/biodefenserelated/biodefense/publicmedia/Pages/image_library.aspx (accessed 10 July 2015).

48. De la Maza L. M., *Color atlas of medical bacteriology*. Second edition. ed.; ASM press: Washington (D.C.), **2013**; xi, 353 pages.

49. Russo E., Special Report: The birth of biotechnology. *Nature* **2003,** *421* (6921), 456-457.

50. Novick A., Growth of Bacteria. *Annual Review of Microbiology* **1955,** *9* (1), 97-110.

51. Encyclopædia Britannica Online. Encyclopædia Britannica Inc. "Binary fission cell division". http://www.britannica.com/science/binary-fission (accessed 10 July 2015).

52. Avasara Leadership Fellows. "Asexual Reproduction". https://sites.google.com/a/avasara.in/educational-resources/academic-resources/science/10th-standard/chapter-12-the-life-cycle (accessed 10 July 2015).

53. Cooper S., *Bacterial growth and division : biochemistry and regulation of prokaryotic and eukaryotic division cycles*; In Academic Press: San Diego ;Toronto, **1991**; 501 p., Chapter 1.

54. Instruction Manual for Inothech ENCAPSULATOR RESEARCH IE-50 R. Inotech Biosystems International: Rockville, MD, 2005.

55. Bradford M. M., A rapid and sensitive method for the quantitation of microgram quantities of protein utilizing the principle of protein-dye binding. *Analytical Biochemistry* **1976,** *72* (1–2), 248-254.

56. Compton S. J.; Jones C. G., Mechanism of dye response and interference in the Bradford protein assay. *Analytical Biochemistry* **1985,** *151* (2), 369-374.

57. Instruction Manual for Bio-Rad Protein Assay. Bio-Rad Laboratories, Inc.: USA.

58. Ghafourifar G. Characterization of Glutaraldehyde-Immobilized Chymotrypsin and an In Situ Immobilized Enzyme Reactor Using Capillary Electrophoresis-Based Peptide Mapping, Ph.D. Thesis. Université de Montréal, **2015**.

59. Department of Chemistry, Université de Montréal. Elemental Analysis Service. http://en.chimie.umontreal.ca/research/the-departments-analysis-services/elemental-analysis-service/ (accessed 17 July 2015).

60. Migneault I.; Dartiguenave C.; Bertrand M. J.; Waldron K. C., Glutaraldehyde: behavior in aqueous solution, reaction with proteins, and application to enzyme crosslinking. *Biotechniques* **2004,** *37* (5), 790-802.

61. Albarghouthi M.; Abu Fara D.; Saleem M.; El-Thaher T.; Matalka K.; Badwan A., Immobilization of antibodies on alginate-chitosan beads. *International Journal of Pharmaceutics* **2000,** *206* (1-2), 23-34.

62. Gross J. H., *Matrix-Assisted Laser Desorption/Ionization*; In *Mass spectrometry : A textbook*, 2nd ed.; Springer: Heidelberg, **2011**; 753 p., Chapter 11.

63. Hitchman M. L., *Chapter 4*; In *Measurement of dissolved oxygen (Chemical Analysis)*, Wiley: New York, **1978**; 255 p., Chapter 4.

64. The Rank Brothers Oxygen Electrode Operating Manual. Rank Brothers Ltd: Cambridge, England, 2002.

65. Sambrook J.; Fritsch E. F.; Maniatis T., *Bacterial Media, Antibiotics and Bacterial Strains*; In *Molecular cloning : a laboratory manual*, 2nd ed.; Cold Spring Harbor Laboratory: Cold Spring Harbor, N.Y., **1989**; Appendix A.

66. Sezonov G.; Joseleau-Petit D.; D'Ari R., Escherichia coli physiology in Luria-Bertani broth. *Journal of Bacteriology* **2007,** *189* (23), 8746-9.

67. Gåserød O.; Sannes A.; Skjåk-Bræk G., Microcapsules of alginate–chitosan. II. A study of capsule stability and permeability. *Biomaterials* **1999,** *20* (8), 773-783.

68. Tiwari P. M.; Vig K.; Dennis V. A.; Singh S. R., Functionalized Gold Nanoparticles and Their Biomedical Applications. *Nanomaterials* **2011,** *1* (1), 31-63.

69. Li D.; He Q.; Cui Y.; Duan L.; Li J., Immobilization of glucose oxidase onto gold nanoparticles with enhanced thermostability. *Biochemical and Biophysical Research Communications* **2007,** *355* (2), 488-493.

70. Pandey P.; Singh S. P.; Arya S. K.; Gupta V.; Datta M.; Singh S.; Malhotra B. D., Application of Thiolated Gold Nanoparticles for the Enhancement of Glucose Oxidase Activity. *Langmuir* **2007,** *23* (6), 3333-3337.

71. Ma Z. F.; Ding T., Bioconjugates of Glucose Oxidase and Gold Nanorods Based on Electrostatic Interaction with Enhanced Thermostability. *Nanoscale Research Letters* **2009,** *4* (10), 1236-1240.

72. Song Y.; Chen J.; Liu H.; Song Y.; Xu F.; Tan H.; Wang L., Conformation, Bioactivity and Electrochemical Performance of Glucose Oxidase Immobilized on Surface of Gold Nanoparticles. *Electrochimica Acta* **2015,** *158*, 56-63.

73. Turkevich J.; Stevenson P. C.; Hillier J., A Study of the Nucleation and Growth Processes in the Synthesis of Colloidal Gold. *Discussions of the Faraday Society* **1951,** (11), 55-75.

74. Kireyko A. V.; Veselova I. A.; Shekhovtsova T. N., Mechanisms of peroxidase oxidation of o-dianisidine, 3,3′,5,5′-tetramethylbenzidine, and o-phenylenediamine in the presence of sodium dodecyl sulfate. *Russian Journal of Bioorganic Chemistry* **2006,** *32* (1), 71-77.

75. Amachi S.; Kimura K.; Muramatsu Y.; Shinoyama H.; Fujii T., Hydrogen Peroxide-Dependent Uptake of Iodine by Marine Flavobacteriaceae Bacterium Strain C-21. *Applied and Environmental Microbiology* **2007,** *73* (23), 7536-7541.

76. Haiss W.; Thanh N. T. K.; Aveyard J.; Fernig D. G., Determination of Size and Concentration of Gold Nanoparticles from UV−Vis Spectra. *Analytical Chemistry* **2007,** *79* (11), 4215-4221.

77. Heller A., Electrical wiring of redox enzymes. *Accounts of Chemical Research* **1990,** *23* (5), 128-134.

78. Pazur J. H.; Kleppe K., The Oxidation of Glucose and Related Compounds by Glucose Oxidase from Aspergillus niger*. *Biochemistry* **1964,** *3* (4), 578-583.

79. Guerrero M. P.; Bertrand F.; Rochefort D., Activity, stability and inhibition of a bioactive paper prepared by large-scale coating of laccase microcapsules. *Chemical Engineering Science* **2011,** *66* (21), 5313-5320.